A LATE QUATERNARY SUBMARINE OUTWASH FAN AT ST. LAZARE, QUEBEC

by

Geoffrey Harrison Burbidge

A thesis submitted to the School of Graduate Studies of the University of Ottawa in partial fulfillment of the requirements for the degree of M.Sc. in Geology

OTTAWA CARLETON CENTRE FOR GEOSCIENCE STUDIES,
OTTAWA, ONTARIO, CANADA, 1985

ABSTRACT

A plateau of Quaternary glacial outwash sand, approximately 30 km in extent, at St. Lazare, Quebec, is interpreted as a subaqueous outwash fan, or subwash fan. Its relatively flat top is due to littoral reworking during regression of the Champlain Sea, which submerged the area to a depth of more than 112 m during ice retreat. The fan was deposited in a reentrant of the ice margin, which in turn was controlled by a steep bedrock knoll beneath the fan. It is the major component of a complex of ice contact outwash deposits in the lee of Oka and Rigaud mountains. The mountains acted as obstacles to ice flow, inducing down-ice calving and crevassing. Multiple subaqueous ice tunnels supplied sediment to the fan.

In the distal areas of the fan the sediments consist primarily of proximal varves, the peak flow units of which are composed of units of well sorted fine to medium sand containing traction current structures. The "winter" deposits are poorly sorted horizontally laminated clayey silt to very fine sand. The abundance of trace fossils is evidence of extensive faunal colonization of the distal fan.

The proximal fan sediments are dominated by channelized crossbedded sand. Units of silt to very fine sand are

evidence of the rapid facies variation in proximal subwash deposits. A shallow channel over 100 m wide contains a bank-attached cross channel bar over 3 m high. A >30 m wide lens of contorted silty clay resulted from the infilling of a kettle hole.

The traction current structures in the fan sediment indicate that the sediment concentrations in the debouching glacial tunnels were sufficient to form continuous turbidity underflows across the fan surface. When the deposition of sediment reduced the density of the underflow to less than the surrounding seawater, the underflow lifted from the fan surface and continued as an interflow. Interflow sediments are horizontally laminated and poorly sorted, with significant amounts of clay and silt.

A prominent littoral unconformity is present at 3 m depth mid-fan and can be correlated across the fan. Storm beach and beachface stratification overlies the unconformity.

Vertical, planar water escape fissures that resemble fossil frost veins are present in the proximal facies. The fissures consist of a narrow central fissure with an average of 4 cm of downturning of adjacent strata. They are attributed to the channelization of fluidized sediment during release of water from buried remnant glacier ice.

ACKNOWLEDGEMENTS

I wish to thank my advisor, Dr. Brian Rust, for his support throughout the thesis and his prompt and excellent criticism of the manuscript. I am indebted to Jan Terasmae of Brock University for processing the radiocarbon dates, to Guy Narbonne of Queen's University for his help with the trace fossil identification, and to Henry Richard of the Terrain Science Division of the Geological Survey who suggested the project and provided advice and field guidance. Dr. Hugh French of the O.C.C.G.S. co-supervised during Dr. Rust's absence, providing very useful input concerning frost wedges and veins. Several people gave excellent assistance in the field, in particular Lorne Bennett, and my father, Harrison Burbidge. Iain Muir, Bill Parkins, and Dana Naldrett gave welcome support and advice during the initial bewildering stages. Our former thin section technician, Bob Taylor, provided technical support and ideas throughout the field season. Thanks to Dave Sharpe, Carlos Salas, Penny Henderson, and Heather Blois for their advice and help during the later stages of the project.

Financial support was supplied for the entire project by Dr. Rust from National Research Council grants.

TABLE OF CONTENTS

LIST OF TABLES

LIST OF FIGURES

CHAPTER 1: INTRODUCTION

1.1 LOCATION AND PURPOSE OF STUDY

A large plateau of Quaternary glacial outwash sand lies beside the Ottawa River at St. Lazare, near Vaudreuil, Quebec, just west of the island of Montreal. Fig. 1.1a locates the study area with respect to Ottawa and Montreal. The purpose of the field investigations was to examine and describe the sedimentology of the feature, as exposed in a series of borrow pits across the plateau. The plateau was mapped as ice-contact stratified drift by Richard (1982). Other deposits of ice-contact sand or gravel have been mapped in the Champlain Sea Basin (Richard 1982; Gadd, 1963). The St. Lazare plateau is among the largest and most remarkable of these deposits.

1.2 LATE QUATERNARY HISTORY OF THE AREA

1.2.2 ISOSTACY AND PONDING OF GLACIAL MELTWATER

The Wisconsinan continental ice sheet attained a minimum thickness of 3500 m (Robin, 1962). The weight of the

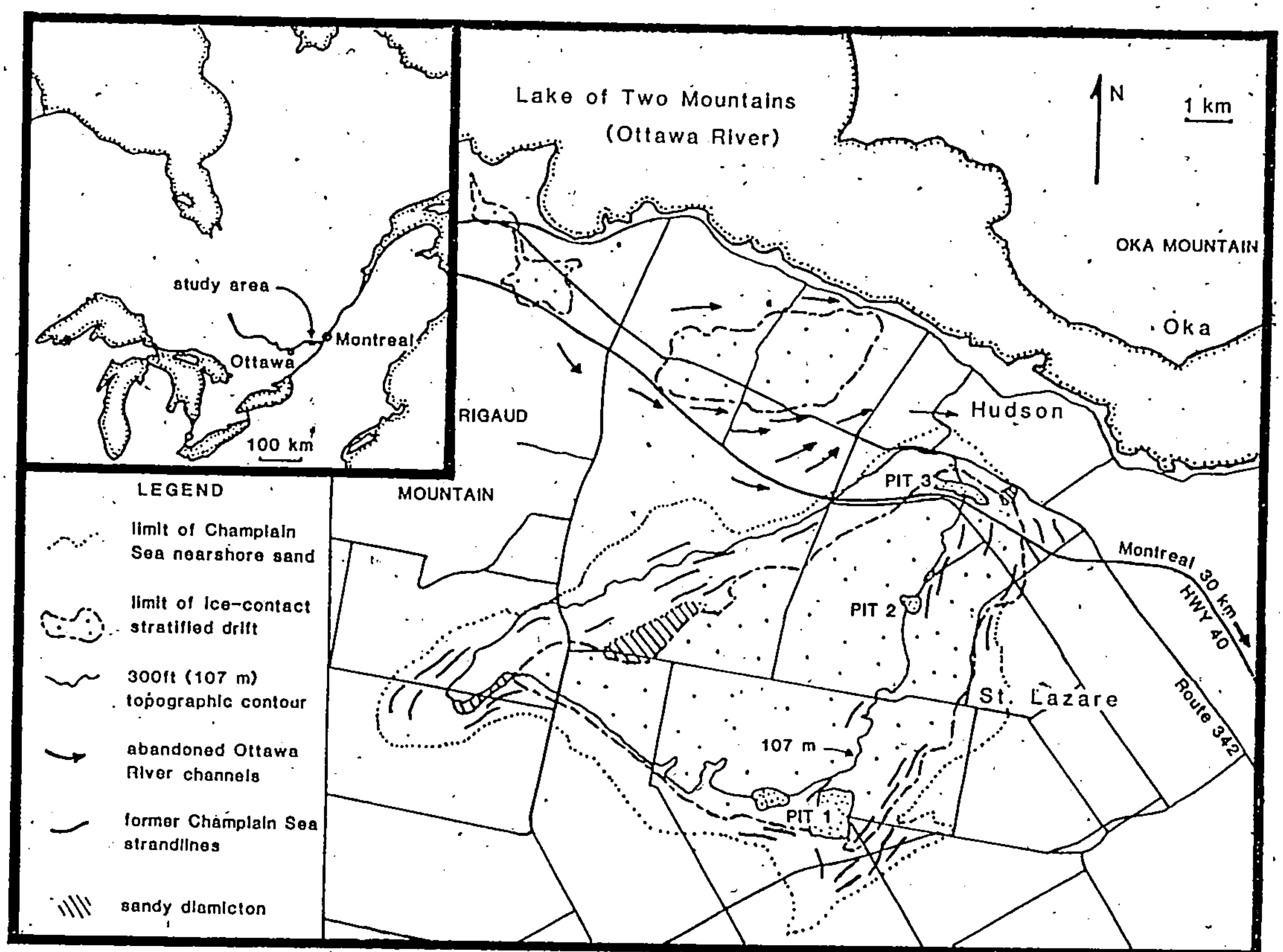

Fig. 1.1a Surficial geology of study area, southwestern Quebec, after Richard, (1982).

accumulated ice caused an isostatic response of the Earth's crust, that is, depression of the land surface beneath the ice sheet and to a certain distance in front of its terminus. The resulting upward slope away from the terminus tended to keep glacier meltwater accumulated at the front of the glacier (Andrews, 1970), and in many areas the ice sheet retreated in standing water, either lacustrine or marine. Hillaire-Marcel (1979) estimated the maximum depth of the Champlain Sea at 150 m. An estimate of the depth of water at the terminus of the Laurentide sheet in the Ottawa area is 100 m (Rust and Romanelli, 1975). In the Ottawa and St. Lawrence River valleys, marine fossils in clay deposits which overlie tills and other glacial material provide proof that there was marine water in the lowlands after the ice retreated, and by the above argument, ponded against the ice front. Rapid isostatic recovery immediately following deglaciation outstripped eustatic fluctuations and provided for an uninterrupted regression of the proglacial waters and a continuous offlap sequence in the sedimentary record (Andrews, 1968; Gadd, 1977).

1.2.3 THE CHAMPLAIN SEA

Early concepts

In 1845, Sir Charles Lyell proposed that there had been a marine invasion of the St. Lawrence Valley and that the sea-ice rafted boulders into the basin to be deposited with the shelly marine clay there. In the early years of the twentieth century the boulder clays were recognized as products of continental glaciation (Karrow, 1961, p. 98).

The Champlain Sea was named by E. Hitchcock in his Report on the Geology of Vermont (1861). The sediments of the Champlain Sea have been described recently by Terasmae (1959, 1965), Elson (1959, 1969), Karrow (1961), and Gadd (1972, 1977), among others. Richard (1982) has mapped the surficial deposits of part of Eastern Ontario and Western Quebec as part of an ongoing 1:50,000 map series. A recent work on the post-glacial marine bodies of Quebec is by Claude Hillaire-Marcel (1979).

Extent and phases of the Champlain Sea

Atlantic waters were free to enter the St. Lawrence Lowlands when the Wisconsinan ice sheet retreated past the narrows of the St. Lawrence River at Quebec City. Prior to that, there was a series of fresh meltwater lakes in front of the ice in the Lowlands. In support of this hypothesis, Terasmae (1965) found sections of varved lacustrine-like clay that grade upward to marine clays in the Cornwall area.

Correlation of strandlines and former water planes indicate that Glacial Lake Iroquois (of the Lake Ontario basin) extended into the St. Lawrence Lowlands. The Sydney and Belleville phases of Lake Iroquois were continuous with water in the Champlain Valley of New York State, after the ice sheet retreated past the northernmost part of the Adirondack Mountains (Prest, 1970; Clark and Karrow, 1984). Recently re-interpreted rythmically bedded lacustrine sediments between the diamictons and the overlying marine clays indicate the existence of a pre-Champlain Sea freshwater phase in the upper Ottawa Valley (Naldrett, Ph.D. thesis in preparation, University of Ottawa). Evidence presented in this thesis shows that to the southeast of Ottawa, in the St. Lazare area at least, marine sediments directly overly Wisconsinan till.

The concept of a connection between the St. Lawrence and Lake Ontario basins across the Frontenac Axis at the time of the Champlain Sea has long been a point of contention among workers. As early as 1907 this possibility was considered (the "Gilbert Gulf" of Fairchild). Hough (1958) referred to the the "St. Lawrence marine embayment" in the Lake Ontario basin. The main objection to this concept had been that unequivocal evidence of marine fossils or brackish water sediments have never been found to the west of the Frontenac Axis (Terasmae, 1965; Dreimanis, 1977). Anderson et al (1985) have identified glacilacustrine clay (based on the presence of fresh water ostracodes) beneath glacimarine deposts in the upper Ottawa Valley. Even if there were a connection between the two basins, the influence of the reservoir of fresh water in the

Great Lakes, added to the meltwater input from the ice sheet, would have kept water in the Lake Ontario basin too brackish for the development of a marine or euryhaline fauna (Anderson et al, 1985). Certainly the earliest phase of the Champlain Sea was brackish, because of the large amount of fresh water already ponded in the Lowlands. Cronin (1977) identified both fresh water and marine ostracodes from the highest beaches of the Champlain Sea, and called this earliest episode the Transitional Phase of the Champlain Sea. Schroeder and Bada (1978) suggested that high concentrations of certain amino acids in Lake Ontario cores indicate marine conditions. These considerations, and reinterpretation of strandline and isobase data, led Clark and Karrow (1984) to correlate the Trenton phase of Lake Algonquin in the Lake Ontario basin with marine shell-bearing strandlines of the early Champlain Sea, indicating that there was a connection between the Lake Ontario basin with the St. Lawrence Lowlands. According to Clark and Karrow (1984, p. 813), shortly after inception of the Champlain Sea, isostatic uplift of the Frontenac Arch severed the connection with the Great Lakes and the Champlain Sea entered its most saline phase.

Examination of O.D.M. map 2227, (Chapman and Putnam, 1972), showing the physiography of the eastern portion of Southern Ontario, indicates the large areas of clay deposits of the Champlain Sea. The eastern edge of the Frontenac Arch forms the western boundary of these deposits. In the Ottawa

Valley the deposits extend as far west as Petawawa. The southern edge of the Gatineau Hills and Laurentian Highlands bounded the sea to the north, and there were various short-lived incursions up river valleys such as that of the Gatineau River (Romanelli, 1975).

Elson (1969) has estimated the total area submerged by the Champlain Sea at 53,000 km^2. That it reached its maximum depth immediately following its inception is borne out by the fact that the oldest radiocarbon dates are from the highest strandlines, and that only offlap sequences have been identified relating to the Champlain Sea (Clark and Karrow, 1984).

Elson and Elson (1959) identified three phases of the Champlain Sea based on relative abundance of certain macrofauna. These subdivisions were supported by the microfaunal work of Cronin (1977). Elson named the first phase after the arctic bivalve <u>Hiatella arctica</u>, and the second after a boreal species, <u>Mya arenaria</u>. The third, or latest, phase is represented by a freshwater bivalve, <u>Lampsilis siliquoidea</u>. Cronin added a Transitional Phase (mentioned above) of brackish conditions which predated the Hiatella Phase.

The beginning of the Hiatella phase is radiocarbon dated at approximately 12,500 yrs BP (Hillaire-Marcel, 1979). This was the coldest and most saline episode. As the influence of the retreating ice front lessened, marine temperatures increased (Mya Phase). Salinities decreased in response to lessening of the size of the connection to the Atlantic at Quebec, and the continued influx of meltwater and Great Lakes drainage (Elson, 1969). Dates on the early Mya phase range from 10,800 (Elson, 1969) to 10,600 (Cronin, 1977). The Lampsilis episode represents freshwater remnants in isolated basins in the lowlands. These basins persisted after the connection to the Atlantic was terminated by isostatic uplift of the sill at Quebec City, at about 10,000 BP (Cronin, 1977; Hillaire-Marcel 1979).

Hillaire-Marcel (1979) divided the marine events in the St. Lawrence into three parts, the boundaries of which are marked by conspicuous moraines and are dated from shells within these moraines. His approach serves to point out the diachronous nature of the marine limits of the Champlain Sea. Phase 1 represents the period from the incursion of the Champlain Sea to the construction of the Drummondville Moraine in Southern Quebec, dated at 12,000 to 11,800 BP (Hillaire-Marcel and Occhietti, 1977). Phase 2 occurred during retreat from the Drummondville system to the St. Narcisse Moraine. Morainal segments north of the Ottawa River are correlated with the St. Narcisse system, which is dated at +11,000 BP (Parry and Macpherson, 1964), and 10,800 BP (Hillaire-Marcel and Occhietti, 1980). Phase 3 is the episode which accompanied withdrawal of the ice mass from the St. Narcisse position into the Laurentian Highlands.

1.3 REGIONAL GEOLOGY

1.3.1 BEDROCK GEOLOGY

The northern edge of the Ottawa - Bonnechere graben is situated 10 km north of St. Lazare, where the Laurentian Highlands begin (Kumarapeli and Saull, 1966). Flat-lying Lower Paleozoic clastic and carbonate rocks are preserved within the graben, and are underlain at depth by a basement of crystalline Precambrian rocks of Grenvillian age, which comprise the Laurentian Highlands to the north. The graben system is complicated by subsidiary faults that have exposed inliers of the basement at Oka and Rigaud (Wilson, 1941). These now form two prominent hills, Rigaud and Oka Mountains, which dominate the otherwise subdued local landscape (fig. 1.1b).

St. Lazare is situated in the centre of a large area of thick drift which obscures the bedrock. Borehole data (Tremblay and Hobson, 1962) reveal the presence of the Paleozoic Nepean Formation beneath the St. Lazare plateau. Paleozoic limestone, dolostone and sandstone are exposed south and north of the area. Specifically, to the north, there is the moderately consolidated, well sorted medium to coarse grained sandstone of the Nepean Formation; the March and Oxford Formations, composed of limestone, dense blue-gray dolostone, and sandstone similar to that of the Nepean; and

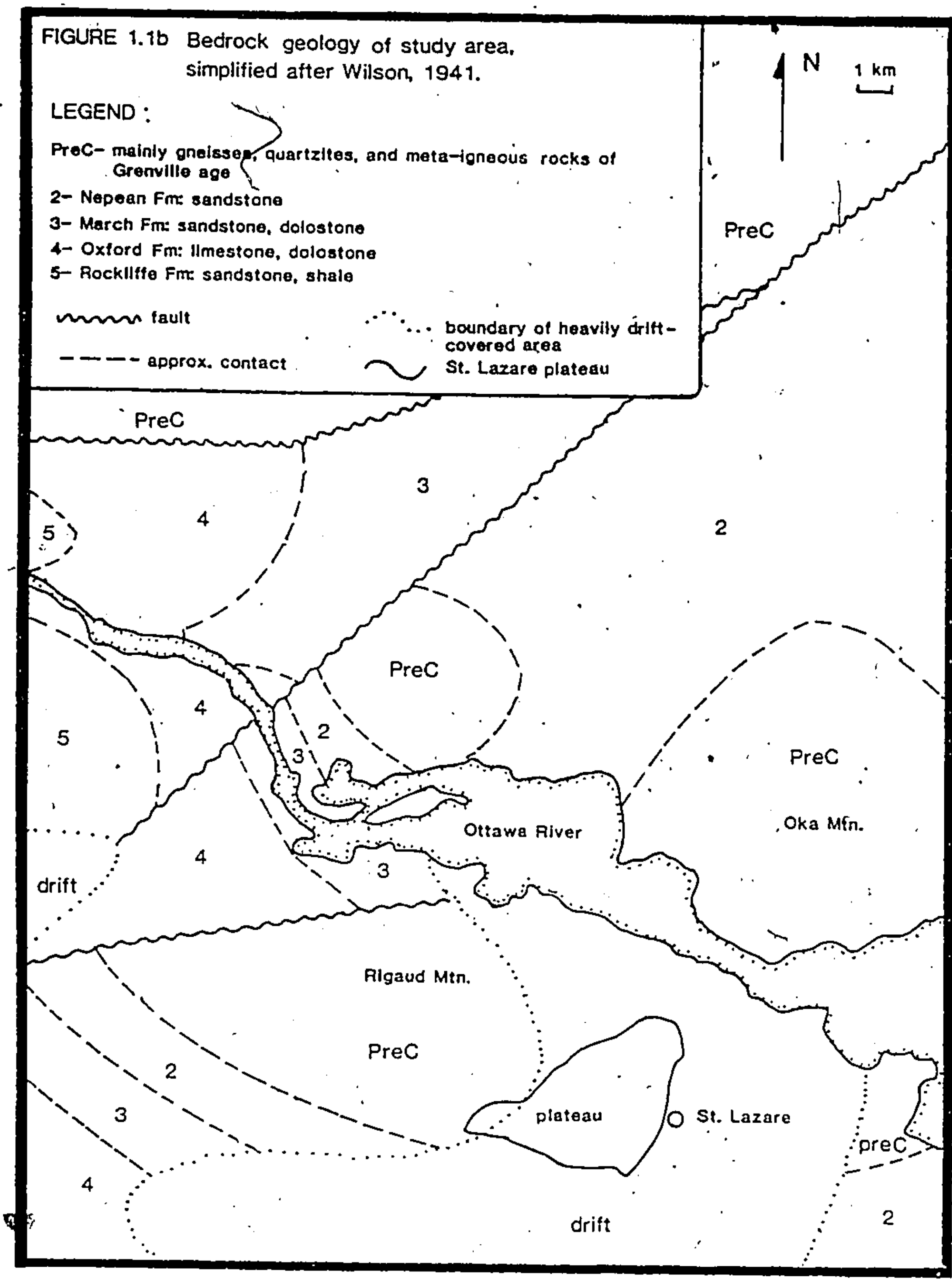
FIGURE 1.1b Bedrock geology of study area, simplified after Wilson, 1941.
LEGEND :
PreC– mainly gneisses, quartzites, and meta-igneous rocks of Grenville age
2– Nepean Fm: sandstone
3– March Fm: sandstone, dolostone
4– Oxford Fm: limestone, dolostone
5– Rockliffe Fm: sandstone, shale
fault
approx. contact
boundary of heavily drift-covered area
St. Lazare plateau
N
1 km
PreC
3
4
5
2
PreC
4
5
2
3
PreC
Oka Mtn.
Ottawa River
4
3
drift
Rigaud Mtn.
PreC
2
3
plateau
St. Lazare
preC
4
drift
2

the shale and fine micaceous sandstone of the Rockliffe Formation.

1.3.2 BEDROCK TOPOGRAPHY

Fortuitously, a seismic refraction survey of the St. Lazare area was carried out by the Geological Survey of Canada in 1961 (Tremblay and Hobson, 1962). Although there are some discrepancies between the bedrock contours and topographic contours on the top of the St. Lazare plateau, borehole data confirmed the general accuracy of the survey and the following observations can be made (fig. 1.2).

1. The St. Lazare sand plateau is perched atop a bedrock knoll with 90 m relief (67 m above the Ottawa River), and the topographic expression of the plateau is partially controlled by the knoll.

2. A steep sided bedrock channel is situated along the northwestern boundary of the knoll.

3. The thickness of the drift in the plateau is much less than would be assumed from the morphology of the plateau.

4. An isopach map of the drift over the bedrock knoll shows a triangular shaped body thickening to the southwest from a relatively thin apex at the northeastern corner of the plateau (fig. 1.2b).

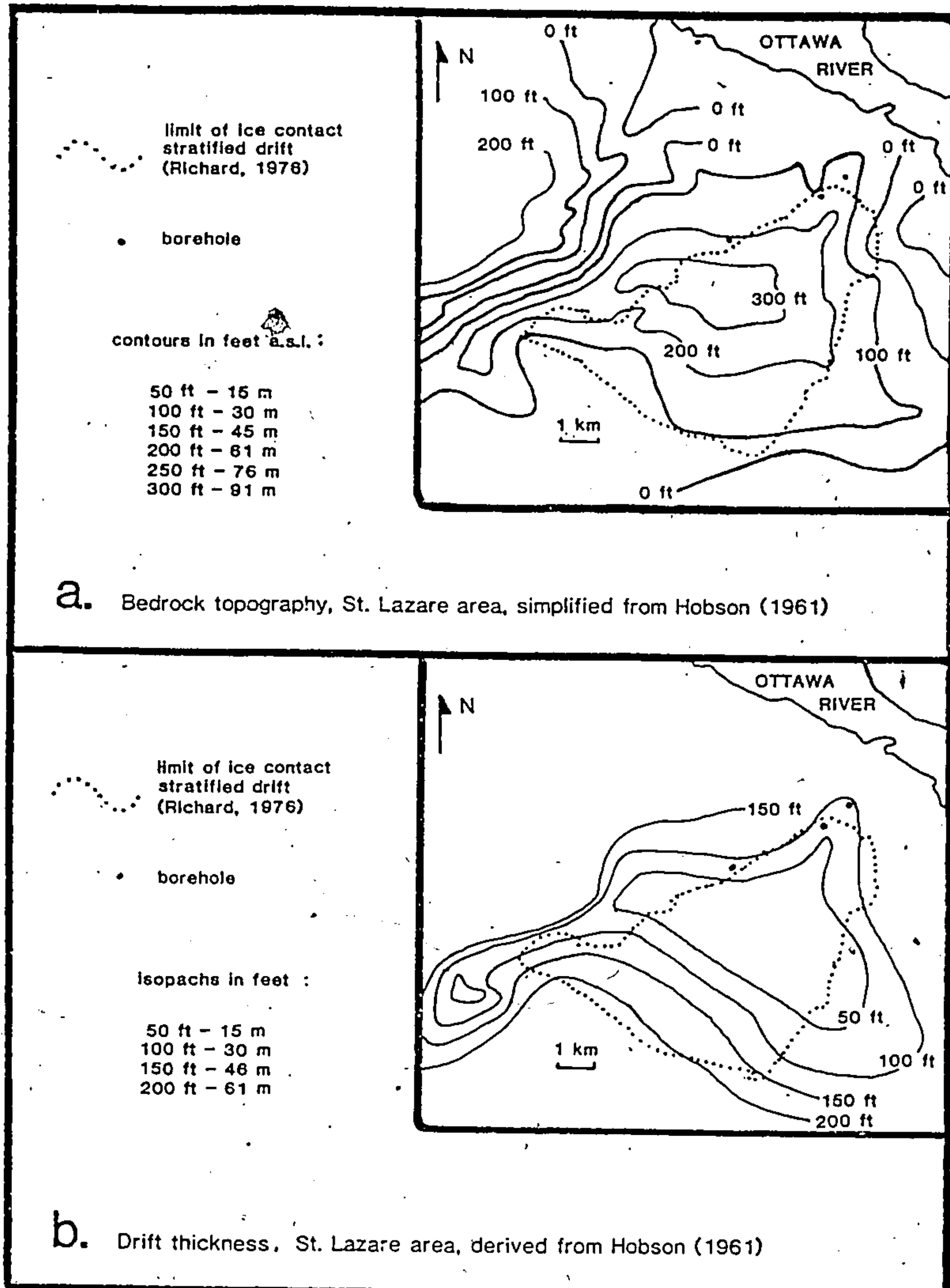

a. Bedrock topography, St. Lazare area, simplified from Hobson (1961)

b. Drift thickness, St. Lazare area, derived from Hobson (1961)

Fig. 1.2 Bedrock topography and drift thickness of the St. Lazare area.

1.3.3 SURFICIAL GEOLOGY

The surficial deposits of the area have been mapped at a scale of 1:50,000 by H. Richard of the Geological Survey of Canada (Richard, 1982). In 1950, a soil survey of the county was published by Lajoie and Stobbe.

The most abundant surficial deposit in the area is marine clay deposited in the Champlain Sea, which blankets much of the area, filling basins and depressions over bedrock and glacial material. Various glacial deposits constitute about a quarter of the map area. Most of these are composed of silty to sandy diamicton, in the form of hummocky or ridged ground moraine. The morainic ridges trend WSW. Ridges and uplands of sandy to gravelly glacifluvial (Powell, 1984, p.2) outwash occur in scattered localities in the area, of which the largest, at St. Lazare, is the subject of the present study. Large areas of sand plains of lower relief also occur in the area, and are interpreted as subaerial fluvial and deltaic deposits of the shoaling remnants of the Champlain Sea and Lampsilis Lake (Richard, 1976). Lambert (1972) noted that glacial striae observed in the Oka region indicate a NE-SW direction of ice transport.

1.3.4 GEOMORPHOLOGY OF THE ST. LAZARE PLATEAU

The St. Lazare plateau is a roughly triangular feature, 13 km along its longest (NW-facing) side and about 30 km in total extent (fig. 1.3). Its NW-facing side is relatively steep, and the plateau reaches its maximum height of over 105 m asl along this side. It is relatively flat-topped, with moderately sloping NE- and SSE-facing margins. The top of the plateau stands over 60 m above the surrounding clay plains. A few small areas of silty to sandy diamicton occur on the plateau (fig. 1.1a). Evidence of aeolian processes (dunes) have been identified on the plateau (Romaine, 1953; Lajoie and Stobbe, 1950). A much smaller accumulation of material forms a separate hill to the NW. It is separated from the main plateau by a meandering, misfit stream in a valley carved by a former Ottawa River channel. A large number of beach ridges can be seen on air photos along the margins of both features.

1.3.5 PALEOCURRENTS

Fig. 1.4 shows the results of 19 groups of paleocurrent measurements (for details see appendix 1). Pit-wide totals for linguoid ripples and trough crossbeds are indicated by the smaller rose diagrams. Vector strengths and means were calculated as outlined by Tucker (1982). The results show a 120° variation in vector means between pits, but strong vector strengths within pits, especially for the crossbeds. The latter may represent sample bias within large channels or an area of similar channel trends.

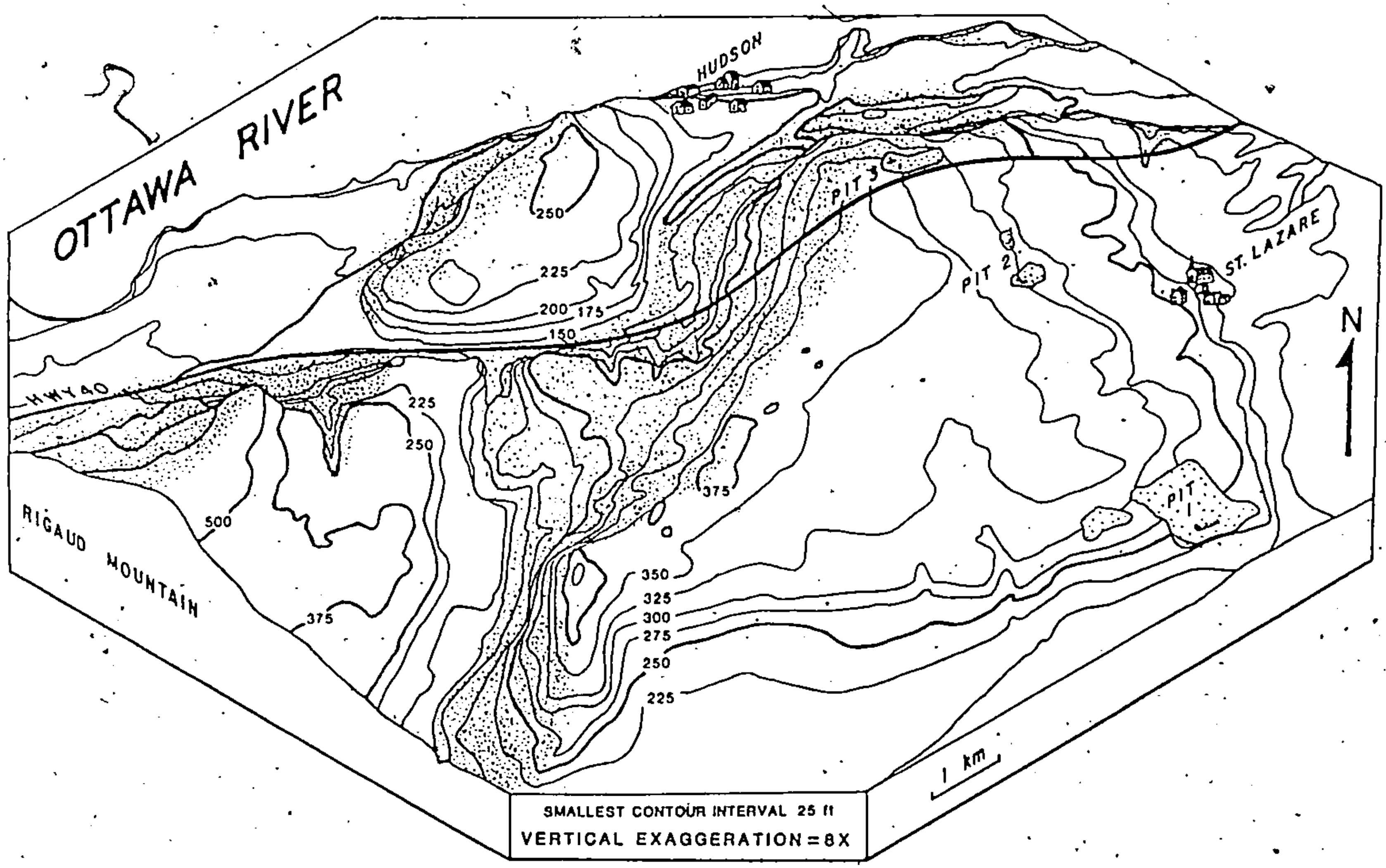

Fig. 1.3 Isometric contour diagram of St. Lazare plateau and part of Rigaud Mountain. 25ft = 7.6m.

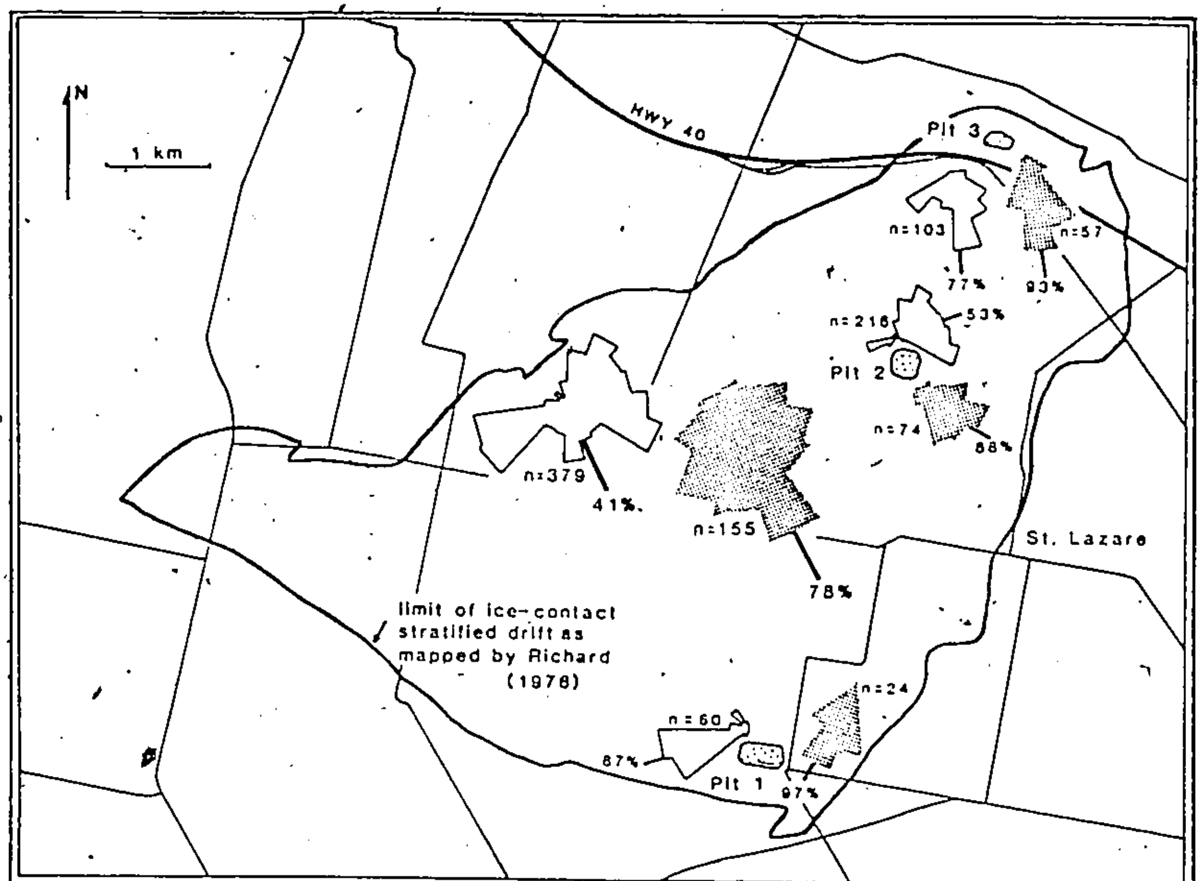

TROUGH CROSS-LAMINATION (RIPPLES)

TROUGH CROSSBEDS

Figure 1.4 Rose diagrams of paleocurrent measurements, St. Lazare plateau. Vector mean for each diagram indicated by radial line segment. n equals number of measurements. Data divided into 20° classes. Vector strength (degree of scattering about the mean) given in %. Vector strength of 100% means that all the measurements fall within a single class. Smaller diagrams are totals for each pit; the two large diagrams in the centre sum all the measurements. Statistics calculated as outlined by Tucker (1982).

The two larger rose diagrams represent the sum of all measurements within the two classes of current indicators. The vector means of these are remarkably similar, although the ripples give a much weaker vector strength (41%) compared with the crossbeds (78%). The diagram summing the ripple measurements for the entire plateau shows a strong bimodality, reflecting the naturally high variability of ripple directions. The overall paleocurrent trend is toward the SSE.

CHAPTER 2: SEDIMENTARY STRUCTURES AND ENVIRONMENTS

2.1 DESCRIPTIONS OF EXPOSURES

2.1.1 FACIES TYPES

The following is a description of the major facies types of the exposures in the three pits studied. (The pits in which each type occurs are indicated in brackets.)

<u>Facies 1</u>: Faintly stratified channel sands, exclusive to pit 1 (distal fan). Strata are 0.5 to 5 cm thick (mode 1.5 cm), straight, parallel, and subhorizontal except near the channel base, where they tend to follow the contours of the base. Most beds fine upward from well sorted medium to coarse sand (average 1.5 ∅, maximum 1 ∅), to well sorted fine sand (3.0 ∅ minimum). In some cases a lamina (average 2 mm thick) of 2.5 to 3.5 ∅ sand high in heavy mineral content separates each bed (fig. 2.1). A few strata are inversely to normally graded (2.5 ∅ to 1.5 ∅ to 2.5 ∅, for example), or massive and relatively coarse. In some cases, discontinous horizontal lamination is present within the beds. Erosional surfaces occur within the channels, cutting the underlying faint horizontal bedding at an angle. The bedding above the erosional surfaces tends to parallel the erosional surface itself, just as the bedding near the

COLOURED PICTURES
Images en couleur

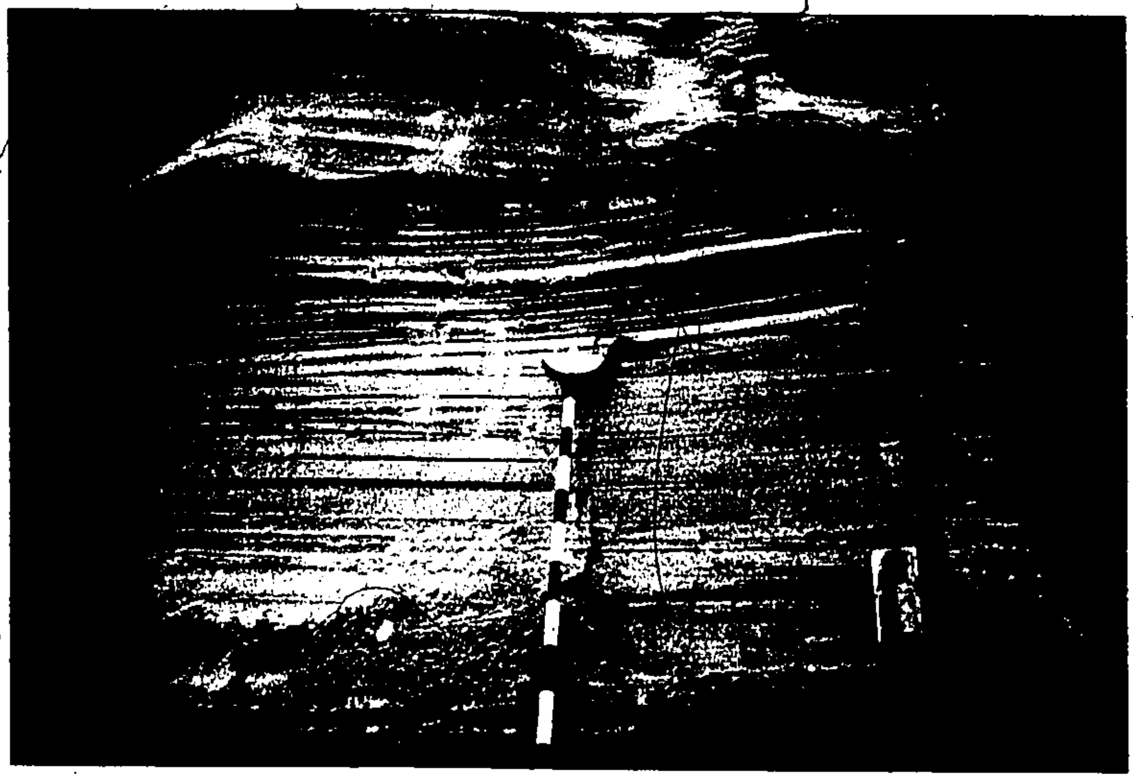

Figure 2.1 Facies 1 channel fill, consisting of medium sand. Bedding is faint, regular, even and parallel. Fine sand at the top of most of the beds has a high concentration of heavy minerals. Individual beds fine upward slightly. Scale in dm.

channel bases is subparallel to the channel floor (fig. 2.2). The sand within the lower 1-2 cm of many channels commonly coarsens upward by about 1 ∅ size grade, and where present this finer basal bed weathers out as a resistant layer helping to accentuate the channel base. This resistant layer usually defines the erosional contacts or reactivation surfaces within the channels. There is no overall grading within the channels.

Small amounts of pebble gravel occur along bedding surfaces at channel margins near the base of some channels, or scattered within the channel fill near channel base, and exhibit normal coarse-tail grading. In places angular rip-up clasts of micaceous clayey silt lie horizontally within the channel (fig. 2.3). Clayey rip-ups are evenly distributed throughout the channels in which they occur. The channels are notably asymmetric, and pebbles, where present, tend to be concentrated toward the steeper side (fig. 2.4).

The channels exposed in pit 1 trend towards the east and southeast, at an oblique angle to the general dip of the bedding and the paleocurrents measured outside the channels. Two channels had undergone sufficient differential wind erosion to enable their trends to be measured at 120° and 094°, which differs by 87° to 113° from the general trend of the crossbeds throughout the pit.

Figure 2.2 Channels filled with facies 1 sand cut into facies 3 beds. Note asymmetry of channels and reactivation surfaces within them. Bedding is subparallel to channel base. Bottom of lowest channel is 5m from top of section.

COLOURED PICTURES
Images en couleur

Figure 2.3 Facies 1 channel cut into facies 3 beds, face 1.1b. Ripped-up clasts of micaceous clayey silt lie horizontally within the channel. Scale in dm.

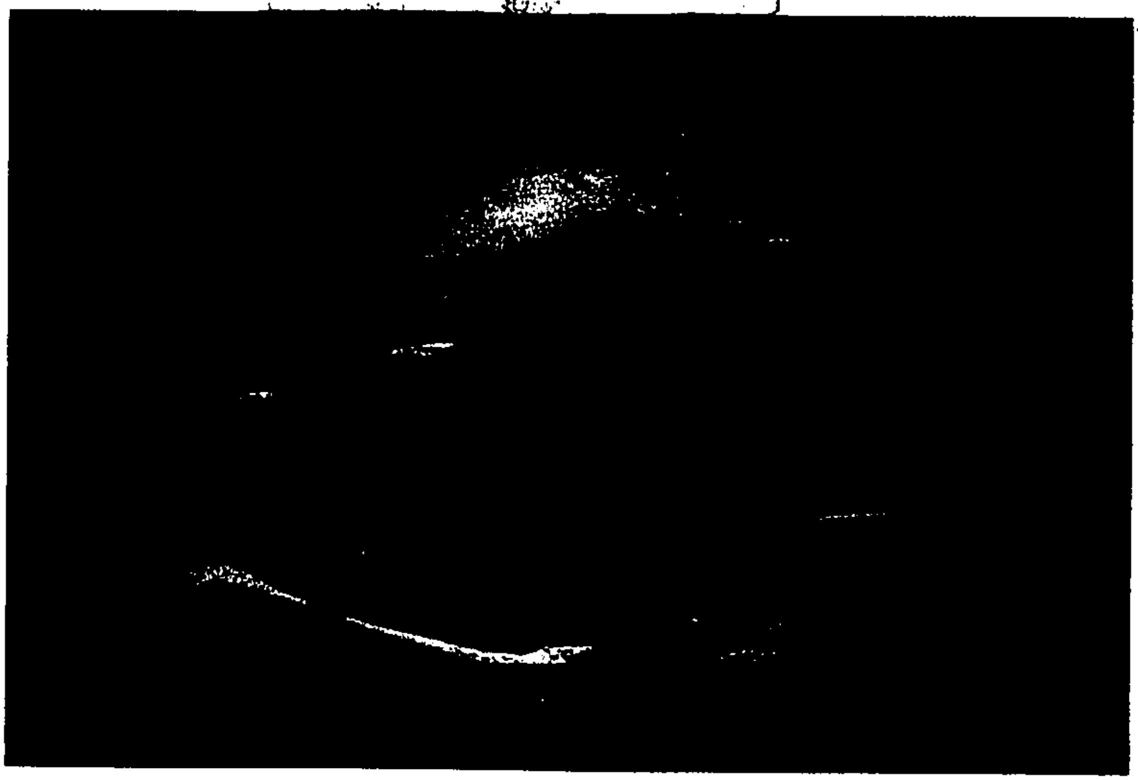

Figure 2.4 Base of facies 1, channel in facies 3 sediment, face 1.1b. Note asymmetry of channel, and concentration of pebbles near the steep side. The light colored layer of material at the base of the channel is an accumulation of loose, windblown sand. Field of view is approximately 2 m wide.

The maximum dip of the channel walls noted in face 1.1b was 70° (fig. 2.5). The channel margins can be smooth and evenly curved (figs. 2.3 and 2.5), but are more commonly irregular, sometimes forming concave steps, where reactivation has enlarged the channel. The bedding near the top of many of the channels is broadly convoluted (figs. 2.6 and 2.7). There are no trace fossils, but disarticulated bivalve shells are present in several channels (Face 1.1b).

<u>Facies 2</u>: Current rippled sand. Asymmetric climbing and non- climbing ripples in well sorted very fine to medium (4 Ø to 2 Ø) sand. This facies generally weathers more massively than facies 3. Silty flasers are common. No symmetric ripples were recorded in any section. (faces 1.1, 2.2, 2.5).

<u>Facies 3</u>: Alternating bed facies. This is a very variable facies characterized by a distinctive stepped (flaggy to slabby) appearance in weathered sections. It consists of alternating, laterally continuous 1 to 50 cm (mode 15 cm) beds of fine, fine to medium, medium, and rarely, coarse sand. The finer sand beds tend to be moderately sorted, bioturbated, and usually horizontally laminated, although ripple cross-lamination is common. The

COLOURED PICTURES
Images en couleur

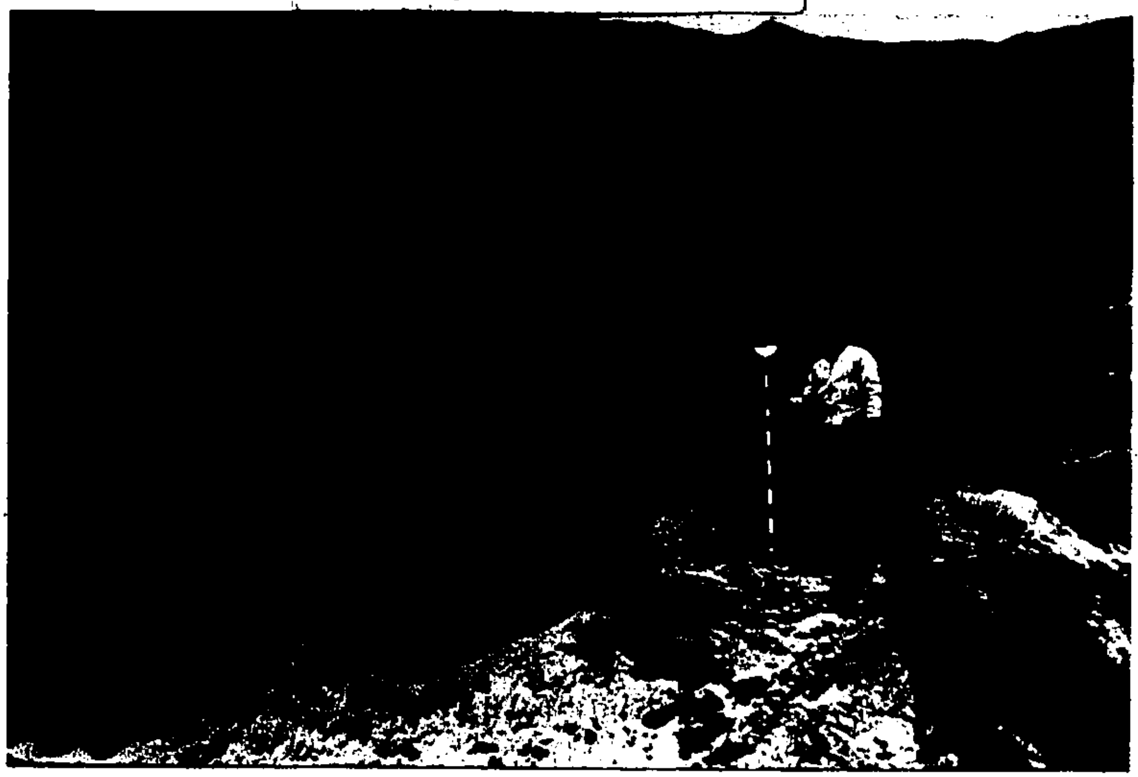

Figure 2.5 Steep-walled facies 1 channel, face 1.1b. Left wall dips at about 70°. Scale in dm.

COLOURED PICTURES
Images en couleur

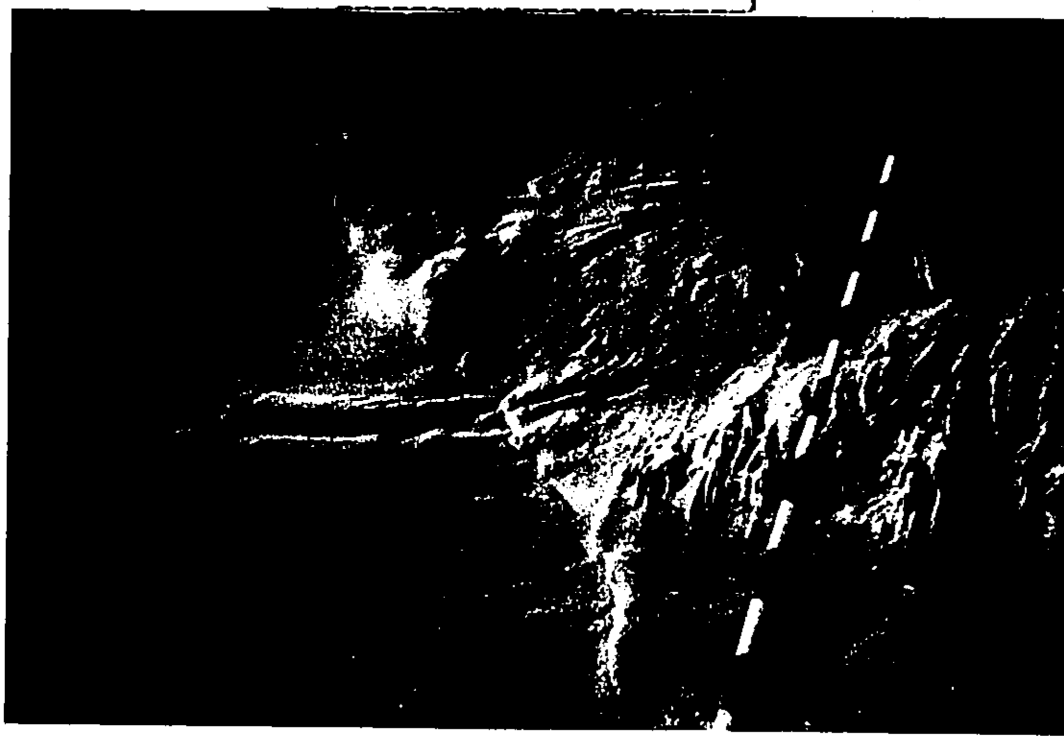

Figure 2.6 Broad convolutions at the top of facies 1 channel, face 1.1b. Scale in dm.

COLOURED PICTURES
Images en couleur

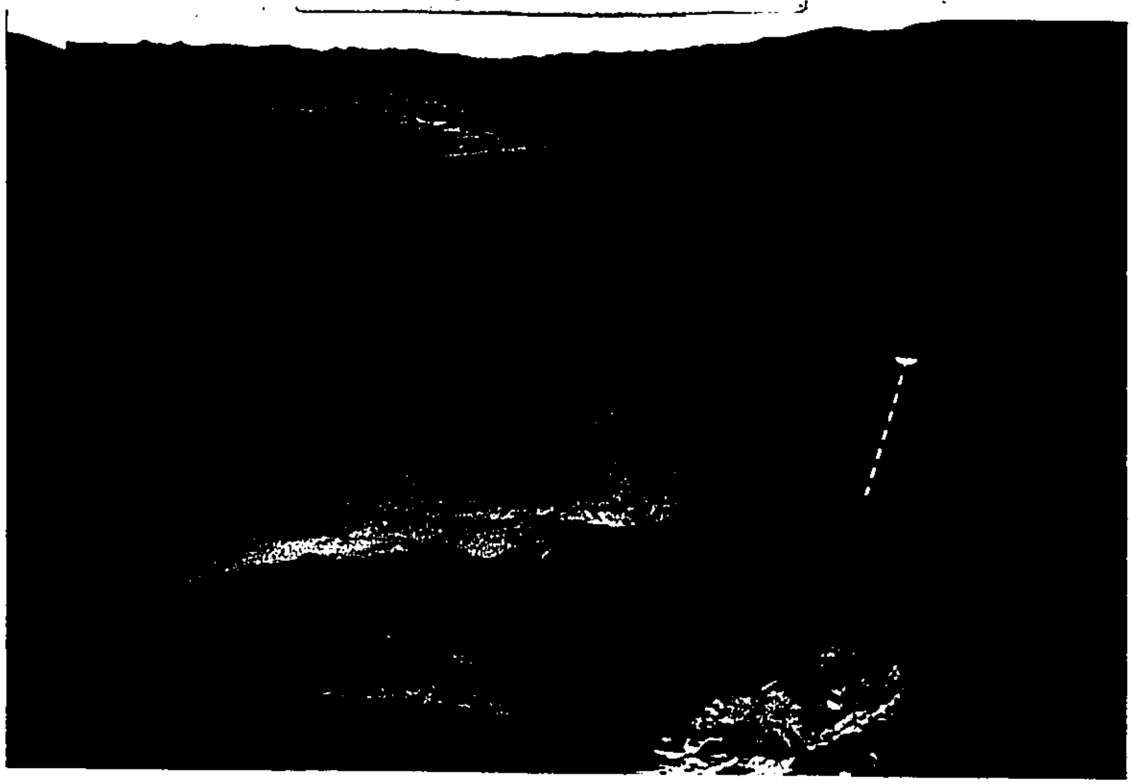

Figure 2.7 Convolutions at top of facies 1 channel fill, face 1.1b. Scale in dm.

silt content of the finer beds makes them cohesive and causes them to resist weathering. The medium grained sand beds are moderately to well sorted and rippled, or consist of very low angle cross-strata. The rare beds of coarse sand are moderately sorted and crossbedded. The medium and coarse beds are non-cohesive and recessive in weathered sections. Monocraterion burrows occur in the coarser beds, although they appear to have extended downwards from a superjacent bioturbated bed of fine sand (face 1.1). Individual beds of facies 3 can be traced laterally for over 100 m in face 1.1a. In face 1.1b, however, some facies 3 sediments appear to be confined within broad channels about 10-50 m wide. Facies 3 beds were observed to grade upwards into trough crossbedding of facies 4 at one locality (face 1.1b, November, 1984) (face 1.1).

Facies 4: Crossbedded sand facies. This facies consists of fine to coarse tabular or trough crossbedded sand. (face 2.5, 3.1, 3.2).

2.1.2 PIT NUMBER 1 (SABLIERE BARBE)

Pit number 1, the largest and most active borrow pit on the St. Lazare plateau, is located at the southeast edge of the fan (or stratified drift, as mapped by Richard, 1982). At the height of construction activity in the summer of 1983, two articulated loaders filled ten to fifteen large gravel trucks an hour. From the beginning of field work in 1983 until present, only one face has been actively worked (face 1.1b). In 1983, this face had a maximum height of 13 m, but since then the height of the exposure has decreased by about one third (as of November, 1984), due to groundwater problems. This is because the depth to the impermeable diamict and to bedrock decreases in that direction, as shown by the bedrock contours. Artesian pressure keeps spring water flowing over the floor of the pit towards the southeast. A spring-fed stream flows constantly along the northern boundary of the property, by the base of face 1.2.

Face 1.1

Face 1.1 consists of two parts, face 1.1a, which is a straight section trending east-west, facing north; and face 1.1b, a continuation of face 1.1a, arcuate in shape, facing east (fig. 2.8). Face 1.1b is the actively worked face of Sablière Barbe; face 1.1a is inactive and badly slumped for the most part. See fig. 2.8 for location map of exposures.

Face 1.1a

Face 1.1a consists predominantly of subhorizontally

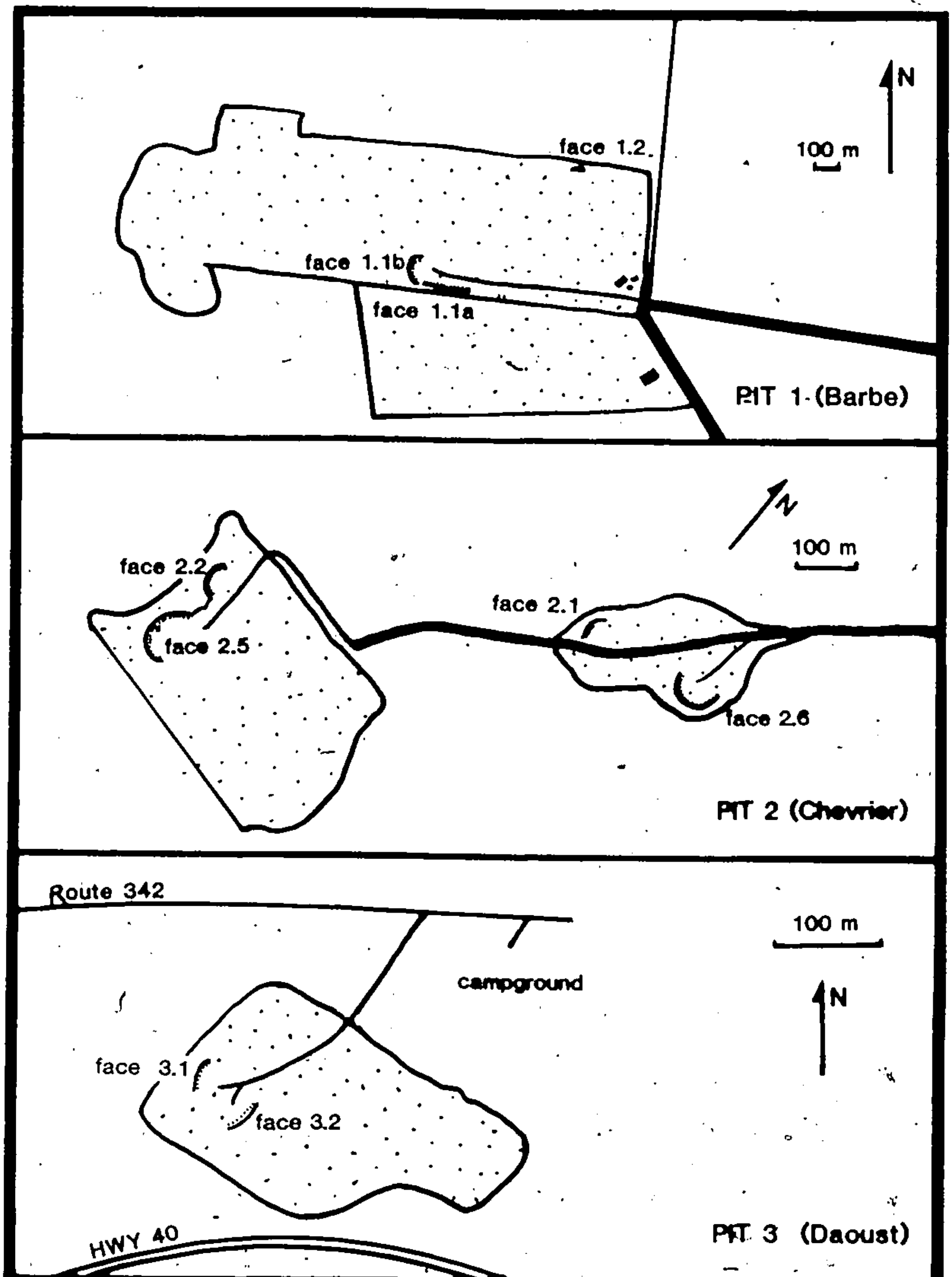

Fig. 2.8 Location and orientation of subcrop faces within the borrow pits on the St. Lazare plateau. Heavy lines are permanent roads located on fig. 1.1a.

bedded moderately to well sorted angular to rounded (mode = subrounded) buff colored fine to medium sand of facies 3 (see composite section, fig. 2.9, and detailed sections, figs. 2.10 and 2.11).

The lowest unit exposed consists of well sorted fine sand, very faintly horizontally stratified (facies 1). Above this unit, at the east end of the measured section (fig. 2.10) is more than a metre of low angle type B climbing ripples in fine sand (facies 2).

A 70 cm unit of horizontally stratified fine sand and an 80 cm coset of tabular crossbedded medium sand overlies this. Within this unit at 2 m along the section (fig. 2.9) occurs a large (>1m) subangular boulder. The uppermost 5 m of sediment at this location consists of facies 3 sediment - irregularly alternating 5 to 20 cm beds of bioturbated, horizontally laminated or, rarely, rippled (non-climbing) moderately sorted fine sand, and burrowed, rippled (non-climbing) well sorted fine sand. The burrows are <u>Monocraterion</u> (see section 2.2, below). The finer beds are generally horizontally laminated, poorly sorted and more cohesive due to the presence of silt. They are prominent in weathered sections, and highly bioturbated, which completely obscures the bedding in places. <u>Monocraterion</u> burrows can be identified in less highly disturbed parts of these units.

These facies 3 strata are generally continuous laterally through the length of the section (140 m), except where

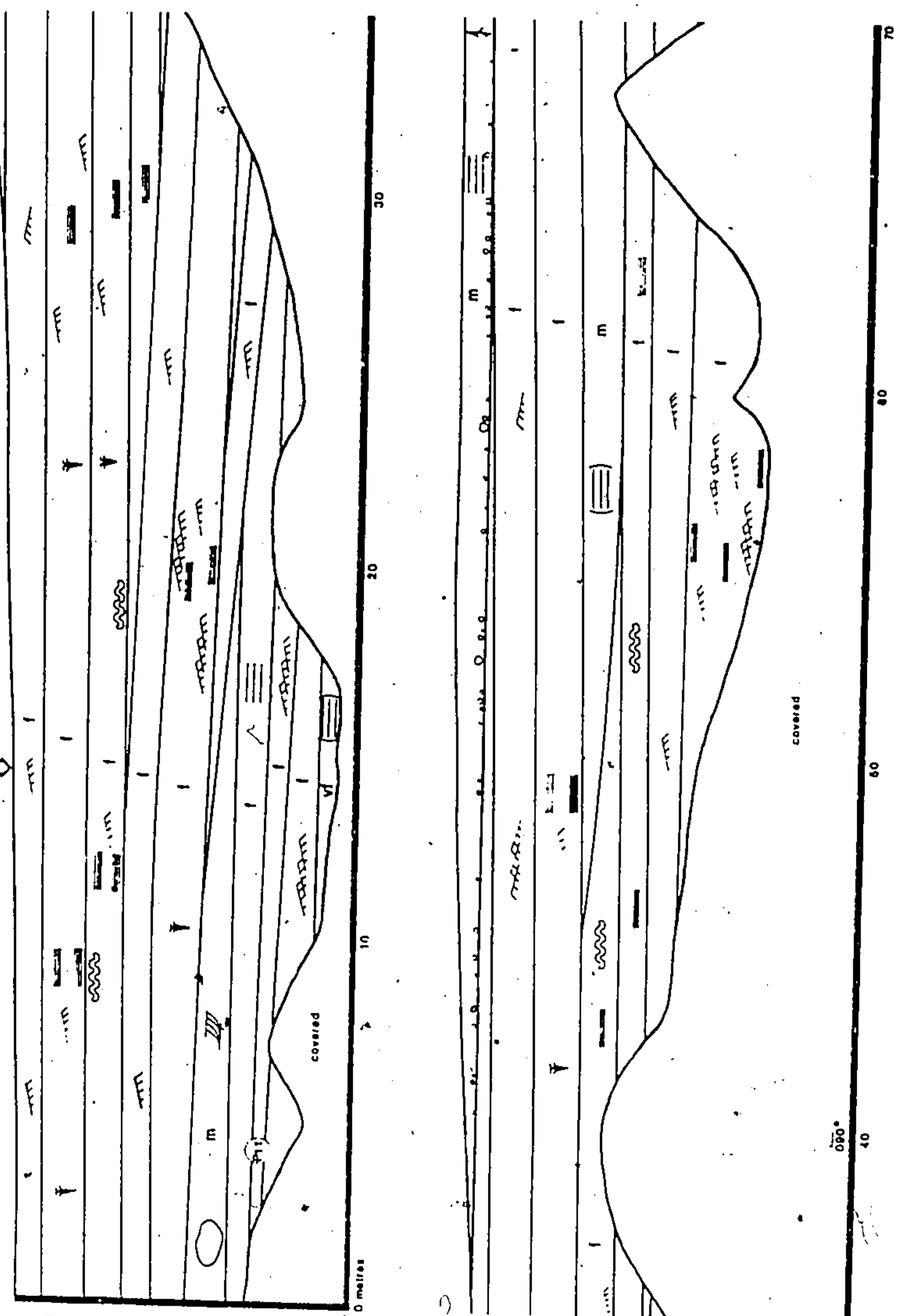

FIGURE 2.9 face 1.1a (Barbe pit), July, 1983 fig. 2.10

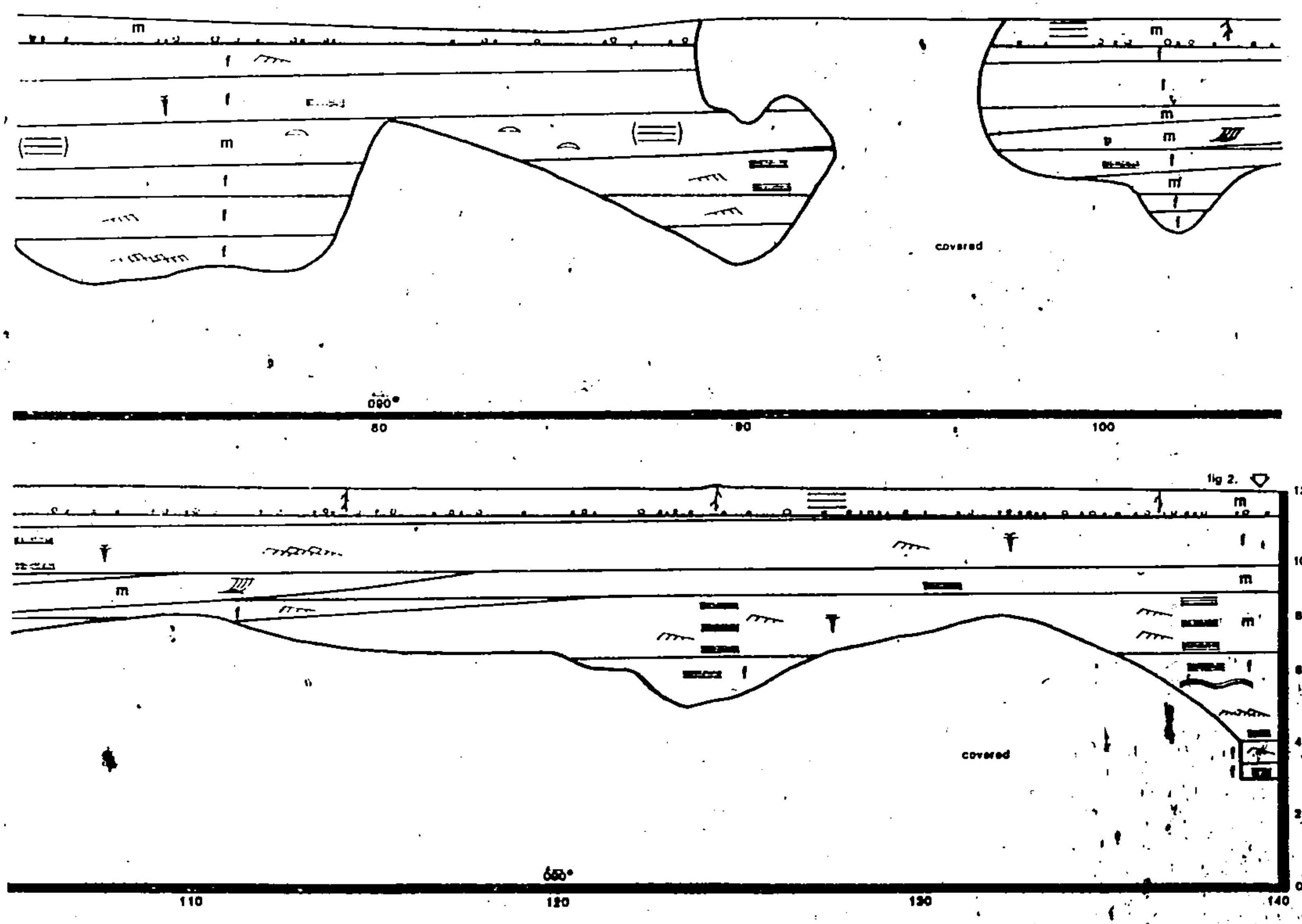

Fig. 2.9 continued

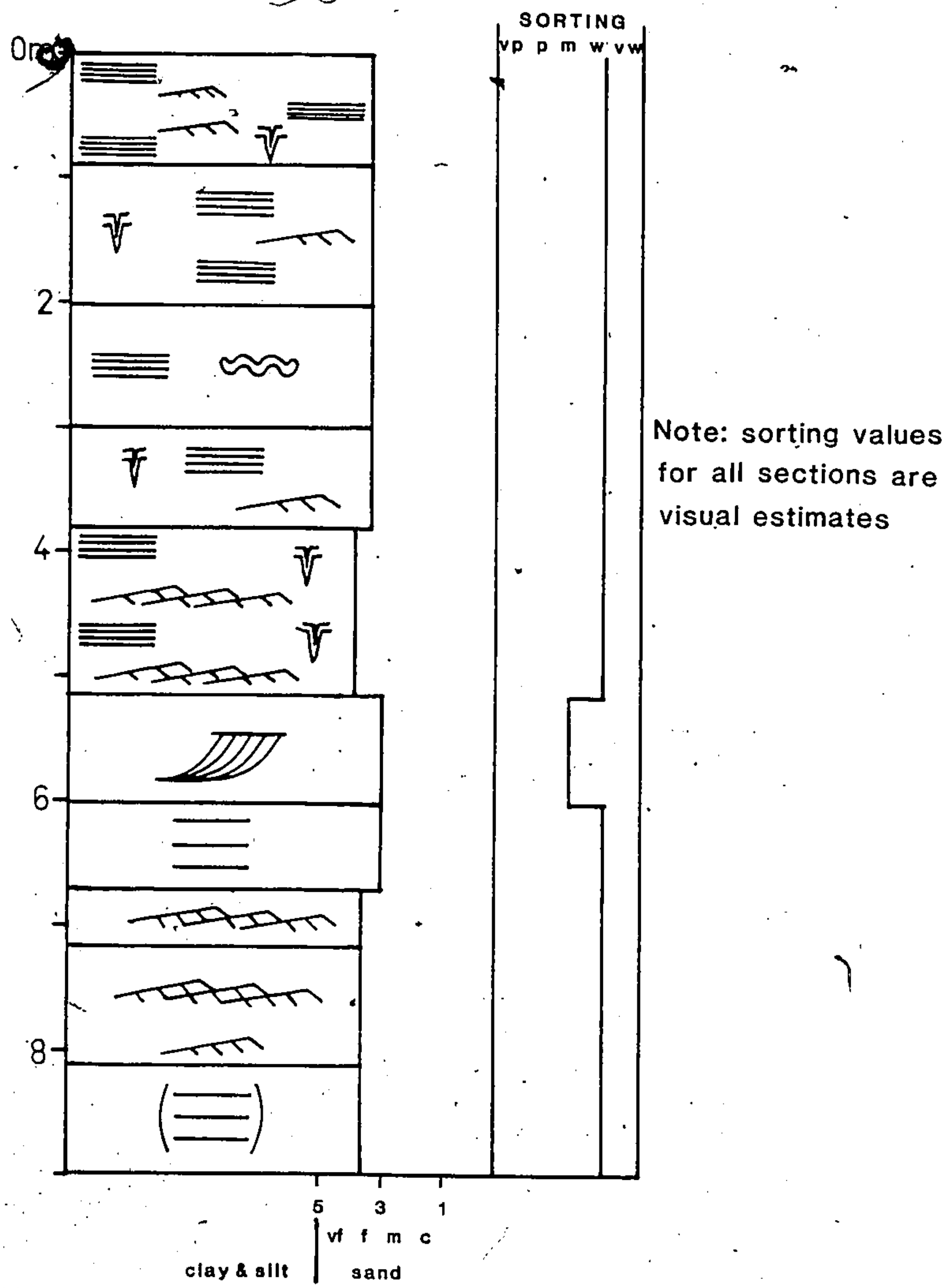

FIGURE 2.10 FACE 1.1a, EAST END

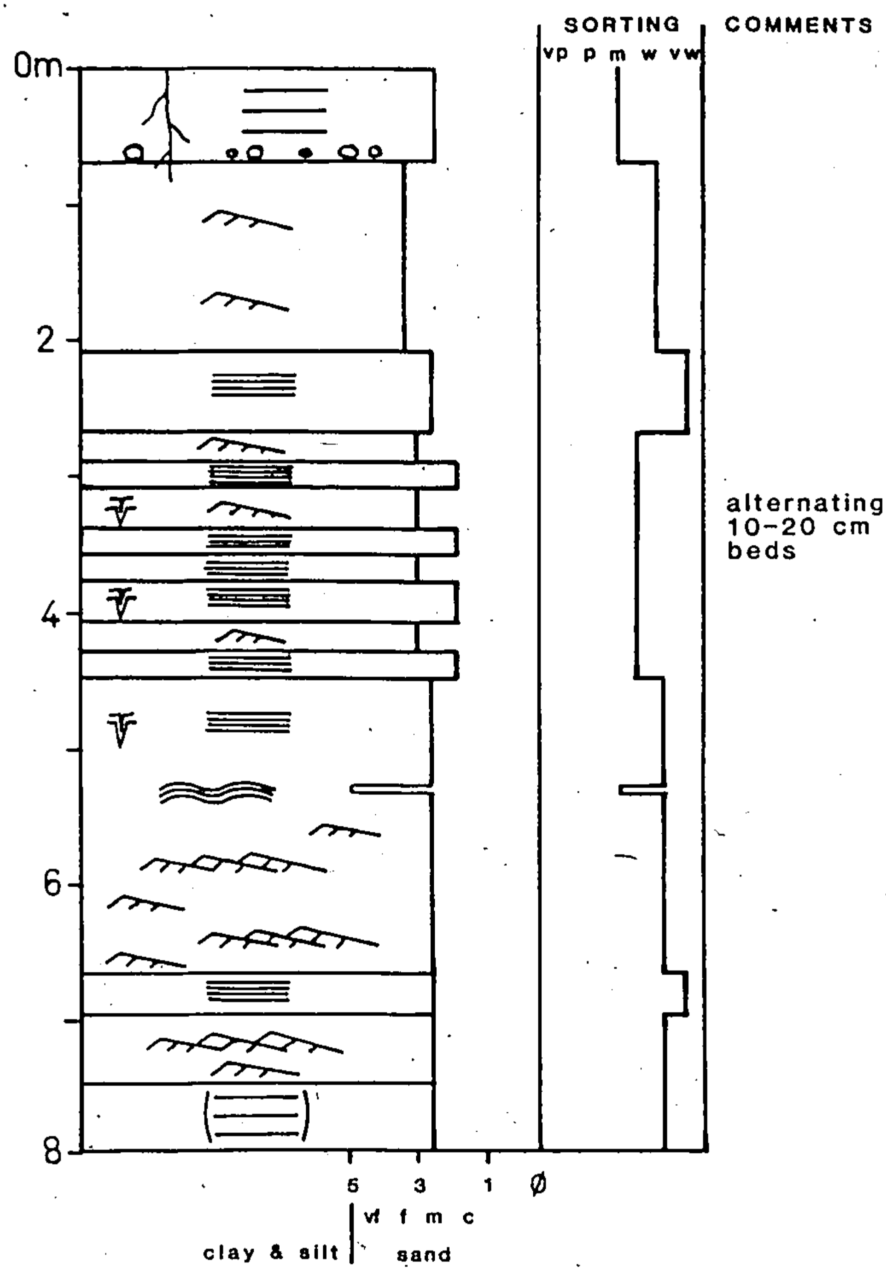

FIGURE 2.11 FACE 1.1a, WEST END

channels are incised into them (composite section, fig. 2.9). The channels, which are more predominant in face 1.1b, are filled with facies 1 sand (well sorted, with a regular, faint horizontal bedding on the scale of 1-3 cm). Isolated disarticulated shells of Macoma balthica and Hiatella arctica were found within several channels. The overall dip of the beds is about 10° towards the SSW. Figs. 2.12 and 2.13 show a representive section of facies 3 beds from the west end of face 1.1a.

The west end of face 1.1a (detailed section, fig. 2.11) is generally similar to the east end. At 5.5 m depth in the section there is a 5 cm thick bed of draped lamination (Gustavson et al, 1975) consisting of silt and fine sand. This bed is continuous for at least 10 m along the section. At 0.7 m depth in the section, there is a pebble lag above a straight, horizontal erosional contact continuous for 100 m along the face. The medium sand above this contact is moderately sorted, orange coloured, and horizontally bedded. Modern plant roots disturb the upper half metre of section.

Face 1.1b

The measured part of face 1.1b begins about 50 m west of the western end of face 1.1a. Face 1.1b is arcuate, as are most actively worked faces, and its strike changes from 275° to 110° along its length (composite section, fig. 2.14, and

COLOURED PICTURES
Images en couleur

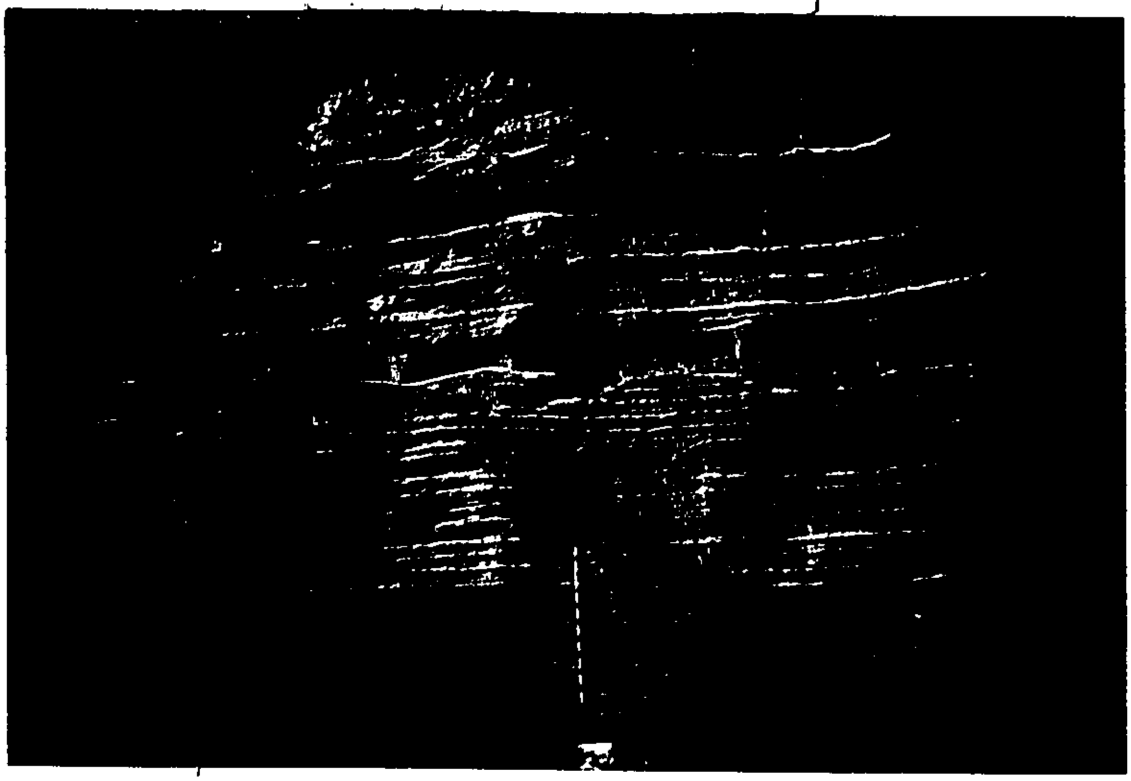

Figure 2.12 Facies 3 beds at west end of face 1.1a. Beds of poorly sorted silty fine sand (prominent units) alternate with moderately sorted medium sand (recessive units). Average thickness of a pair of adjacent units is 30 cm (maximum 110 cm). Beds are laterally continuous (up to 100 m or more). Scale in dm.

COLOURED PICTURES
Images en couleur

Figure 2.13 Close-up of lower part of figure 2.12. Note Monocraterion burrows extending downwards from bottom of finer beds and bioturbation of finer (darker) beds. Coarser beds (lighter) are horizontally laminated or rippled. (Pattern on weathered surface of finer bed to the right of the 9 dm mark on rod is wind adhesion ripples formed since the last rain.)

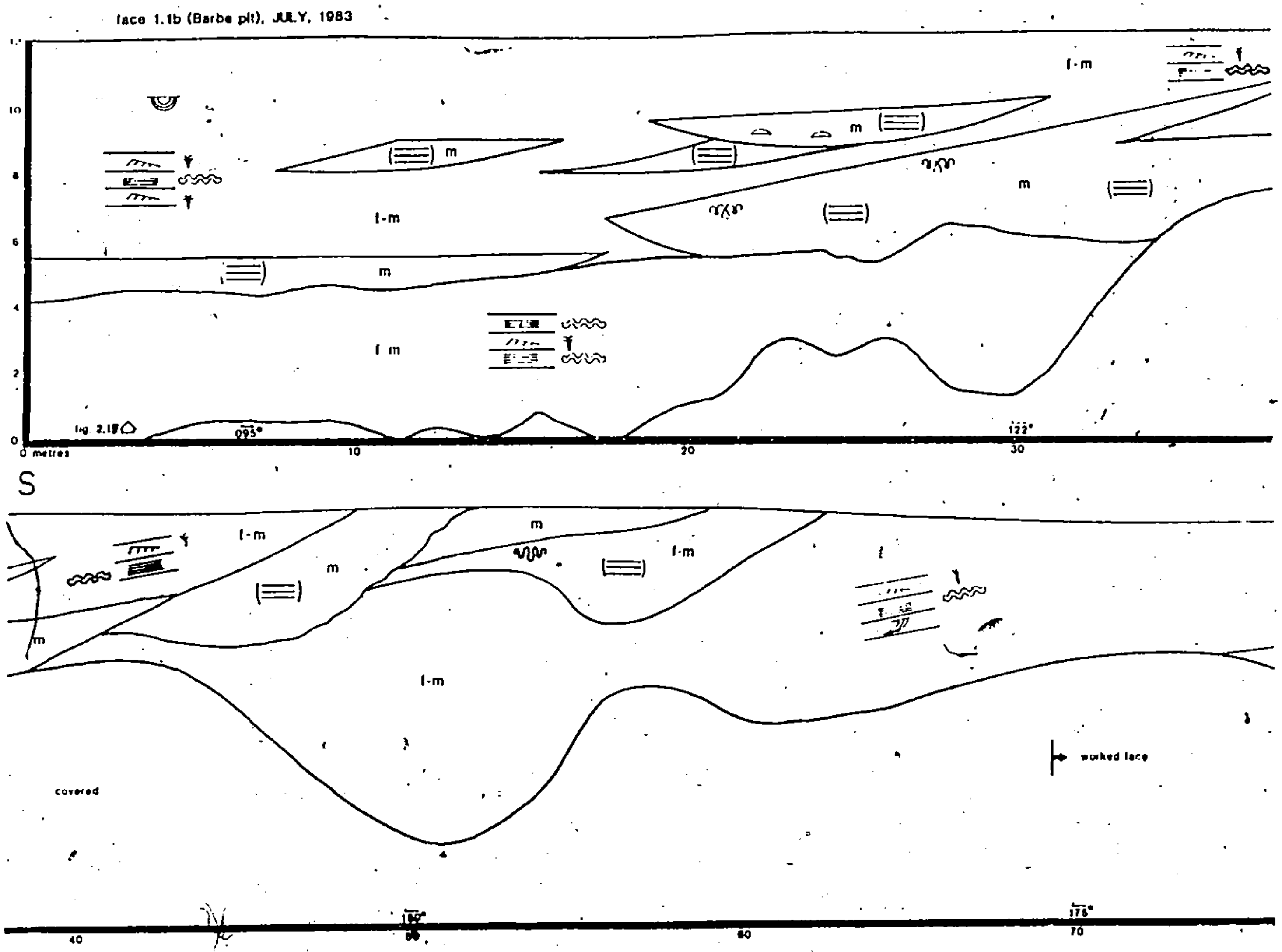

Fig.2.14. See Appendix A for explanation of symbols.

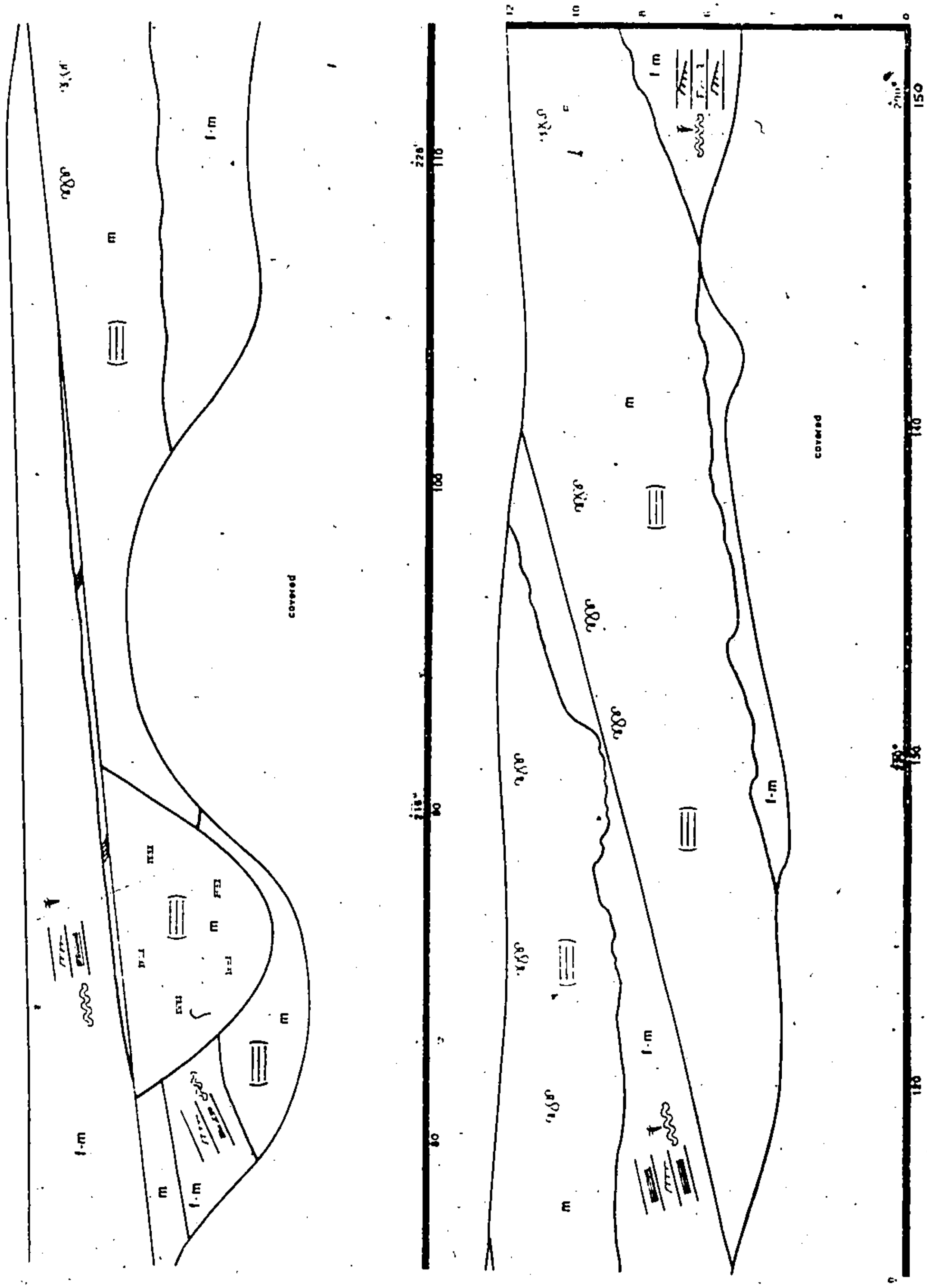

Fig. 2.14 continued

detailed section, fig. 2.15).

Channel fill, or facies 1 sediments, made up half of the sediments exposed in face 1.1b in July, 1983, when the section was first examined. The other half of the face consisted of sediments of facies 3 (alternating thin beds of fine, horizontally or cross laminated sand, and fine to medium, medium, or medium to coarse cross laminated or crossbedded sand). The fine sand beds are heavily bioturbated, and burrows of Monocraterion are common in the subjacent medium or coarse sand beds. The dip of these beds is also about 10° towards the SSW.

Face 1.2

Face 1.2 is located at the northeastern corner of Sablière Barbe. It is extensively slumped and much digging is required to expose a section (fig. 2.16). 3.3 m of massive to faintly stratified medium gray diamicton is accessible at face 1.2 in a drainage ditch along the northern boundary of the pit. The diamicton has a matrix of very poorly sorted clay to coarse sand and granules (mode = fine to medium sand). A framework of pebbles to boulders makes up not more than 2 % of the diamicton. A lag of boulders eroded from the diamict by the small drainage stream at the base of the section shows that blue-gray dolostone makes up a large part of the framework component (>30%), probably derived from the March

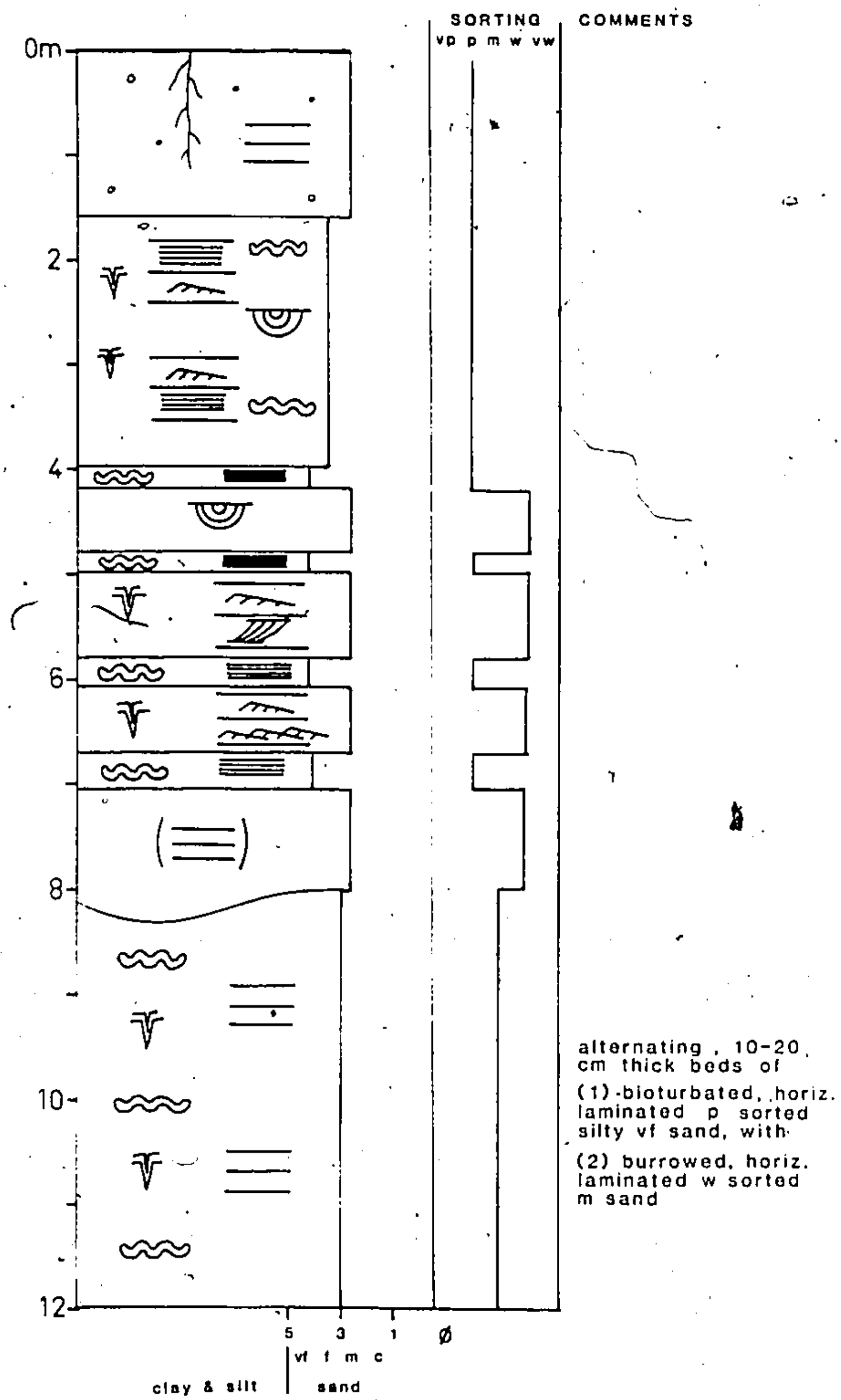

FIGURE 2.15 FACE 1.1b, SOUTH END

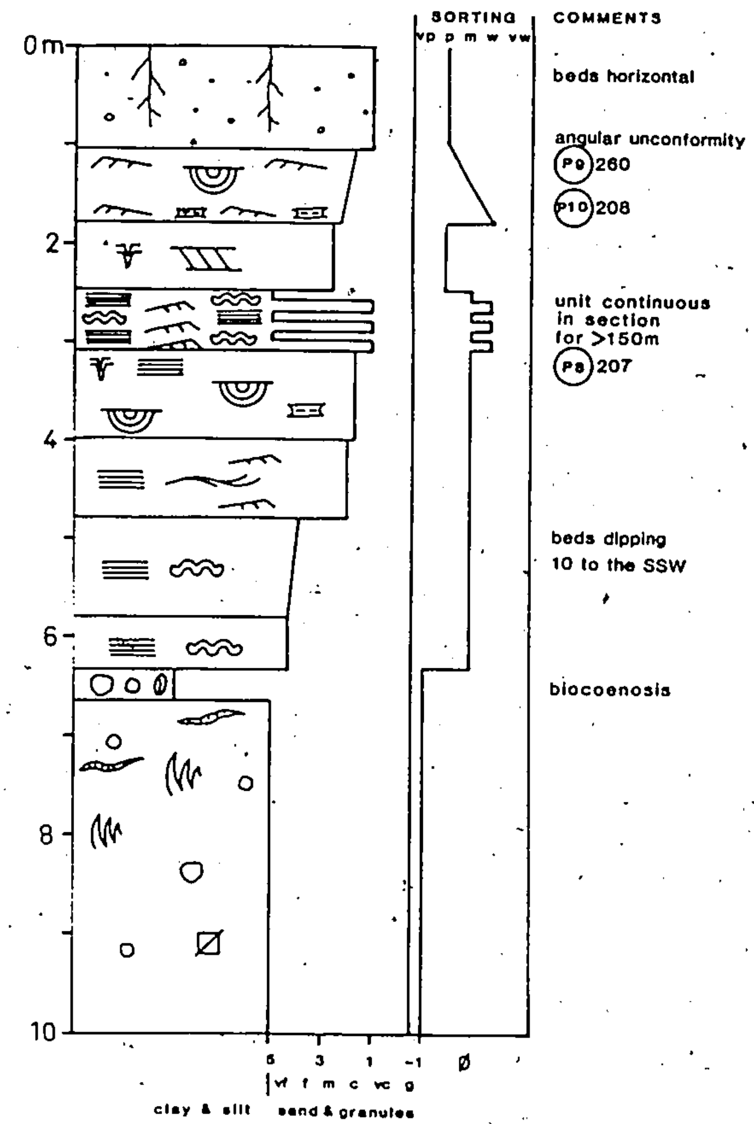

FIGURE 2.16 FACE 1.2

and Oxford Formations, which outcrop north of the study area, between the Ottawa River and the Precambrian rocks of the Laurentian Highlands. Gneissic or meta-igneous and other Grenvillian metamorphic rocks constitute the rest. Many of the dolostone boulders are faceted, and most are striated. Wisps and irregular lenses of fine sand are scattered throughout the diamicton. The upper metre and a half of the diamicton consists of contorted laminations of clayey, silty sand and scattered boulders and pebbles (fig. 2.17). This unit was exposed in the centre of pit 1, near face 1.1b, less than a metre below the pit floor in a drainage ditch dug in the spring of 1985.

A 30 cm bed of massive clay diamicton containing scattered pebbles and boulders overlies the sandy diamicton. Within the clay are isolated pockets and lenses of bivalves in growth position. A diverse assemblage of macrofossils is also found in the clay. This boulder clay is also present above the diamicton in the ditch near face 1.1b.

Above the upper diamicton occurs 3.5 m of coarsening upward horizontally laminated to cross bedded very fine to medium sand, with abundant <u>Monocraterion</u> burrows. Overlying this unit is 1 m of alternating beds of fine and coarse sand (facies 3), also burrowed. The upper 2.5 m of the section is composed of coarsening upwards planar and trough cross bedded medium to coarse sand, the upper metre consisting of orange, poorly sorted coarse pebbly sand.

COLOURED PICTURES
Images en couleur

Figure 2.17 Sandy pebble- and boulder-poor diamicton at face 1.2. Note contortion of wispy lamination. Scale in dm.

2.1.2 PIT NUMBER 2 (CHEVRIER PIT)

Chevrier pit is located towards the northeast corner of the area of stratified drift mapped by Richard (1982) (fig. 1.1a). It is owned and operated by Gerard Chevrier, assisted by his young sons. Material was being steadily removed from face 2.5, and several other faces were being sporadically worked throughout the summers of 1983 and 1984 (fig. 2.8).

Face 2.2

See fig. 2.18 for composite section of face 2.2, and figs. 2.19 and 2.20 for detailed stratigraphic sections. Face 2.2 consists primarily of climbing and non-climbing ripples in well sorted fine buff-coloured sand (facies 2). The climbing ripples are predominately of type B (Jopling and Walker, 1968). Paleocurrents measured within the rippled beds yield highly variable directions, with a combined (pit-wide) vector mean of 53% towards the ESE. Two or three per cent of the facies 2 sediment in face 2.2 are type A climbing ripples (fig. 2.21). Several thin beds of draped lamination occur within the rippled sediments (fig. 2.22). Near the bottom of the section at the southern (left) end, horizontal lamination grades upward into non-climbing ripples (fig. 2.23). Interspersed within the facies 2 sands are medium thick beds

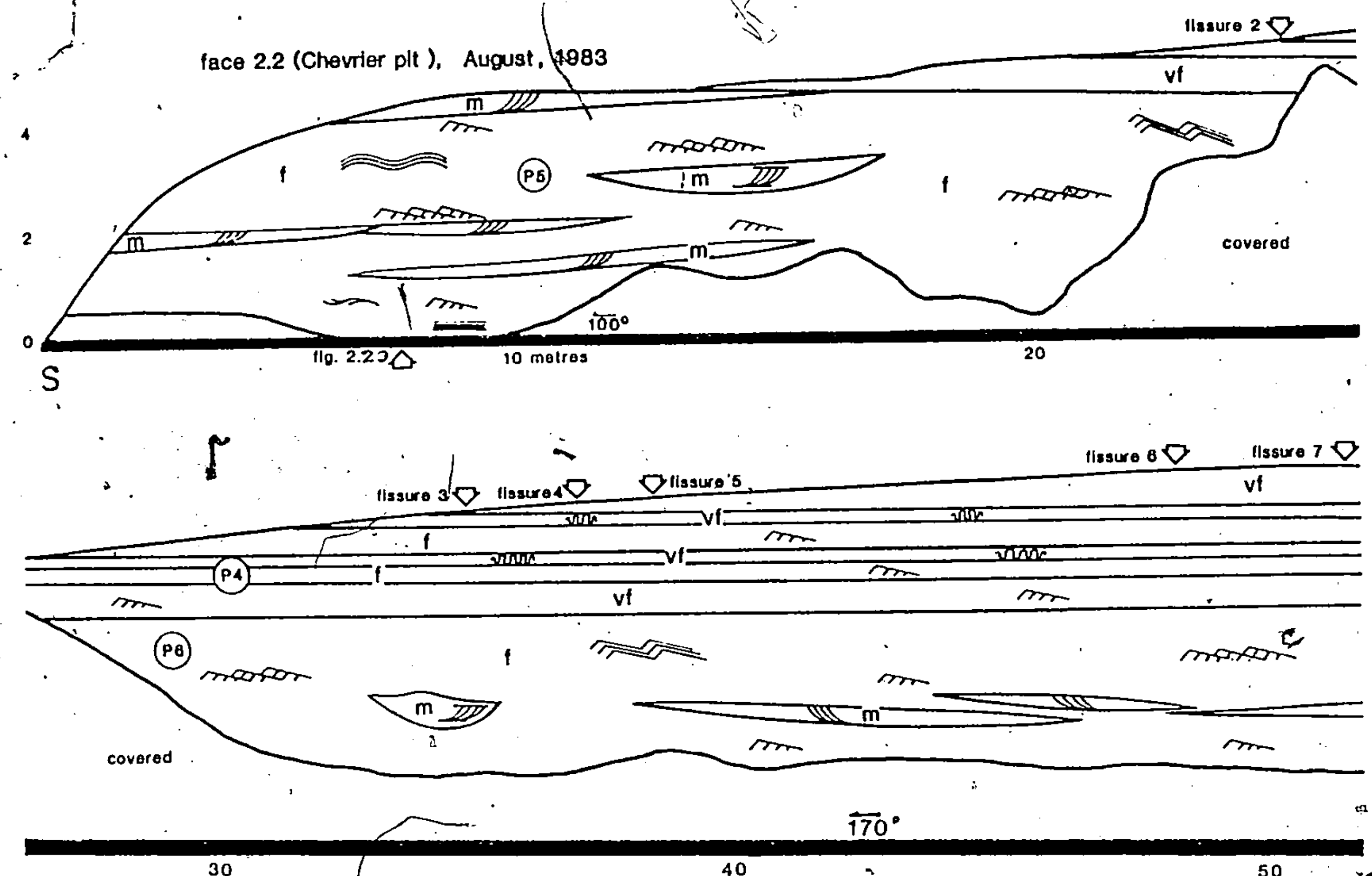

Fig. 2.18. See Appendix A for explanation of symbols.

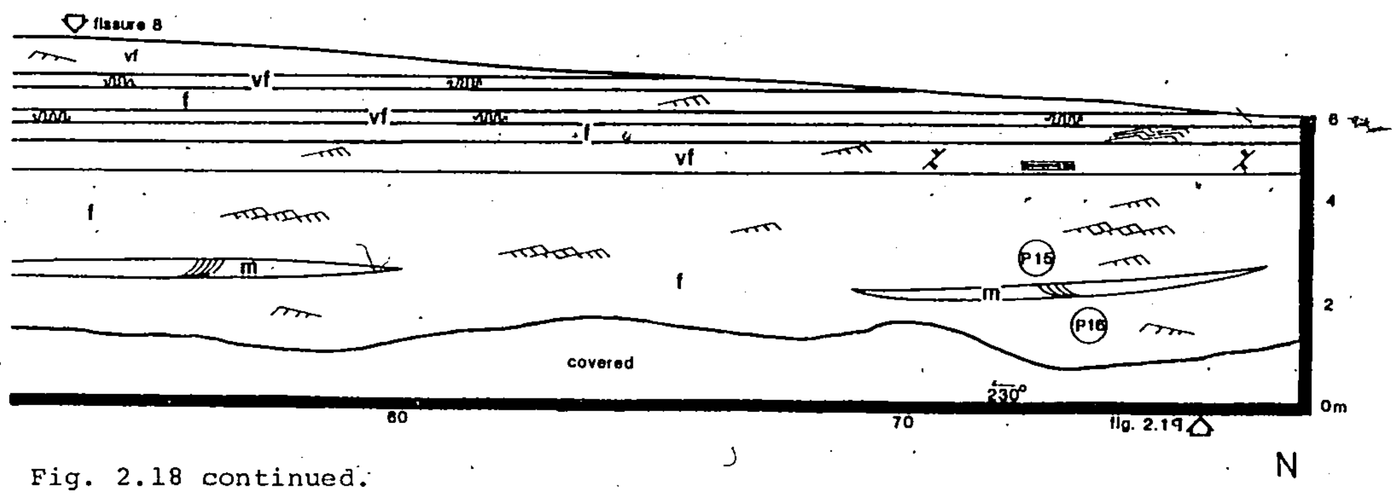

Fig. 2.18 continued.

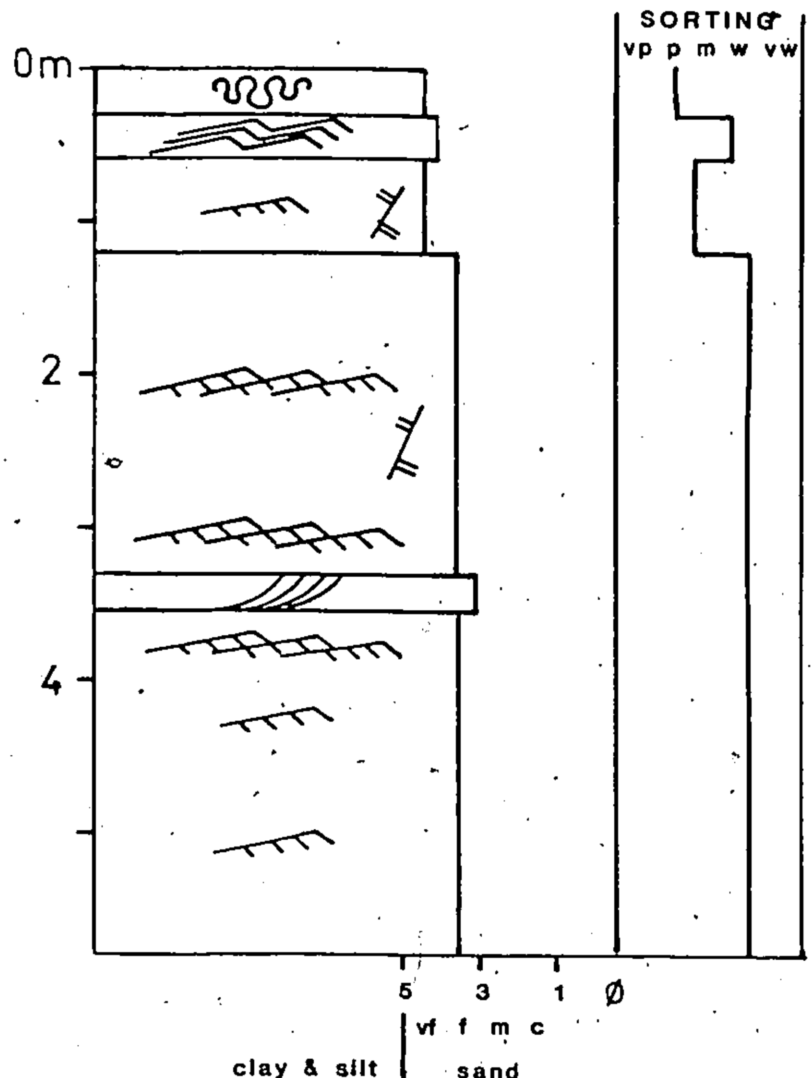

FIGURE 2.19 FACE 2.2, NORTH END

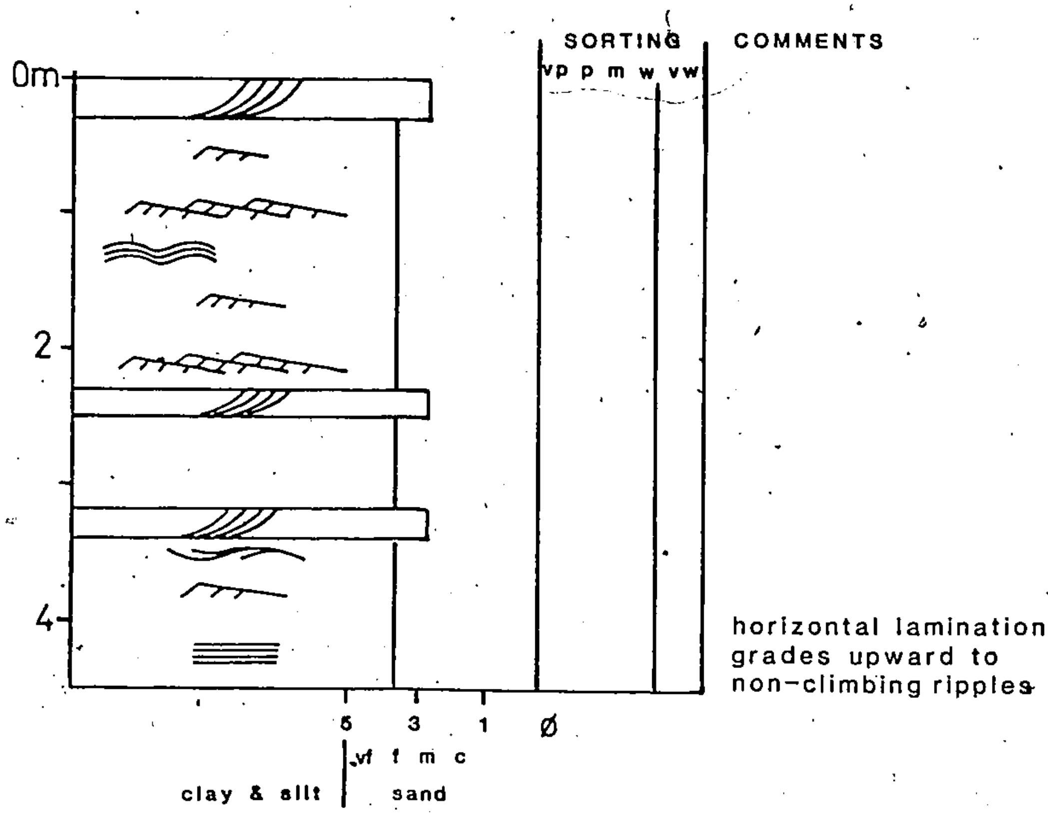

FIGURE 2.20 FACE 2.2, SOUTH END

COLOURED PICTURES
Images en couleur

Figure 2.21 Type A climbing ripples, face 2.5. The ripple foresets have been oversteepened by current shear. Knife handle 8 cm long.

COLOURED PICTURES
Images en couleur

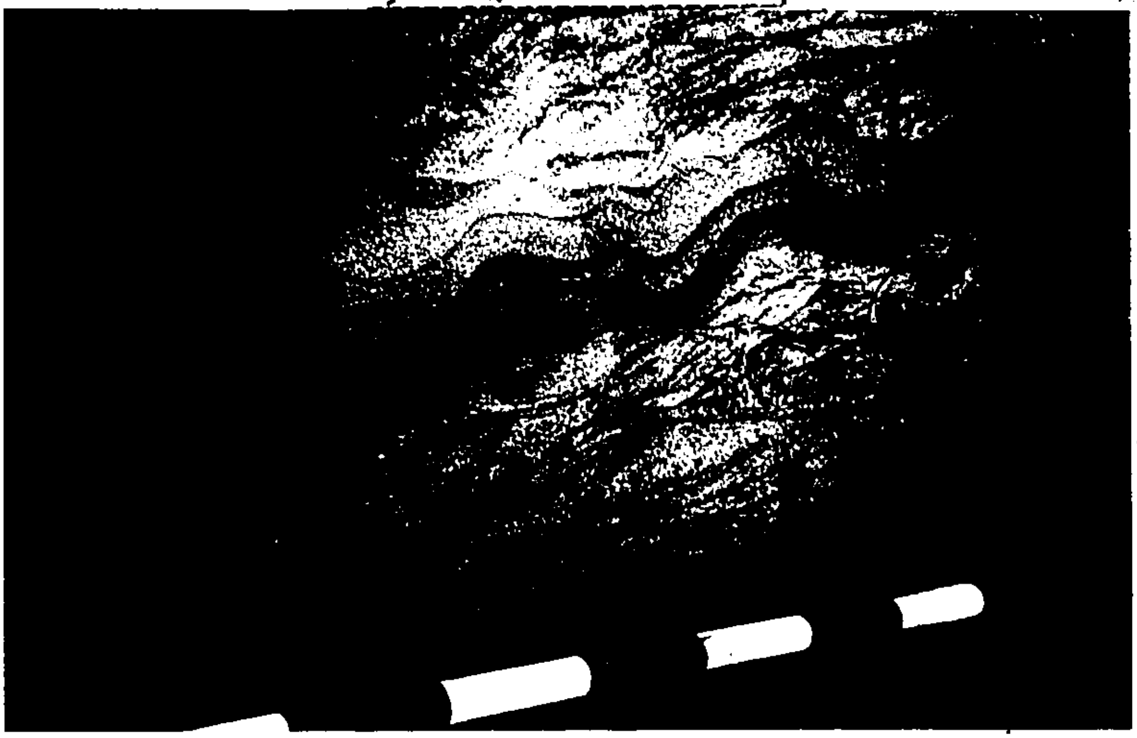

Figure 2.22 Draped bedding, face 2.2. (Thin ferruginous bands follow the bedding). Scale in dm.

COLOURED PICTURES
Images en couleur

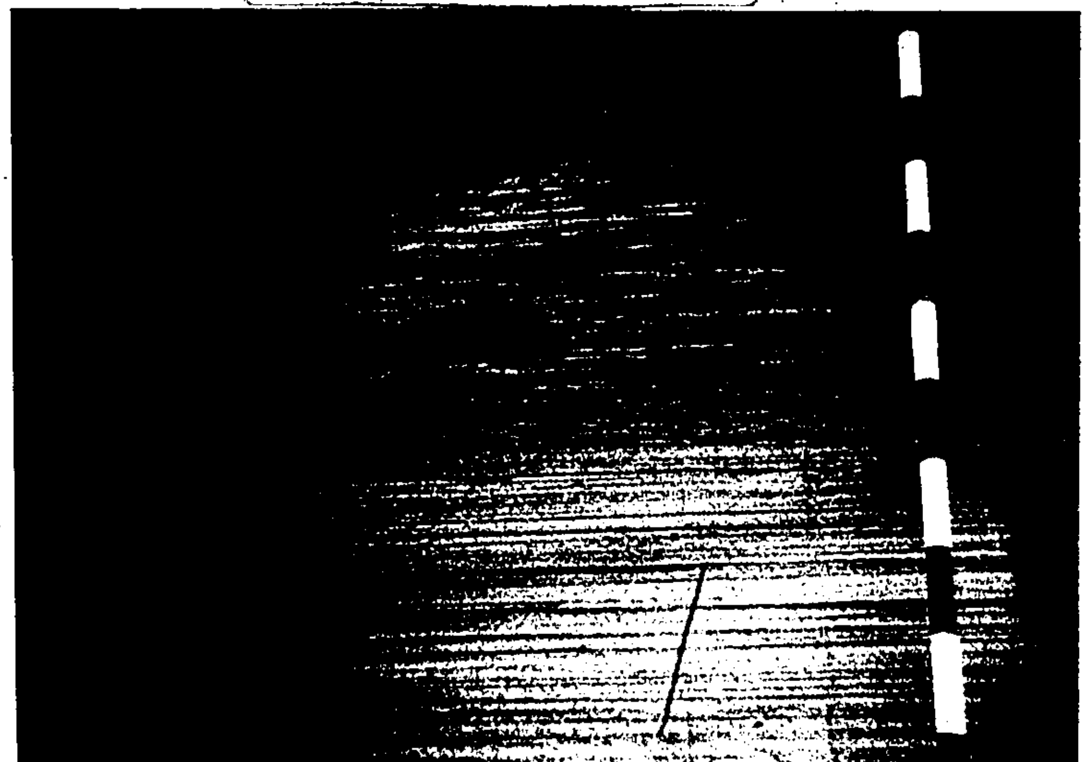

Figure 2.23 Upper flow regime plane lamination grading upward to non-climbing ripples, indicating waning flow. Scale in dm.

of medium grained planar and trough cross-stratified sand.

Above the facies 2 sediments are thin, laterally continuous beds of moderately to poorly sorted silty fine and very fine sand, with horizontal and ripple laminations. These beds are dipping at about 3° towards the east. Flaser-like drapes of clayey silt are present in non-climbing ripples (fig. 2.24). These clay drapes are not exactly as defined by Reineck and Wunderlich (1968), rather they tend to be more prominent along ripple foresets, but they do indicate periods of low or nil traction current activity (suspension sedimentation). Two laterally continuous convoluted beds occur above this (fig. 2.25). Small high angle reverse faults with an average offset of a few cm are present throughout face 2.2.

Face 2.5

See fig. 2.26 for composite section of face 2.5, and figs. 2.27 and 2.28 for detailed stratigraphic sections. At the north end of face 2.5 occur discontinuous, lens-like medium thick beds of trough and planar crossbedded medium sand, well sorted rippled fine sand, and poorly sorted silty very fine sand. The silty beds stand out prominently in weathered sections. The contacts between most of the beds are erosional, and the lens-like form of the beds appears to be due to the superposition of a number of shallow channels. A

COLOURED PICTURES
Images en couleur

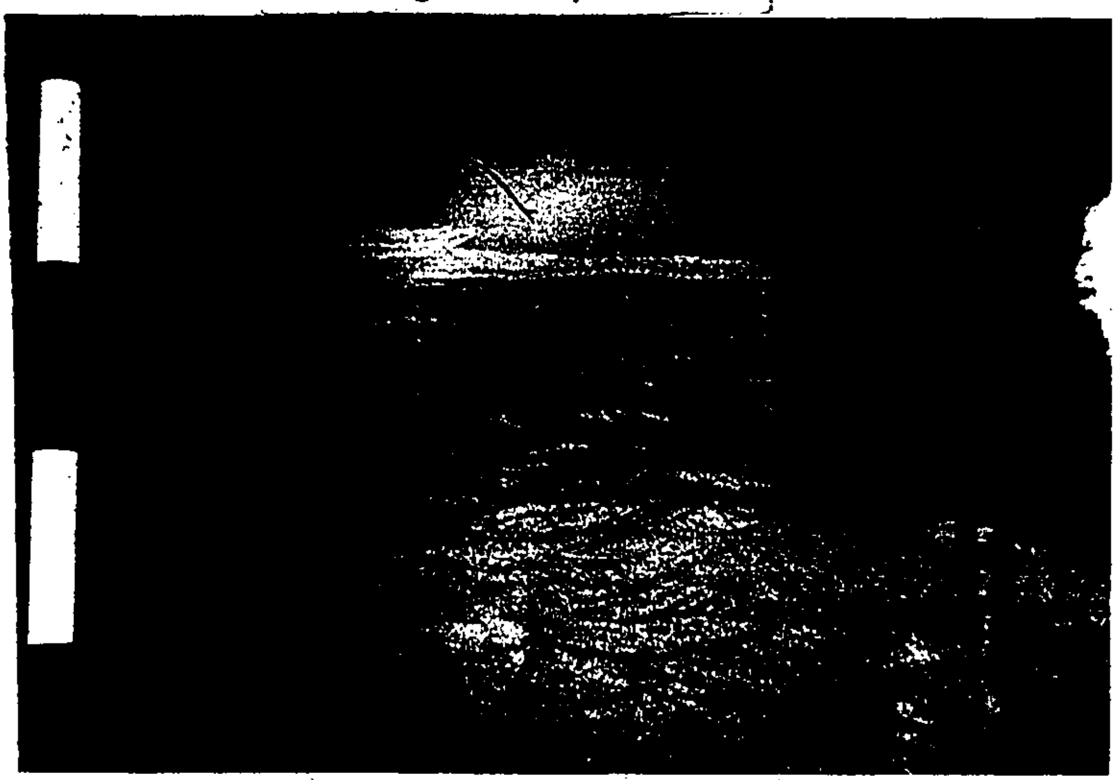

Figure 2.24 12 cm thick bed of rippled fine sand with silty flaser-like drapes. Scale in dm.

Figure 2.25 Convoluted bed at face 2.2. Laterally continuous for >50m. Note sharp upper contact truncating convolutions. Scale in dm.

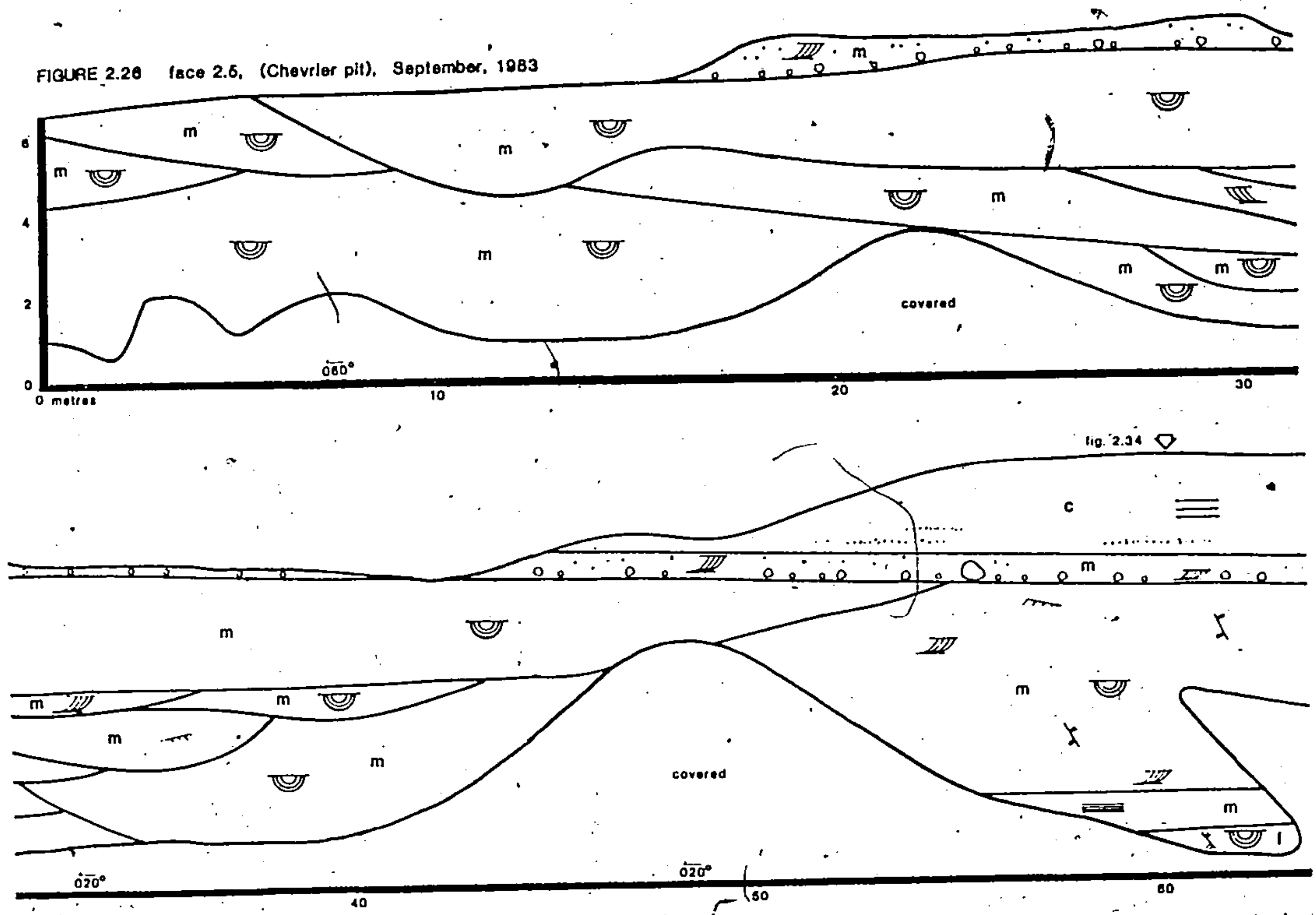

Fig. 2.26. See Appendix A for explanation of symbols.

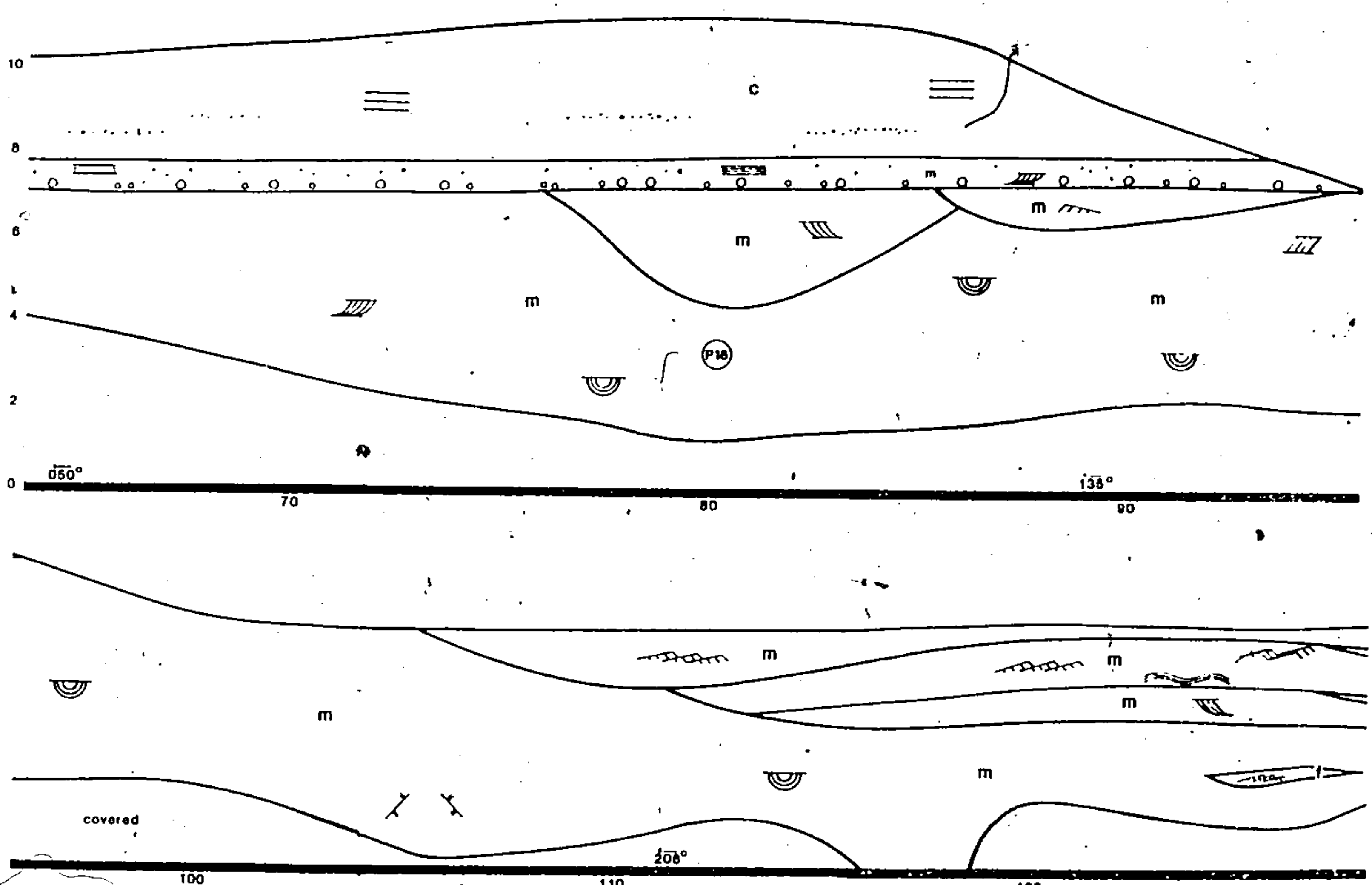

Fig. 2.26 continued.

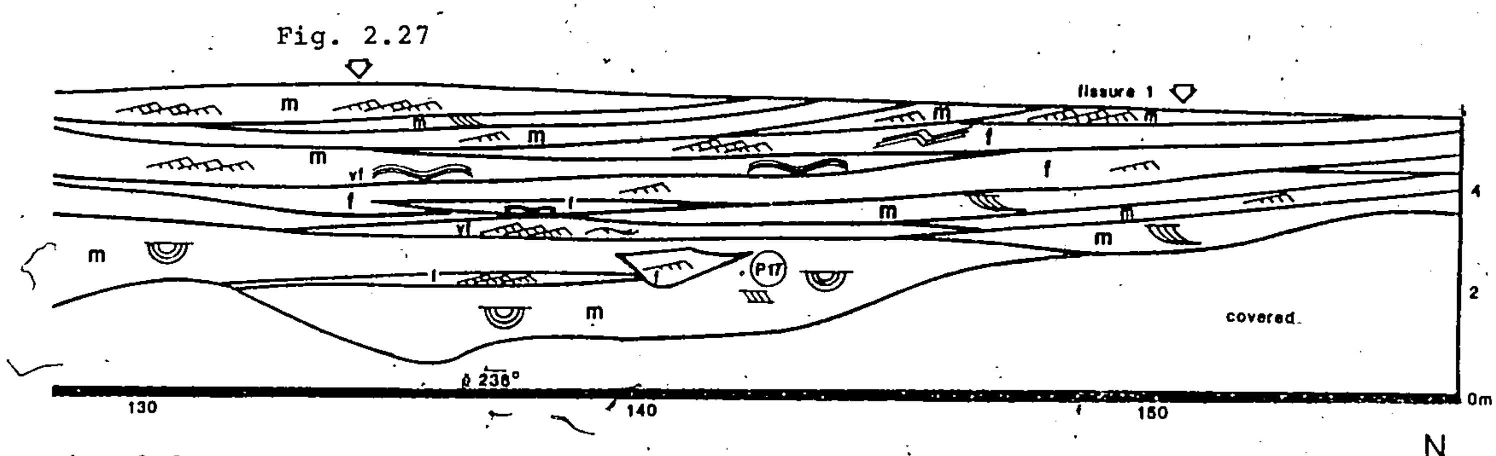

Fig. 2.26 concluded.

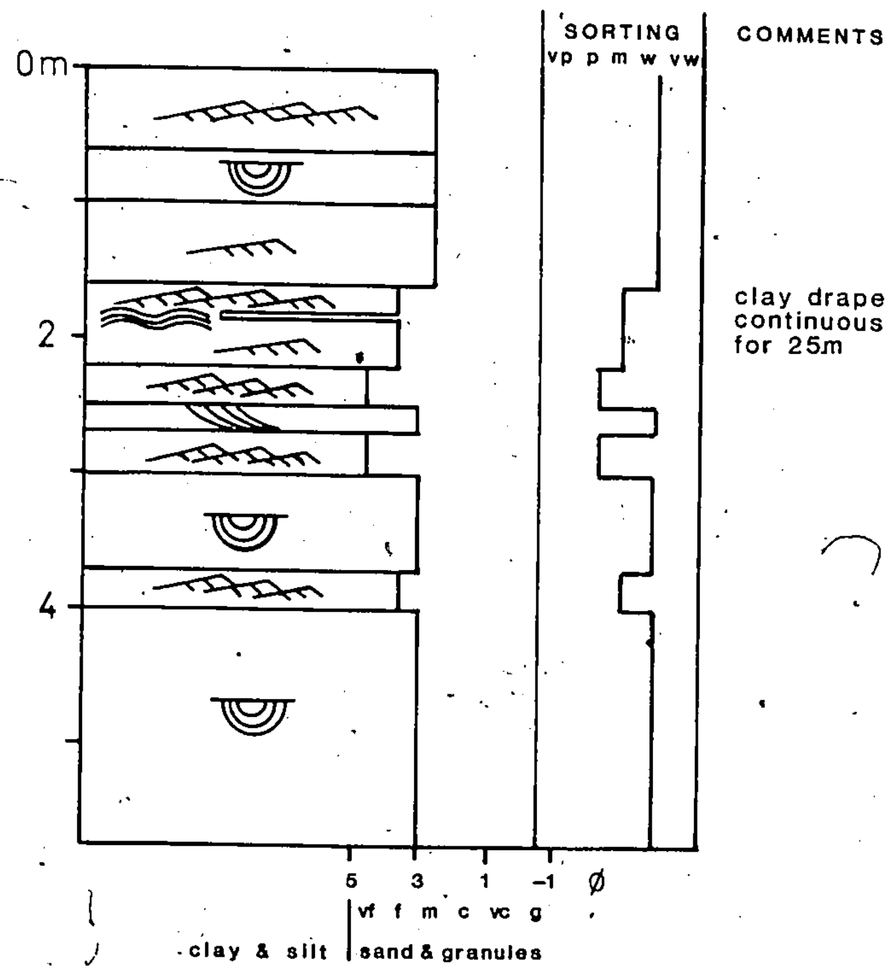

FIGURE 2.27 . FACE 2.5, NORTH END

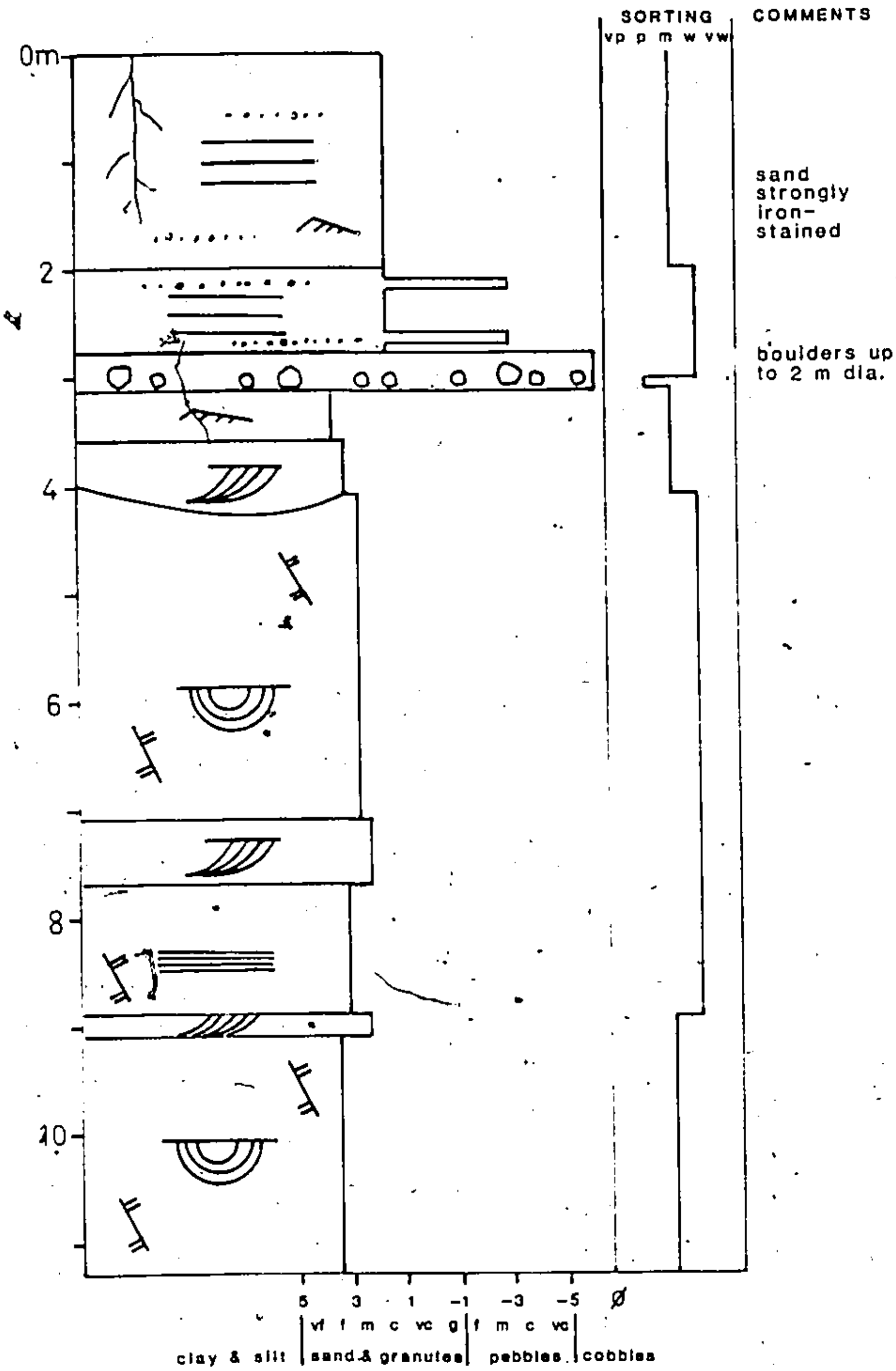

FIGURE 2.28 FACE 2.5, SOUTH END

prominent 4 cm thick bed of draped clayey silt was traced for 25 m along the face (fig. 2.29). Several units of type B climbing ripples are present in the upper third of the section (fig. 2.30). Reverse faults with a maximum displacement of a few cm are present throughout.

The lower half of this part of face 2.5 consists of trough cross-stratified fine to medium sand (facies 4). This style of bedding predominates in the southern three quarters of face 2.5, in slighty coarser sand (medium to coarse).

At 60 m in the section (detailed section, fig. 2.28), the crossbedded units coarsen upwards slightly from fine to medium sand. In the southern two thirds of face 2.5, channels are scoured into the cross-stratified sand, filled with cross-stratified sand, predominantly scour and fill trough crossbeds. The maximum height of the troughs is 1.5 m (fig. 2.31). The maximum dip of channel walls in face 2.5 is about 50°. These channels are relatively deep and narrow (2 m to possibly 10 m in depth, and a depth to width ratio of as high as 1/2). The channel margins are asymmetric. Tabular crossbeds are also present. Fig. 2.32 shows regressive climbing ripples preserved on the toesets of a planar-tangential crossbed set. Near the southern end of face 2.5, displacement of up to 10 cm was noted on reverse faults. Conjugate sets of reverse faults were noted (fig. 2.31). The crossbeds between 85 and 105 m were disturbed or contorted (fig. 2.33).

COLOURED PICTURES
Images en couleur

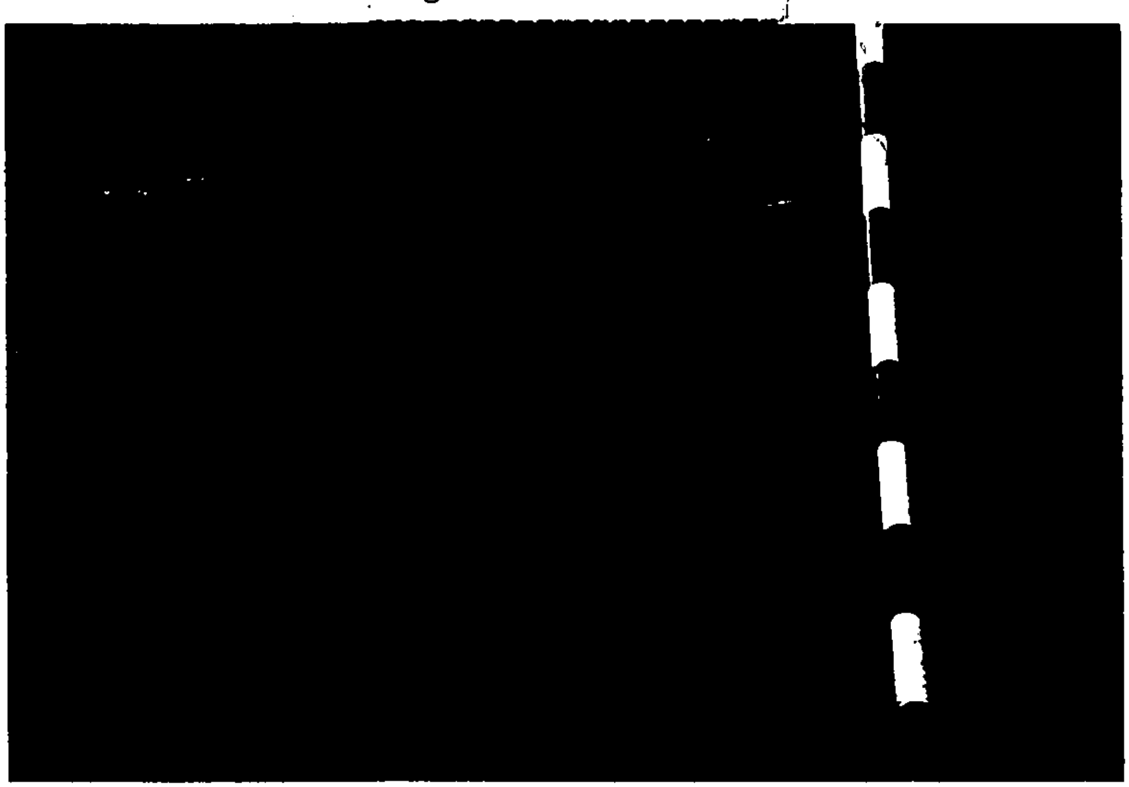

Figure 2.29 Clayey silt strata draped over ripples in fine sand, face 2.2, traceable for 25 m along the section. Scale in dm.

COLOURED PICTURES
Images en couleur

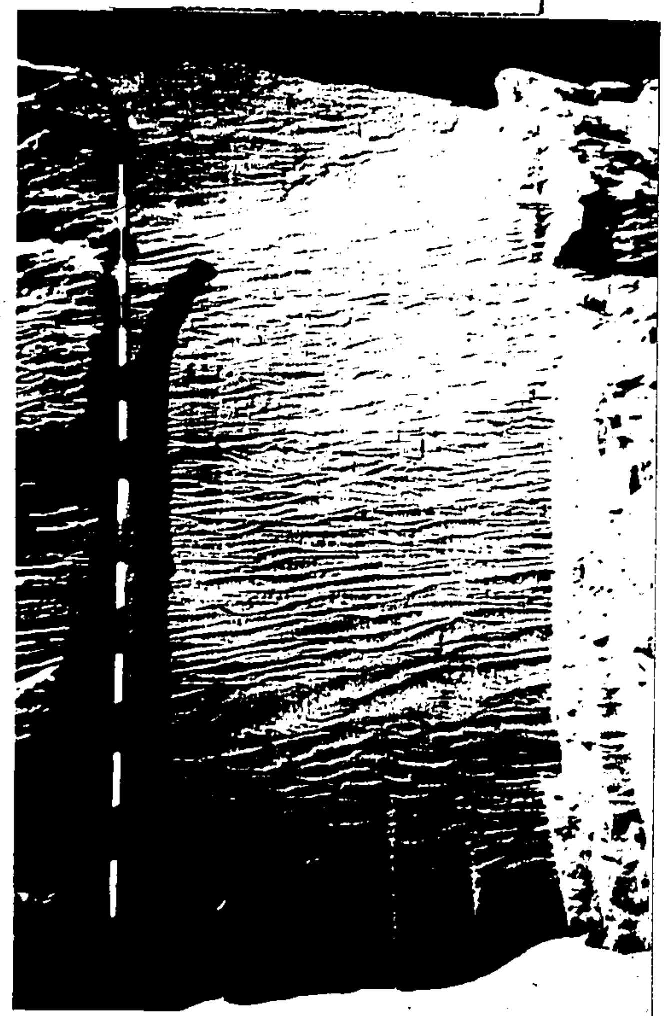

Figure 2.30 Type B climbing ripples, face 1.2. Scale in dm.

COLOURED PICTURES
Images en couleur

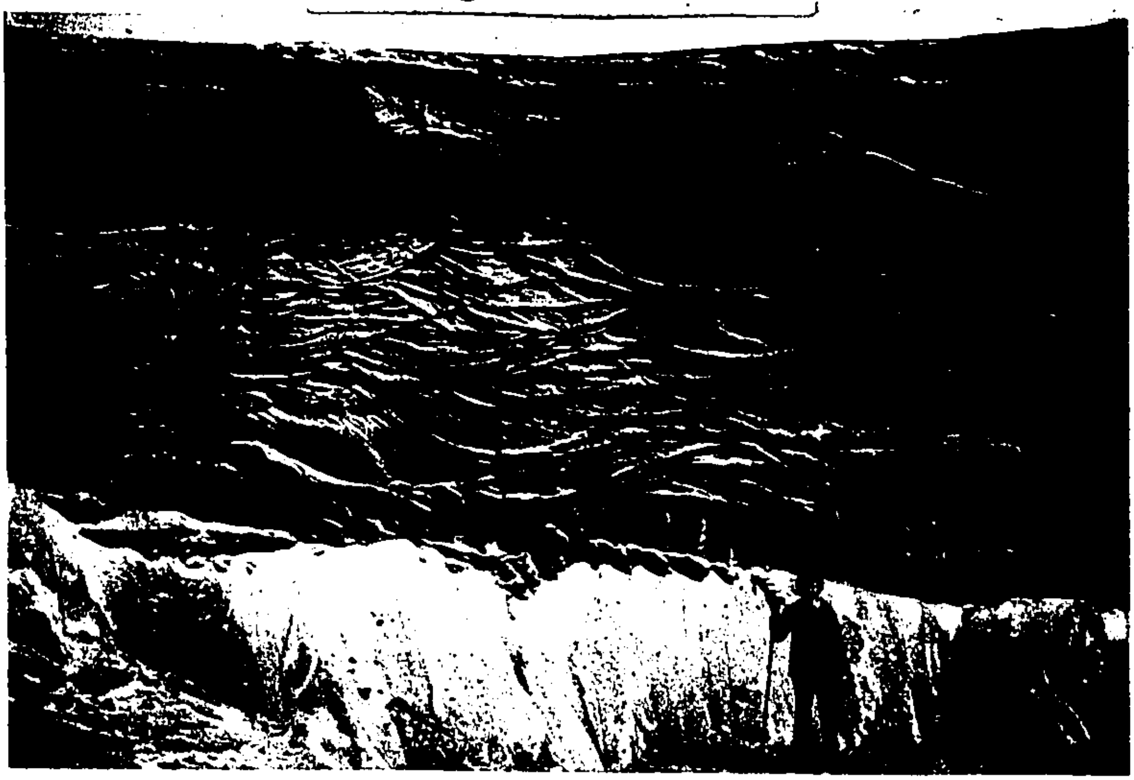

Figure 2.31 Large trough crossbeds in medium sand, face 2.5. Note conjugate sets of reverse faults.

COLOURED PICTURES
Images en couleur

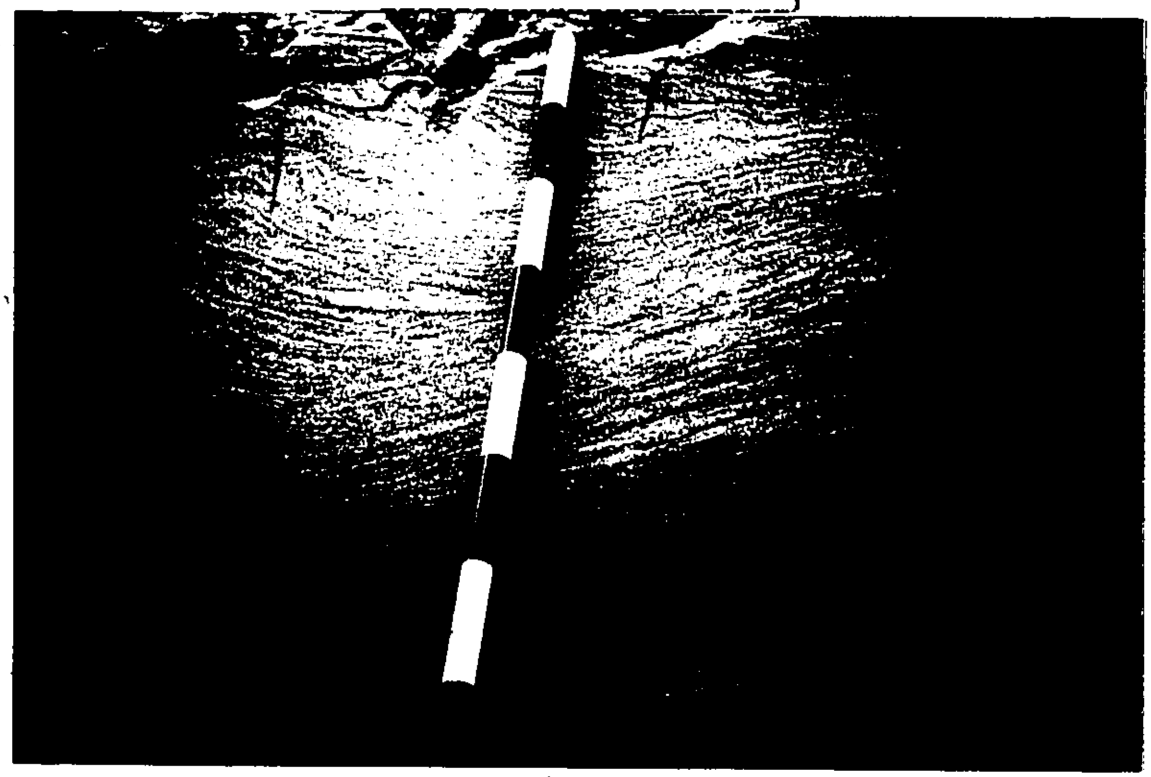

Figure 2.32 Regressive climbing ripples on dune foresets, face 2.2. Scale in dm.

COLOURED PICTURES
Images en couleur

Figure 2.33 Contorted crossbeds, face 2.5. Scale in dm.

The uppermost 4 m of face 2.5 consists of a unit of parallel to subparallel, horizontal beds of poorly sorted pebbly medium to coarse orange sand, with a few interbeds of fine and medium rippled sand, crossbedded medium sand, and pebble to cobble gravel (figs. 2.34, 2.35). The gravel interbeds occur more frequently near the base of the unit. The lower contact of the unit is erosional, and a 20-40 cm thick bed of cobbles and boulders occurs directly above the contact. Boulders up to 2 m in diameter occur at this horizon (fig. 2.34). This cobble lag occurs at a similar stratigraphic position in faces 2.1 and 2.6, and is overlain there by similarly bedded orange sand.

Face 2.6

See fig. 2.36 for schematic composite section of face 2.6. Face 2.6 is a 4 m high by 120 m long arcuate exposure (fig. 2.8) excavated during the summer of 1984. When examined that October, the upper 2 m consisted of the same orange, horizontally bedded medium to coarse pebbly sand as in face 2.5, also with a gravel lag above a straight, horizontal erosional base. Below this is a channel filled with a single continuous coset of large planar tabular crossbeds with straight foresets, in moderately sorted fine to coarse sand, which can be traced for 100 m along the face. The foresets extend for 3 m below the pebble lag, and dip towards the SE

COLOURED PICTURES
Images en couleur

Figure 2.34 Boulders along unconformity at top of section, face 2.5, overlain by coarse grained, horizontal storm beach bedding and finer, subhorizontal beachface bedding. Scale in dm.

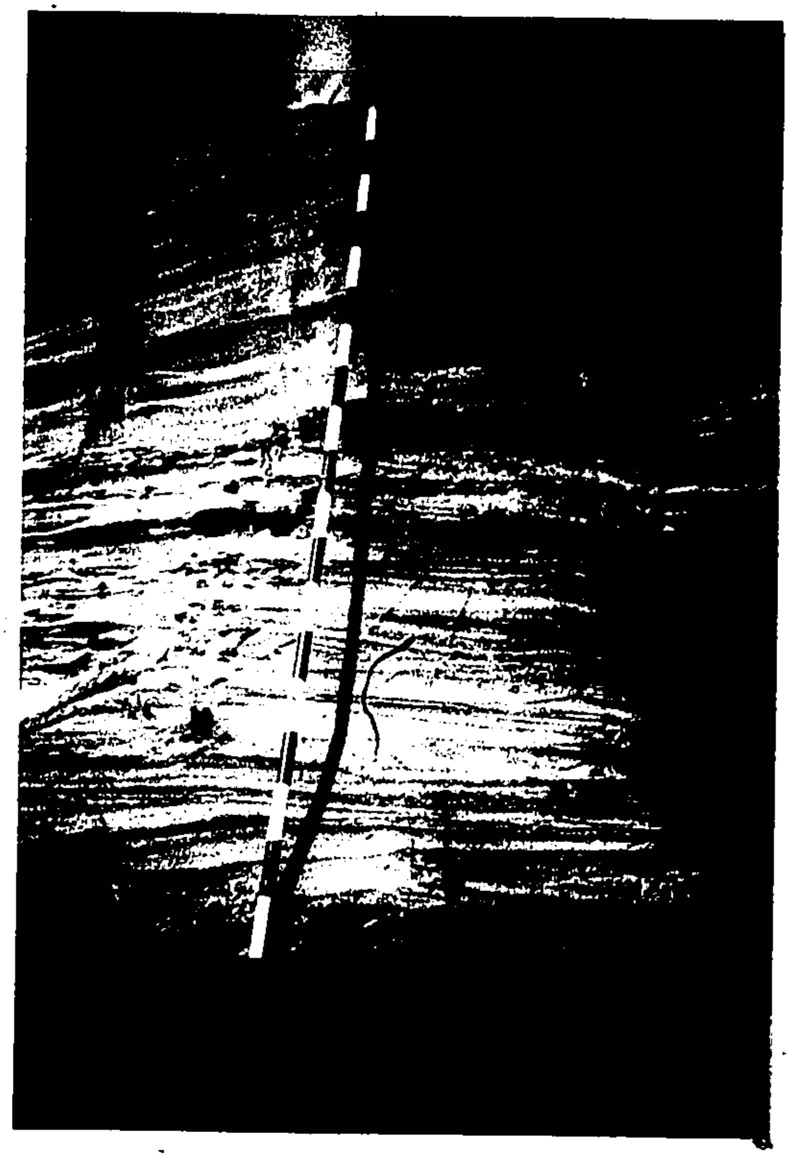

Figure 2.35 Beachface stratification, face 2.5. Scale in dm.

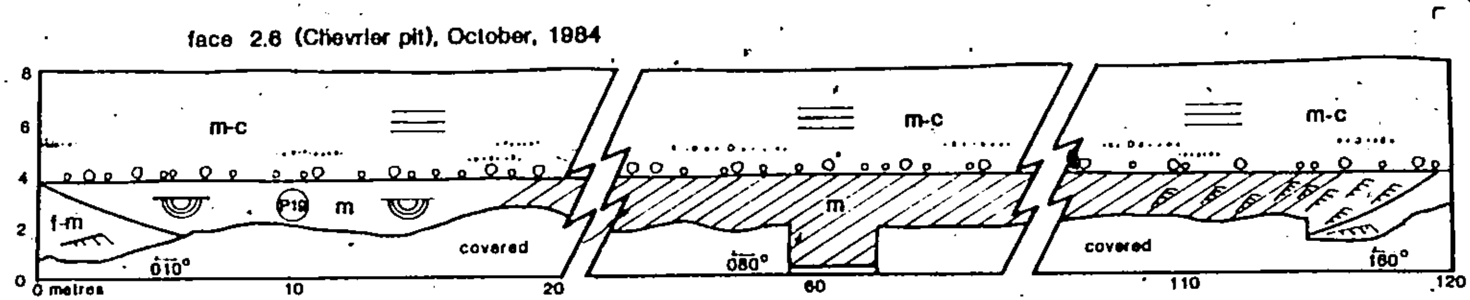

Fig. 2.36 See Appendix A for explanation of symbols.

(130°)(fig. 2.37). Regressive ripples are present on some of the crossbed foresets (fig. 2.38), and at the west (right) end, the foresets grade laterally into rippled beds which decrease in dip until they parallel the western channel margin. On the east (left) end, the tabular foresets grade into medium sized (average 15 cm high) trough crossbeds which yield a strong mean paleocurrent direction (134°) parallel to the direction of dip of the large planar crossbed foresets.

2.1.3 PIT 3 (DAOUST PIT)

Pit 3 is located at the northeast corner of the ice-contact stratified drift of Richard (1982), 2 km NNE of pit 2. It is just north of Highway 40, beside Dauost campground. It is owned and operated by Claude Daoust, who lives on the property, on Route 342.

Face 3.1

The upper metre of sediment of face 3.1 consists of horizontally bedded pebbly medium to coarse orange sand, similar to the upper units of faces 2.5 and 2.6. A pebbly lag is present along the erosional base of this unit, just as in pit 2 (see composite section, fig. 2.39).

Figure 2.37 Foresets of large cross-channel bar at face 2.6.

COLOURED PICTURES
Images en couleur

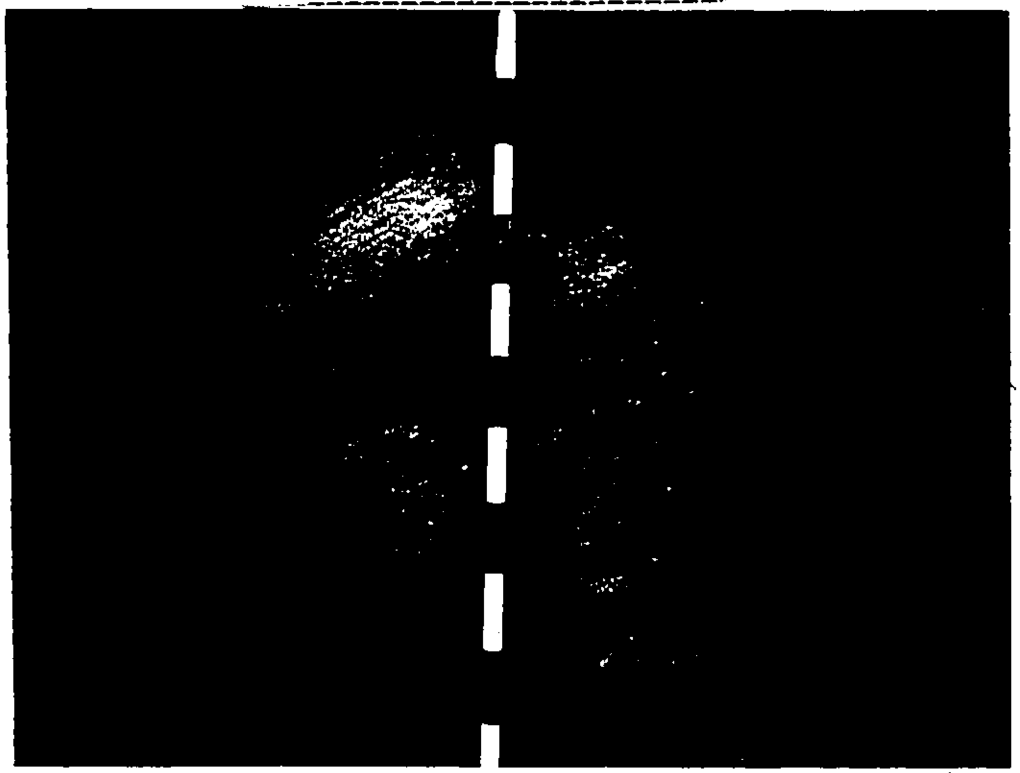

Figure 2.38 Regressive ripples (arrowed) on foresets of cross-channel bar of fig. 2.37. Scale in dm.

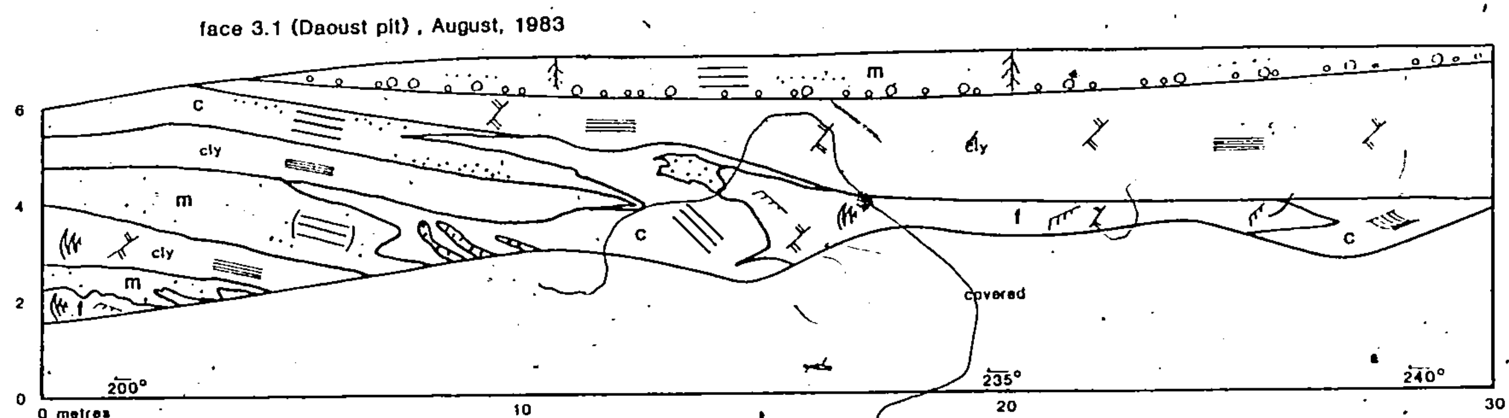

Fig. 2.39. See Appendix A for explanation of symbols.

Below this is a thick lens-shaped unit (max. 3 m) of horizontally laminated blocky silty clay. The clay is light buff-gray in colour from a distance, but at close inspection can be seen to consist of variegated discontinuous lenses and laminae of pale greenish-gray silty clay and pale reddish-gray silty clay. The bedding is contorted, with small normal and reverse faults of various orientations present throughout. The pit owner reported that the clay is present to 30 or 40 m behind this exposure (severely reducing the value of his land for borrow pit use!). The lower contact of the clay unit is relatively straight and uniform. Some foundering of the clay into the underlying sand was noted.

Beneath the clay are units of coarse crossbedded sand, fine rippled sand, and poorly sorted coarse pebbly to cobbly sand. Two smaller beds of similar blocky clay are interbedded with the units beneath the large clay unit. The base of this unit is erosional, and is angularly unconformable with the subjacent rippled and crossbedded units. The sand units are disturbed and contorted. The pebbly sand beds are the coarsest sediments observed in any of the pits.

Face 3.2

See fig. 2.40 for composite section. The measured part of this face is straight and strikes WSW. The east (right) half of the face consists of facies 4 tabular crossbedded buff

FIGURE 2.40 face 3.2 (Daoust pit), July, 1983

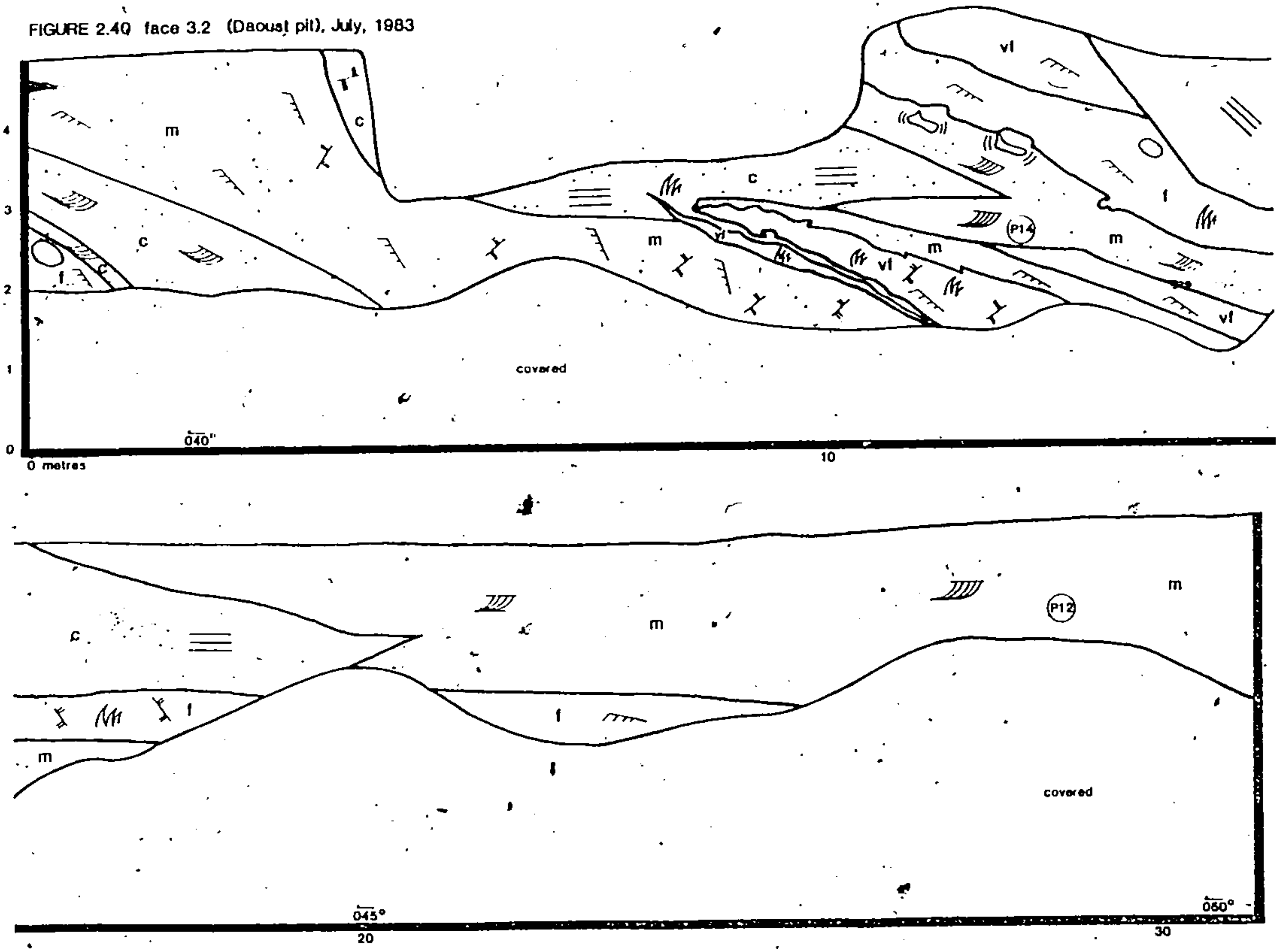

Fig. 2.40. See Appendix A for explanation of symbols.

coloured medium sand. Paleocurrents measured in the crossbeds show a mean direction to the south. The left side of the exposure has units of pebbly coarse crossbedded sand, medium rippled sand, horizontally bedded coarse pebbly sand, and rippled very fine sand. The units are in places highly contorted. The unit of silty very fine sand appears to have been partially injected into an overlying coarse sand unit. Two detached balls of fine sand have foundered into an underlying medium sand (fig. 2.41).

2.2 FOSSILS

A number of species of macrofossils were found in several units in pit 1 (Barbe pit). Very thin, disarticulated valves of <u>Macoma balthica</u> and <u>Hiatella arctica</u> were found within facies 1 sediments (faintly bedded channel fill). The valves lay horizontally at random levels within the channels, and were only locally numerous. They were predominantly convex side up, indicating the influence of currents during deposition.

At 6.2 m depth in face 1.2 (fig. 2.16) there is a 20 cm unit of clay, silty clay, and silty very fine sand containing a diverse biocoenosis. Enough specimens of <u>Hiatella</u> and <u>Macoma</u> were collected (2 kg) to submit for radiocarbon dating (section 2.3). Many of the valves still retained some of their periostracum. Within the same sample, fragments of several

COLOURED PICTURES
Images en couleur

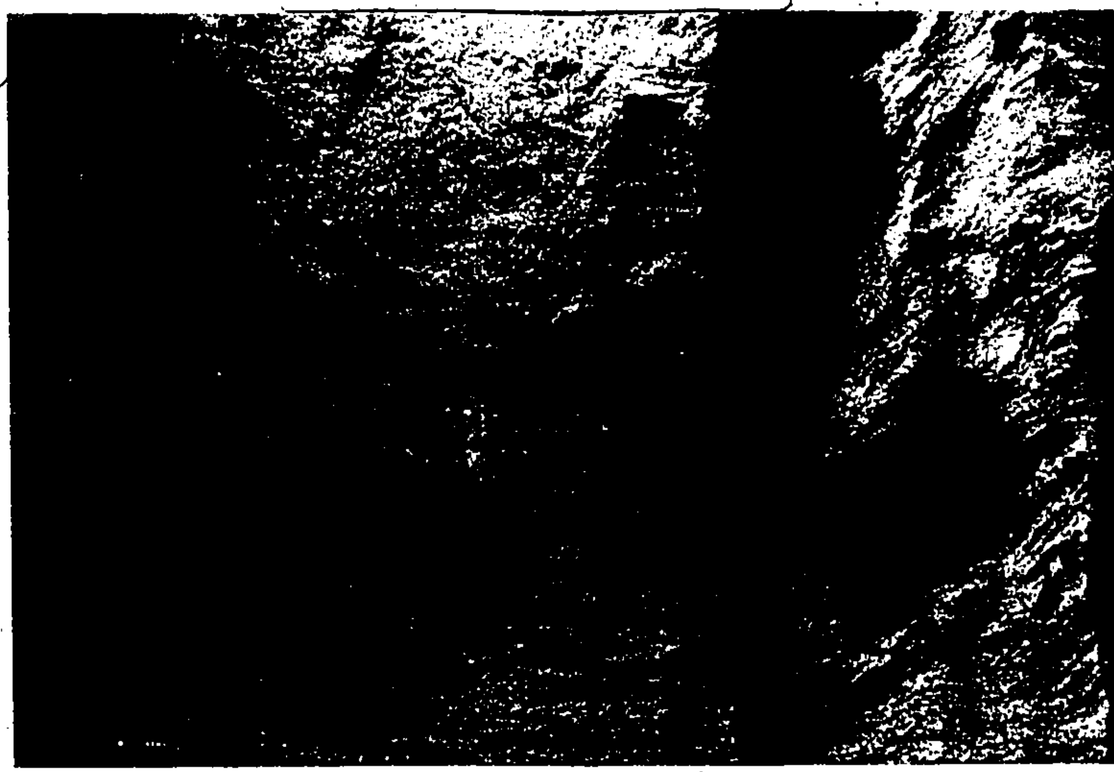

Figure 2.41 Foundered ball of fine sand in medium sand, face 3.2. Ball is 16 cm along its length.

individuals of _Mya_ _truncata_, _Mya_ _arenaria_, and _Mytilus_ _edulis_ were found. A few fragments of _Balanus_ _sp_. were found, along with at least four (unidentified) species of gastropod. Several large specimens of the siliceous sponge _Tethya_ _logani_ were recovered. Numerous small (2-3 mm dia.) very fragile tubes made of well sorted medium sand were present throughout the unit. These are possibly the mucous-cemented tests of organisms similar to the larvae of the modern caddisfly.

Trace fossils were much more abundant within the sediments, although mostly restricted to pit 1. Three ichnogenera were identified:

1. _Planolites_. These are described by Crimes _et_ _al_ (1977, p. 124), as simple, unbranched, straight to curved isolate to dense 1 mm - 1 cm tubes, primarily horizontal. They occur within poorly sorted very fine grained horizontally laminated sand beds of facies 3 in face 1.1 and 1.2. They are abundant enough in places to almost completely obscure the bedding, and are unlined and infilled with homogeneous sand (fig. 2.42). They are most likely formed by worms or worm-like organisms.

2. _Monocraterion_. These are vertical tubes, circular in horizontal cross section (fig. 2.43). In vertical section they consist of concordantly downbent laminae in the shape of nested cones or funnels, 0.5 - 3 cm in diameter,

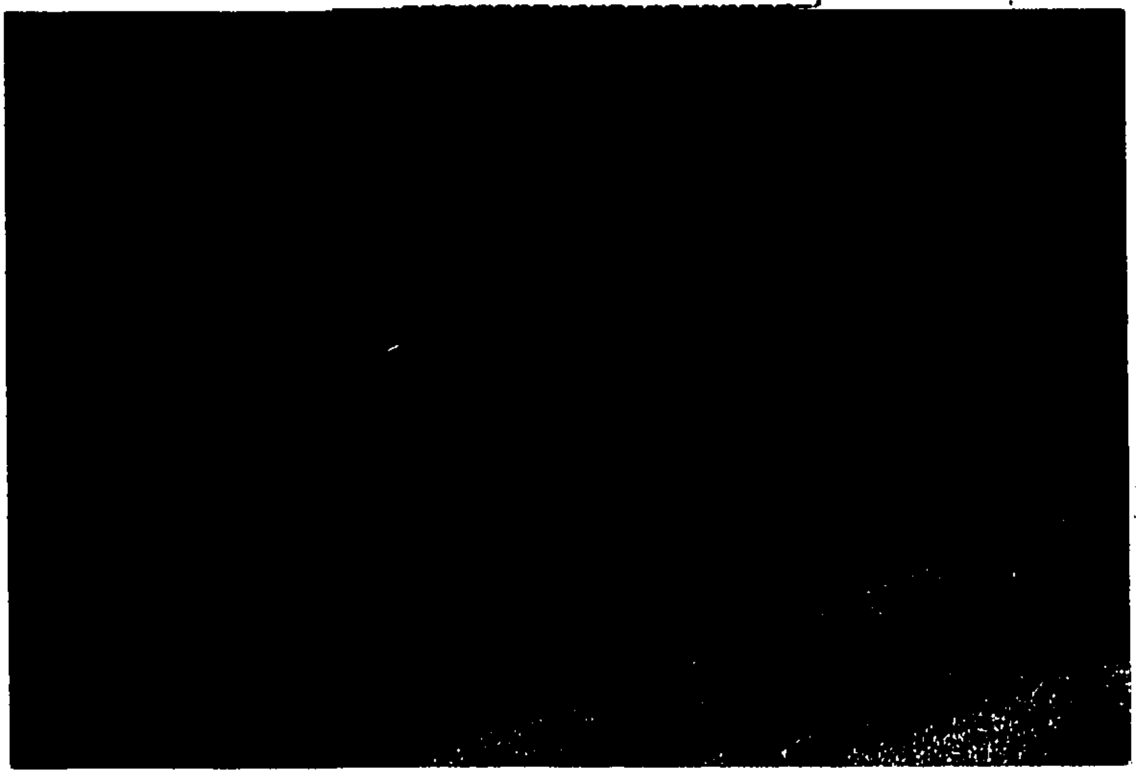

Figure 2.42 Bedding plane view of Planolites traces. Note Skolithos-like burrows extending downward from the silt and clay-rich bed into the underlying coarser, horizontally laminated unit. Face 1.1a. Knife handle 8 cm long.

COLOURED PICTURES
Images en couleur

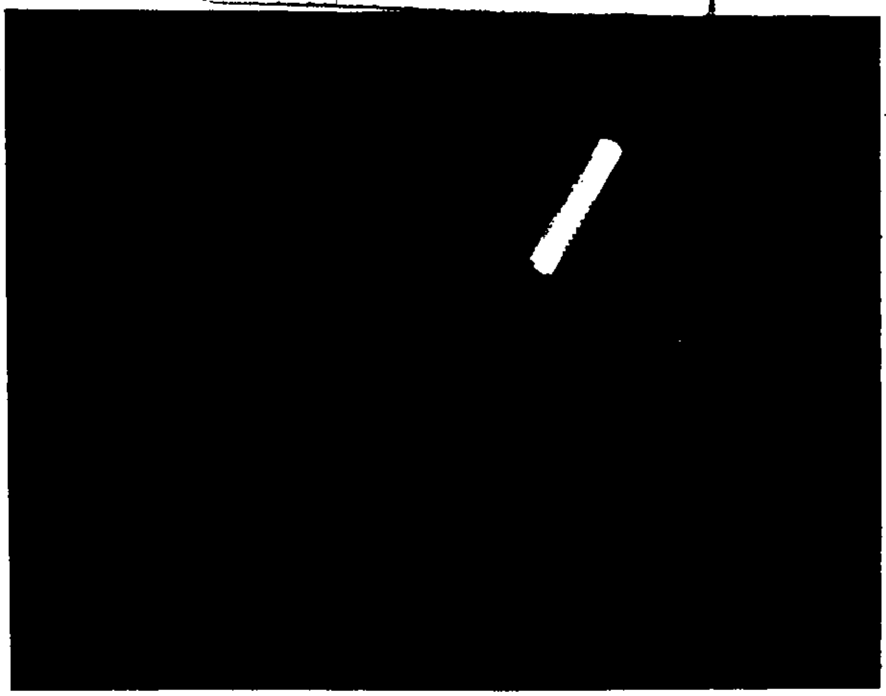

Figure 2.43 Bedding plane view of Monocraterion, face 1.1a
Pen 12 cm long.

and 0.5 to 10 cm in length. The narrow central core described by Crimes _et al_ (1977) was rarely observed. _Monocraterion_ is generally confined to beds of fine to coarse sand, either horizontally laminated, rippled, or occasionally crossbedded (figs. 2.44 and 2.45). Where it occurs in well sorted medium to coarse sand, it appears to have originated in an overlying bed of fine grained material (either still present in the section or missing due to erosion). Annelid worms are believed responsible for these burrows.

3. _Skolithos_. A few 0.5-3 cm wide subvertical burrows are present (fig. 2.42). _Planolites_ burrows may be inclined or vertical for short distances, but the _Skolithos_ burrows were consistently wider than nearby horizontal _Planolites_.

In addition to the traces listed above, rare occurrences of irregular vertical tubes, 2-5 cm wide by 5-15 cm deep, containing irregularly churned or mottled sand were seen at pit 2, and are attributed to the presence of bivalves.

2.3 RADIOCARBON DATES

1.1 kg of _Hiatella arctica_ shells and 0.78 kg of _Macoma balthica_ shells, from the fossiliferous clay unit above the diamicton at face 1.2 were submitted to J. Terasmae of Brock

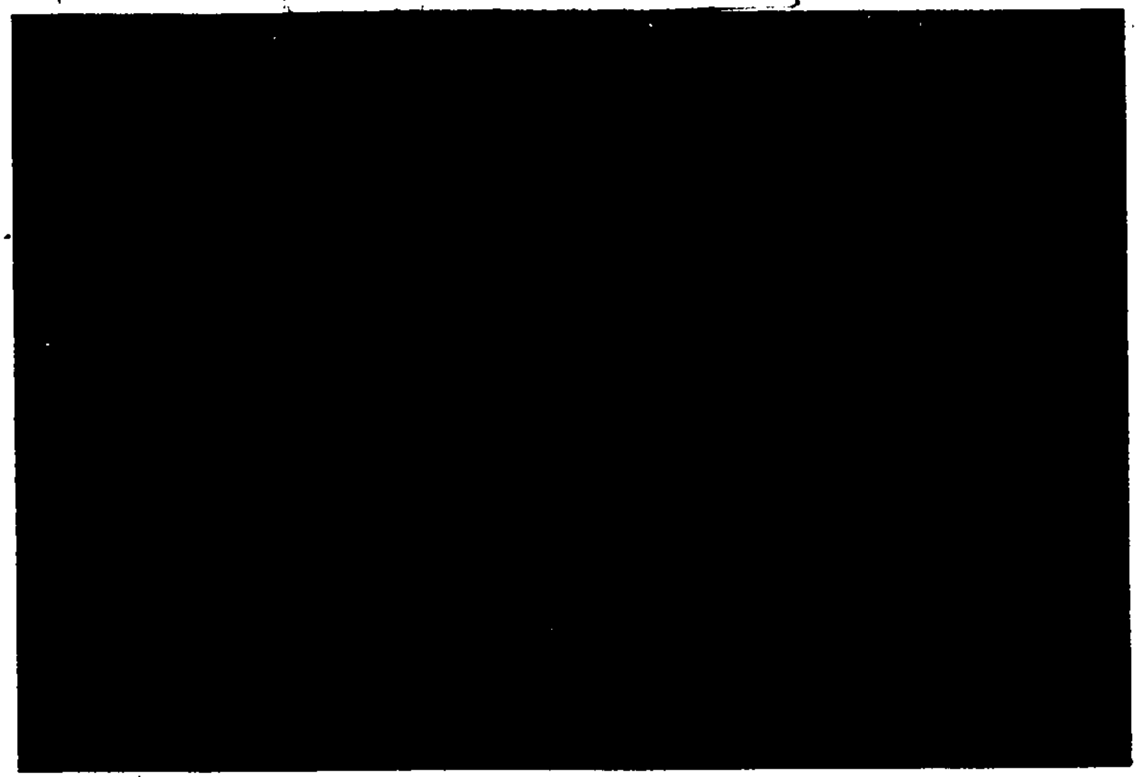

Figure 2.44 Monocraterion in facies 3 sediment (alternating beds), face 1.1b. Burrows appear to have extended down from silt rich layer into plane laminated medium sand. Silt-rich layer has been almost entirely removed by current action preceeding deposition of superjacent plane laminated unit. Knife handle 2 cm wide.

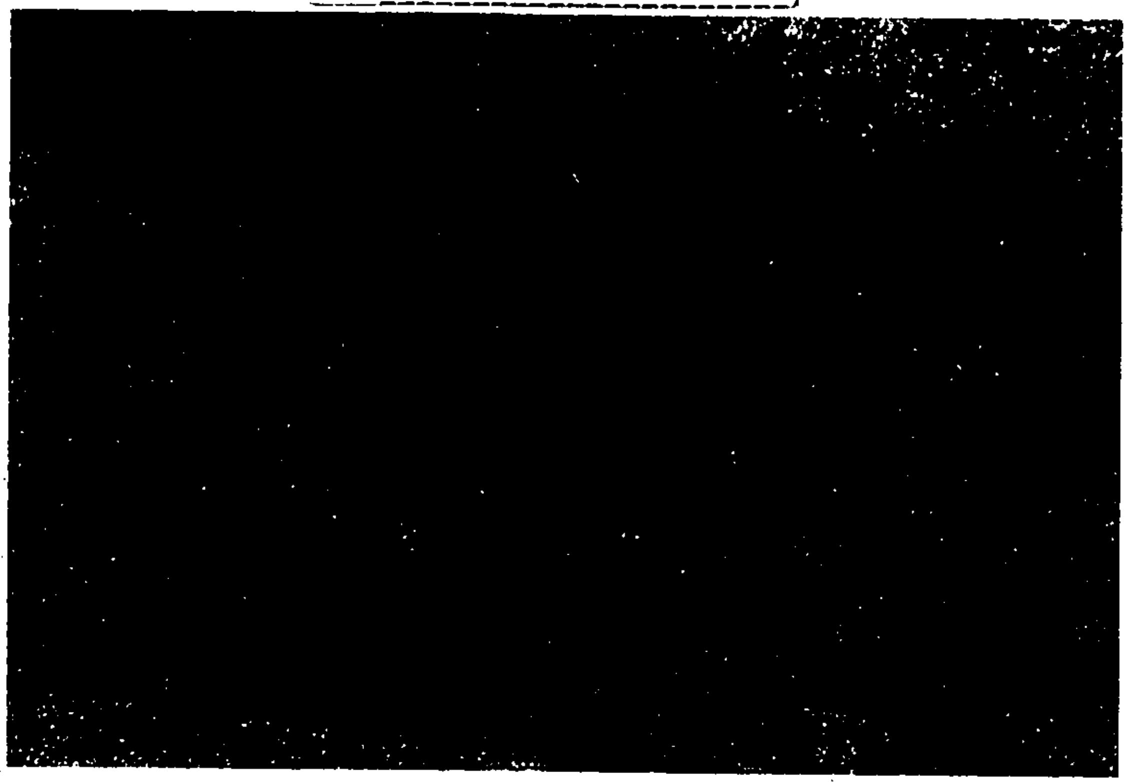

Figure 2.45 Monocraterion burrows in plane laminated (lower) and crossbedded (middle) sand. Field of view 40 cm across.

University for radiocarbon dating. Each sample was divided into two and yielded dates of 9,670 ± 120 yrs and 10,060 ± 120 yrs (Hiatella), and 10,860 ± 160 yrs and 11,190 ± 150 yrs (Macoma). A 50 g sample of compressed wood fragments from the same unit yielded a date of 31,900 ± 1100 yrs, and therefore represents material reworked from a previous interglacial or interstadial period.

TABLE 2.1: RADIOCARBON DATES

Note: after removal of foreign matter, shell samples were pretreated with a distilled water wash and acid leach. Wood fragments were also treated for removal of humic acid. Counting time for all samples was 3000 min.

DECEMBER 1983

SAMPLE NO:	BENZENE PRODUCED:	NO. OF DISINTE- GRATIONS:	CALCULATED AGE:
BGS 913 (Macoma balthica)	2.6204 g 3.9377 g	56,204 66,909	10,860 ± 160 yrs 11,190 ± 150 yrs
BGS 914 (Hiatella arctica)	3.6214 g 3.7082 g	68,924 69,506	9,670 ± 120 yrs 10,060 ± 120 yrs
BGS 915 (wood fragments)	3.4293 g	37,070	31,900 ± 1,100 yrs

CHAPTER 3: POST-DEPOSITIONAL FEATURES

3.1 FERRUGINOUS BANDS

A very common feature of the sections studied in the St. Lazare area is the occurrence of horizontal to subhorizontal bands of hematitic sand, which cross all sedimentary structures within the sediments (figs. 3.1 through 3.4). Slight cementation of the sediments is effected by the hematite and the layers often stand out in relief in weathered exposures (fig. 3.4). These are diagenetic features, and have been called "Liesegang rings" after a laboratory phenomenon involving cyclic diffusion deposits of silver nitrate in contact with potassium chromate, described in the mid nineteenth century (Bertouille 1976). Bertouille (1976) described several different forms of these hematite deposits, and referred to the St. Lazare type as ferruginous bands. They appear to be formed by reactions of zones of colloidal iron or soluble ferrous salts with oxidation fronts within permeable sediments. The ferruginous bands at St. Lazare are generally a few millimeters thick, rarely up to a centimetre or more. They can be irregular (figs. 3.1 and 3.2) or, more commonly, straight and continuous (figs. 3.3 and 3.4). In inhomogeneous sediment the bands tend to follow more permeable zones.

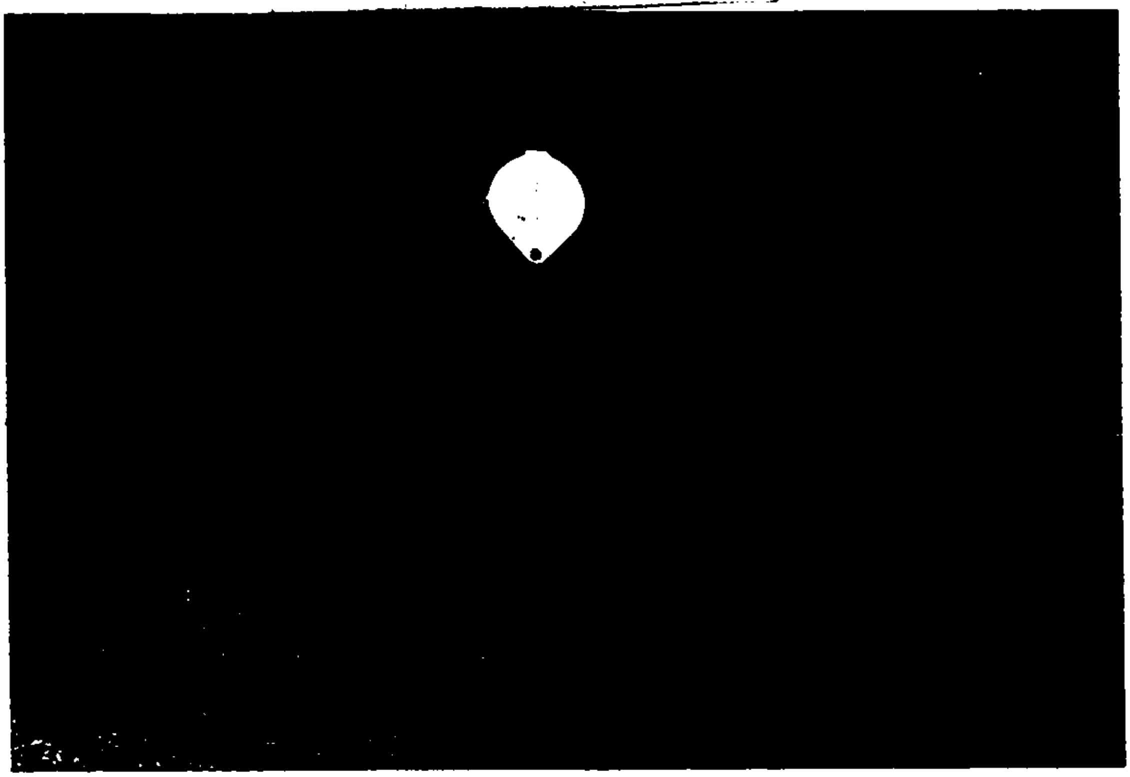

Figure 3.1 Irregular ferruginous band in moderately sorted medium sand, pit 1. Lens 2.5 cm across.

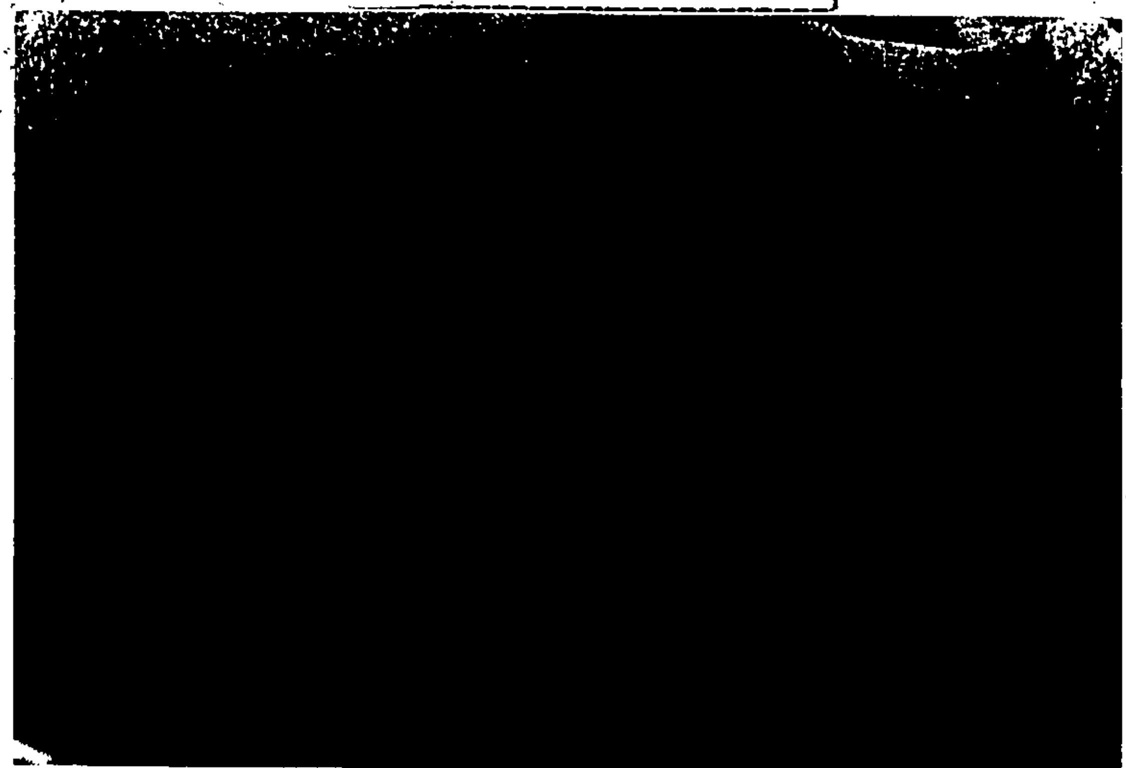

Figure 3.2 Horizontal section through ferruginous band of figure 3.1. Lens 2.5 cm across.

COLOURED PICTURES
Images en couleur

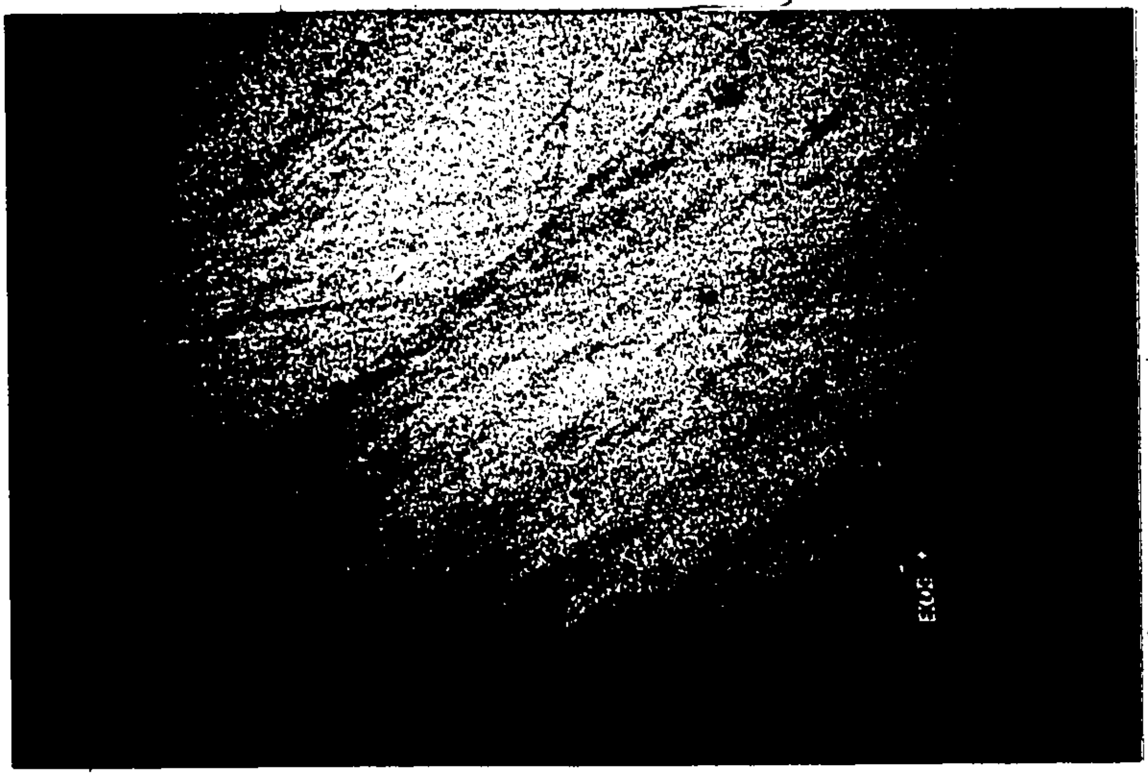

Figure 3.3 Regular, horizontal ferruginous bands in cross bedded medium to coarse sand, in a subcrop east of pit 3, adjacent to Hwy 40. Knife handle 2 cm wide.

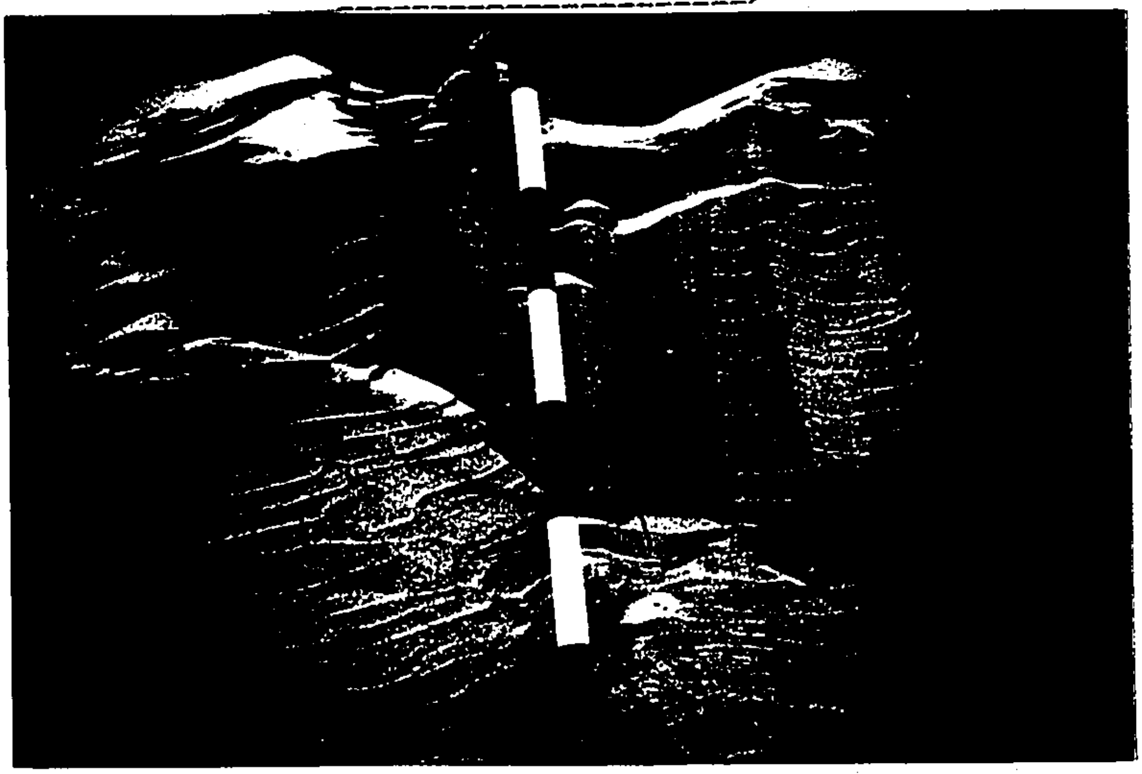

Figure 3.4 Thin, regular and resistant horizontal ferruginous bands in plane and cross laminated fine sands, pit 3. Scale in dm.

3.2 WATER ESCAPE FISSURES

3.2.1 LOCATION, ORIENTATION AND HOST SEDIMENTS

Structures interpreted as water escape fissures were found in several exposures in pit 2 (Chevrier pit). The sediments in which the fissures occur consist of laminated and rippled very fine to fine sand, planar crossbedded medium sand, and minor silt and clayey silt. The sandy facies are well sorted and highly permeable, and are underlain by an unknown thickness of impermeable clayey diamicton.

The fissures are variously oriented subvertical to steeply dipping planes (see fig. 3.5 for location and orientation of fissures). Fissures 1, 3 and 5 strike northwest, and 2 and 9 strike approximately northeast. Fissures 3 and 5 were followed along strike at the top of the section, from the edge of the scarp of the pit back for 5 m. The fissures join at an acute angle 3.5 m from the scarp (fig. 3.6). From the point of intersection back, the fissure changed strike by about 20°. Fissure 9 was followed along the floor of the pit for a distance of 30m; it has an arcuate form and varies in strike by 30° from one end to the other (fig. 3.5). In cross section, the fissures are close to the vertical but vary from it as much as 55° in some places. Some of the fissures vary in dip with depth. The planes of the fissures, therefore, are somewhat irregular. Diagenetic ferruginous

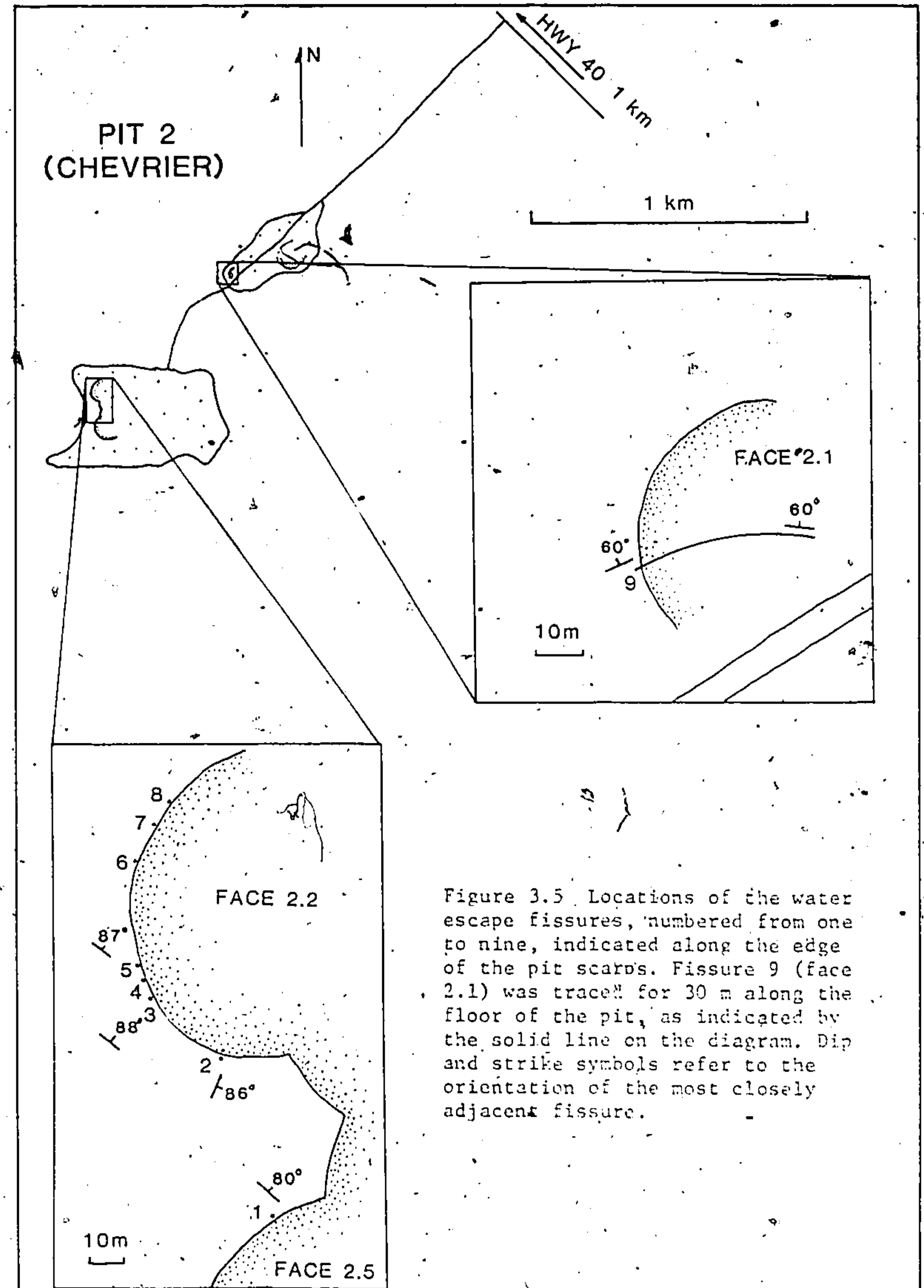

Figure 3.5 Locations of the water escape fissures, numbered from one to nine, indicated along the edge of the pit scarps. Fissure 9 (face 2.1) was traced for 30 m along the floor of the pit, as indicated by the solid line on the diagram. Dip and strike symbols refer to the orientation of the most closely adjacent fissure.

COLOURED PICTURES
Images en couleur

Figure 3.6 Intersection of fissures 2 and 3 (plan view). Scale in dm.

bands are observed to cross the fissures, indicating that the fissures predate the development of the bands.

3.2.2 DOWNTURNING OF THE BEDDING ADJACENT TO THE FISSURES

The fissures are very noticeable in good exposures because of downward displacement of the beds on either side of a narrow central fissure (figs. 3.7 through 3.15). This displacement, or downturning, is a distinctive feature of all the fissures, and extends from the central fissure laterally outward to an average distance of 10 to 15 cm.

The downturning of the bedding next to the central fissure can be smooth and regular, increasing evenly from no displacement at the edge of the deformed zone to maximum displacement along the plane of the fissure, or it can occur in a series of small, stepped normal faults (which generally approximate a smooth curve) (figs. 3.8, 3.9). In a few places there is no downturning associated with the fissure (fig. 3.14), or the downturning occurs only on one side (fig. 3.13). In the three fissures in which the latter phenomenon was observed, the undisturbed beds are always on the underside of the fissure which dips as little as 45°.

3.2.3 NATURE OF THE CENTRAL FISSURE

The widths of the central fissures vary from 1 mm to

COLOURED PICTURES
Images en couleur

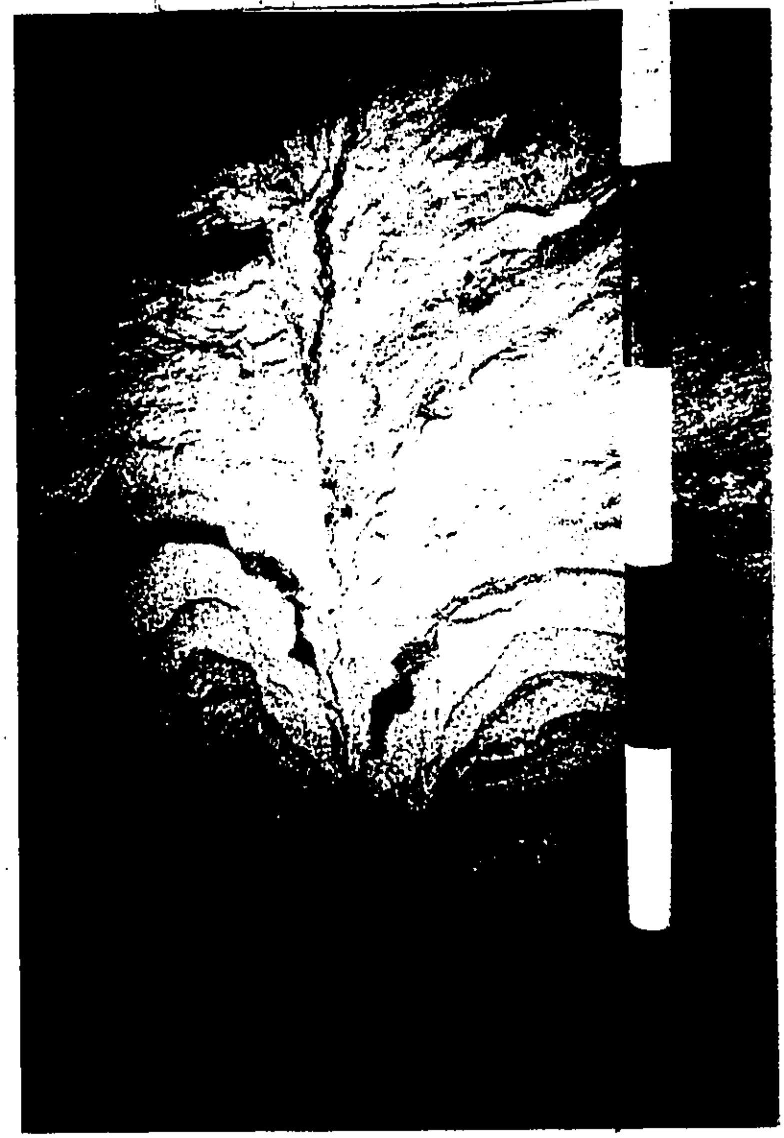

Figure 3.7 Upper part of fissure 2. Note downturning of beds adjacent to the fissure and small, stepped, normal faults. Scale in dm.

COLOURED PICTURES
Images en couleur

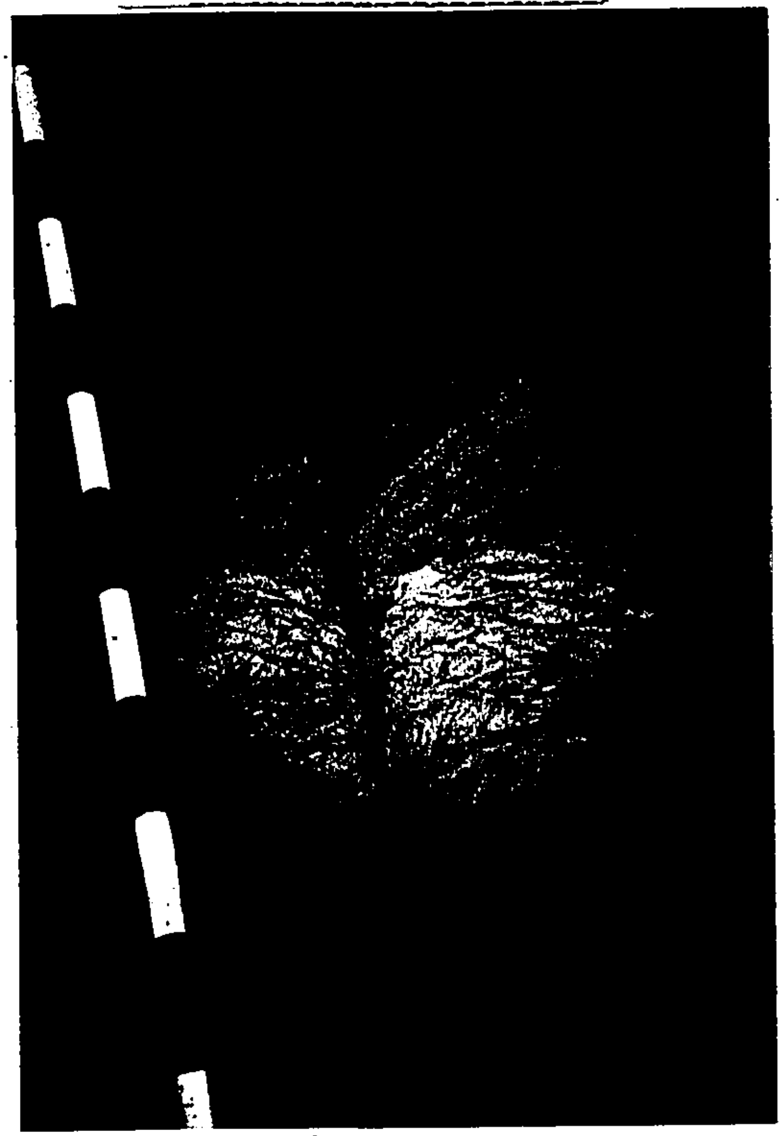

Figure 3.8 Part of fissure 2, about 3 m from the top of the section. Downturning is symmetric, and some microfaulting is present. Sediment is well sorted very fine to medium sand. Scale in dm.

COLOURED PICTURES
Images en couleur

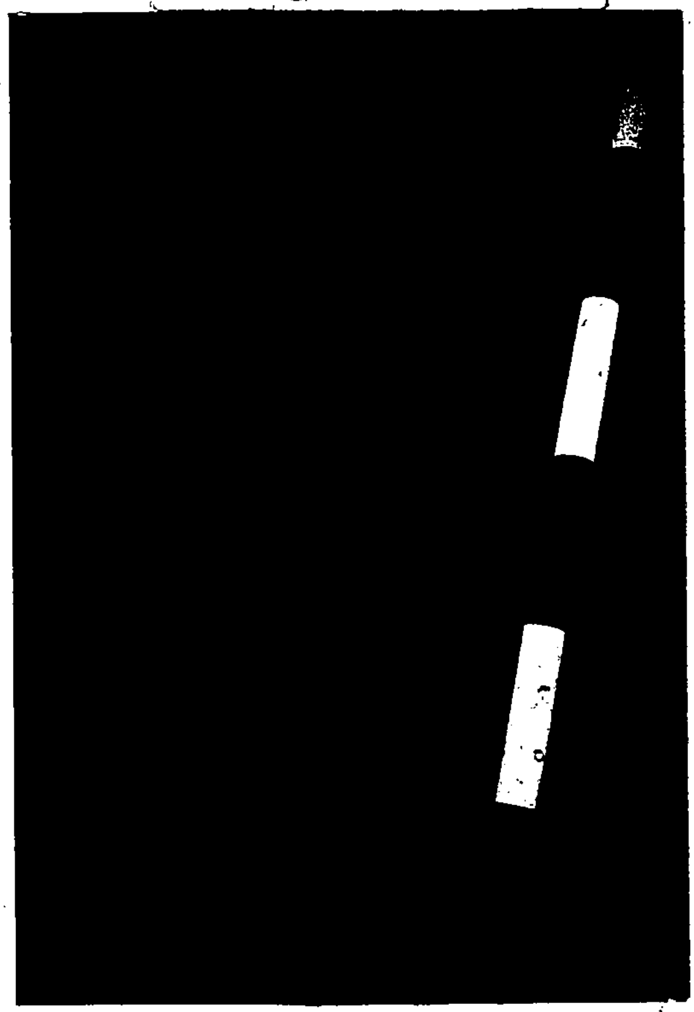

Figure 3.9 Part of fissure 2 subjacent to figure 3.8. Section is cut at about 80° to the strike of the fissure. Scale in dm.

COLOURED PICTURES
Images en couleur

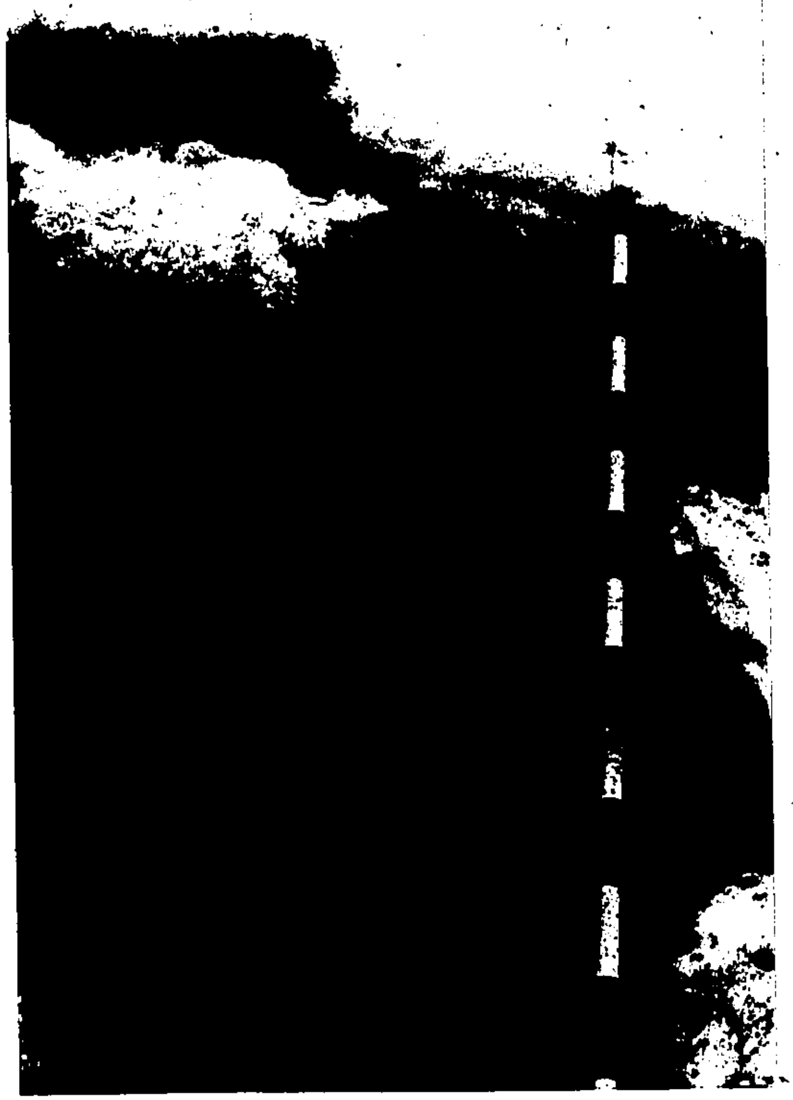

Figure 3.10 Upper 1.5 m of fissure 3. Fissure strikes at about 75° to plane of the section. Note that the central fissure is emphasized by the presence of precipitated iron and manganese. Scale in dm.

COLOURED PICTURES
Images en couleur

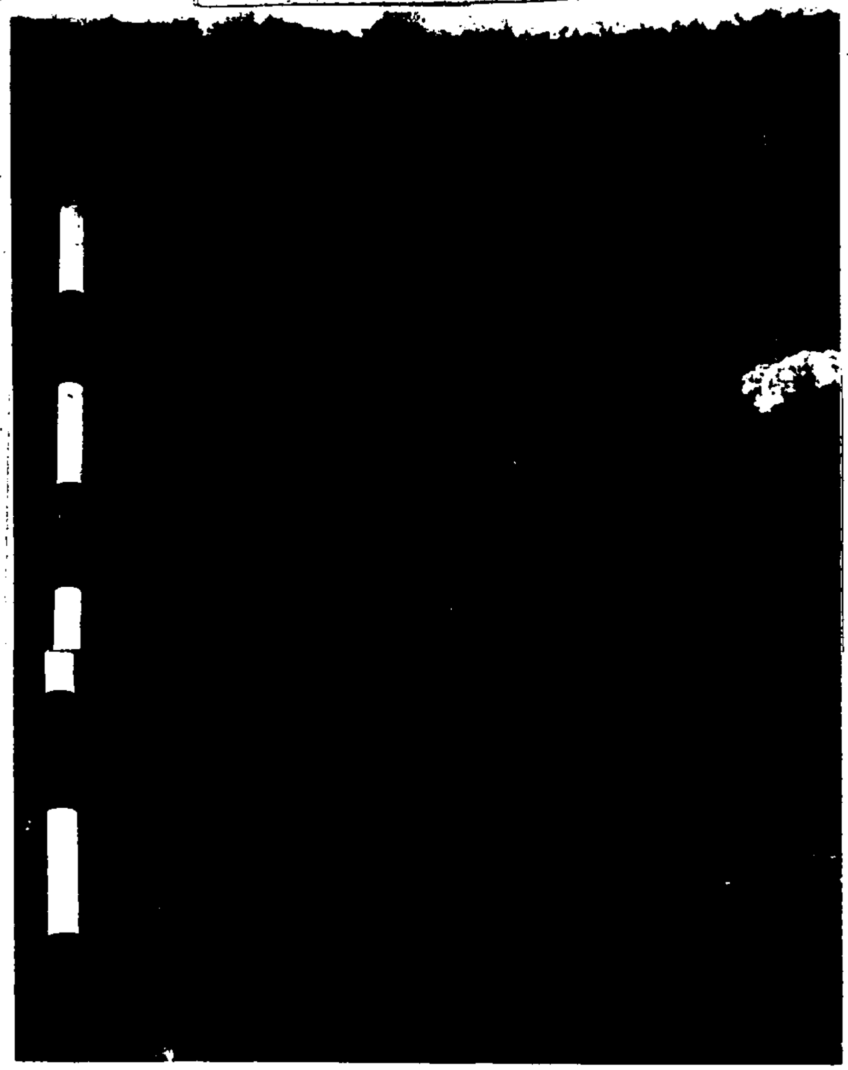

Figure 3.11 Upper metre of fissure 4. Note relatively narrow area adjacent to fissure affected by downturning. Scale in dm.

COLOURED PICTURES
Images en couleur

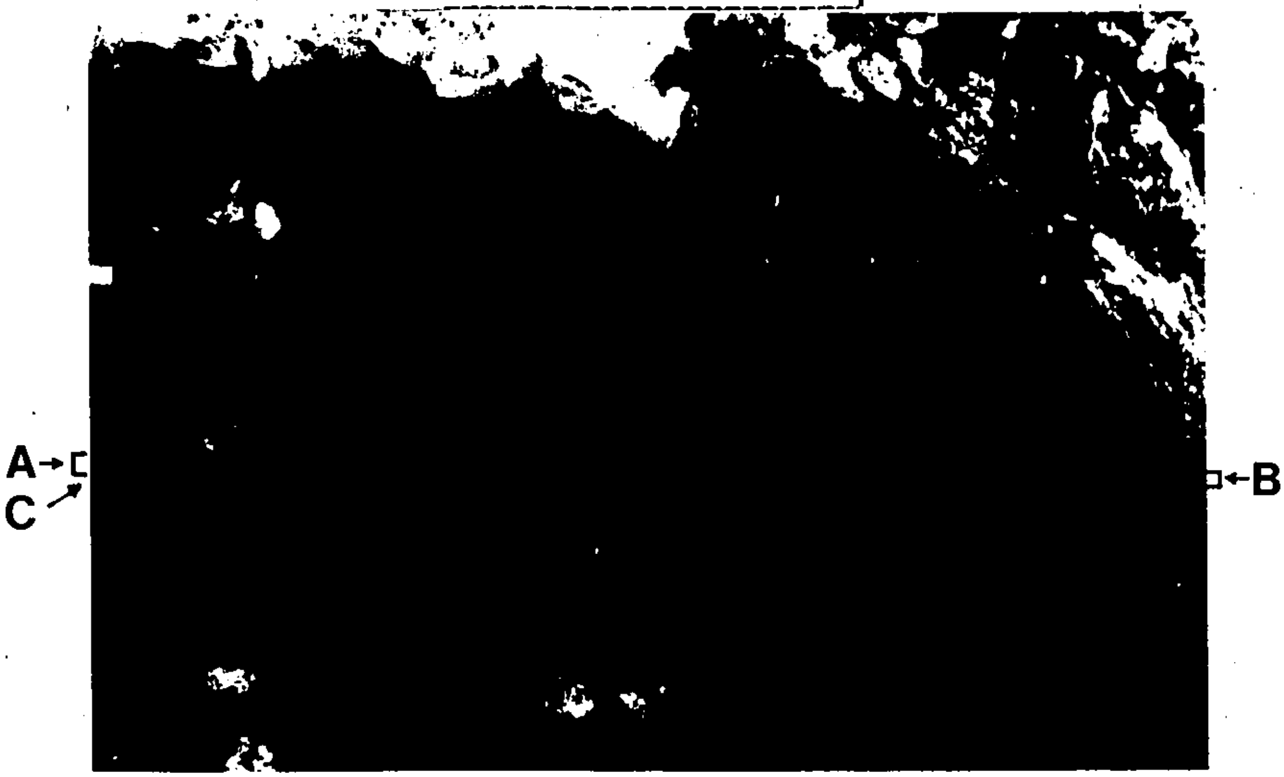

Figure 3.12 Plan view of fissure 3 at top of the section. Note: (1) Apparent lateral movement of sediments adjacent to central fissure is an artifact of the downward displacement of crossbed foresets (the foresets are dipping to the right). (2) Change in thickness of central fissure along strike, from 3 cm at A to 1 cm at B. (3) Diagenetic manganese and iron precipitated along the west side of the fissure. (4) Downturning is a combination of smooth, regular subsidence and microfaulting (5) Vague, irregular, discontinuous lamination within the wide part of the central fissure at A and 50 cm toward B, parallel to fissure walls. 10 cm of scale bar visible at left.

COLOURED PICTURES
Images en couleur

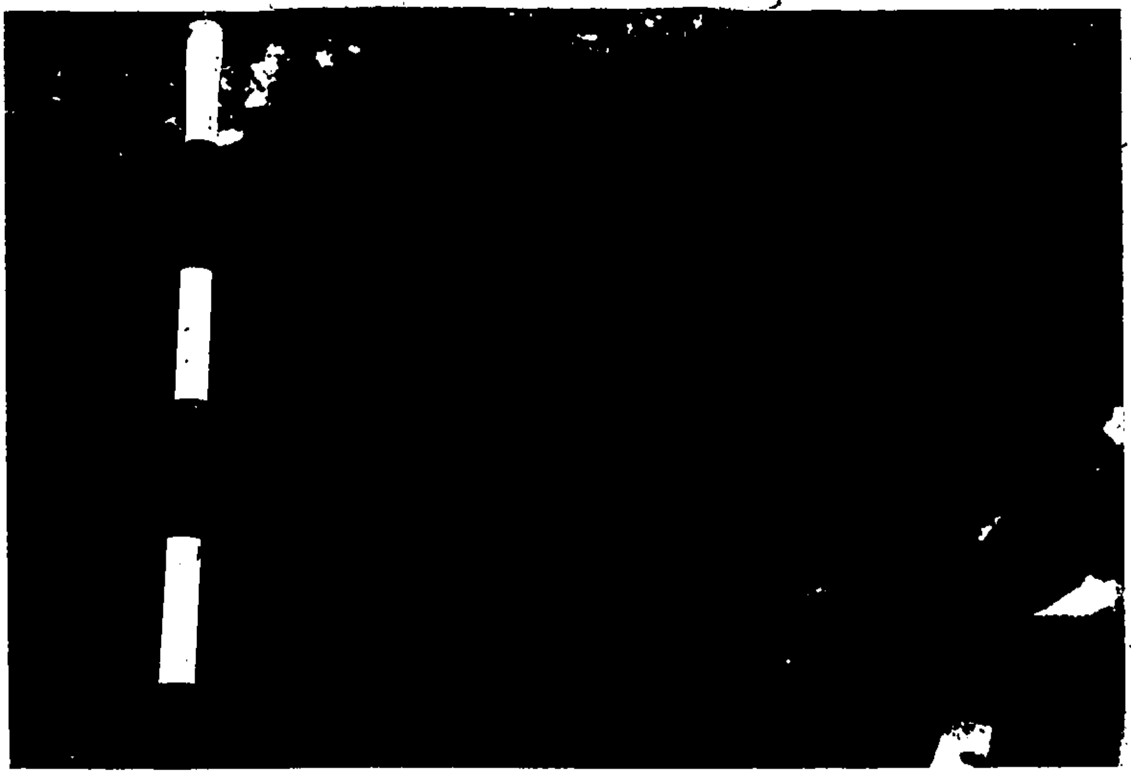

Figure 3.13 Fissure 3, in vertical section. Note absence of downturning of beds on right (lower) side of fissure. Fissure dips about 45° at this point. Scale in dm.

COLOURED PICTURES
Images en couleur

Figure 3.14 Part of fissure 3. Note absence of downturning on the lower side of the fissure and on the upper side in the bottom half of photo. Note alsothe narrowness of the area affected by downturning on the upper side; and the increase of downturning to a maximum of 10 cm higher in the section. Scale in dm.

COLOURED PICTURES
Images en couleur

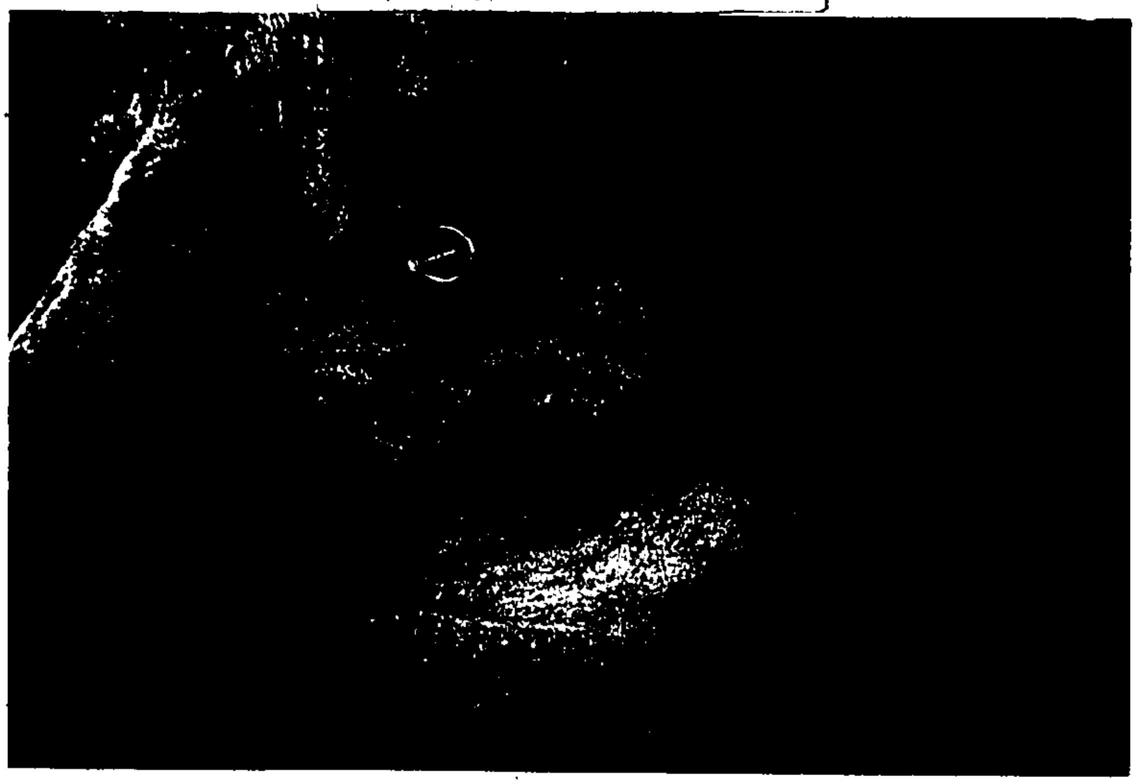

Figure 3.15 Close up plan view of fissure 9, about halfway down the section. Note (unusual) width of central fissure; faint lamination within the fissure, parallel to the walls; and difference in the grain size between the (medium) sand within the fissure and the (fine) sand of the surrounding beds. Lens 2.5 cm across.

(very rarely) more than 2 to 3 cm, and exceptionally 6 cm (fig. 3.15), with an average width of about 2 mm. There is some small-scale relief to the planes of the central fissures, of not more than about 3 cm in most cases (fig. 3.15 shows an exception). The sediment within the fissure is similar to that of the surrounding or nearby beds, that is, well sorted very fine to medium sand. Where they are thicker, the central fissures are well laminated to vaguely laminated parallel to the fissure walls. The lower termination of a fissure (in section) was uncovered in only one instance (fissure 7, fig. 3.16). Here, the fissure gradually tapers to nothing within otherwise undisturbed cross laminated very fine sand. The termination of a fissure in plan view was observed at the eastern end of fissure 3. This termination is also a gradual tapering of the central fissure and adjacent downturned beds.

3.2.4 MULTIPLE FISSURES WITH UPTURNING OF ADJACENT STRATA

Fissures 6, 7, and 8, which have a spacing of about 3 m between them, change in aspect at a specific horizon within the sediments. This horizon is marked by the occurrence of a bed, of varying thickness, of well sorted structureless fine sand (A, fig. 3.17). The expression of the fissures through and above the structureless sand bed is as irregular, roughly vertical, sand-filled planar channels which have either a thin (2-5 mm) central channel with adjacent slight upturning of the

COLOURED PICTURES
Images en couleur

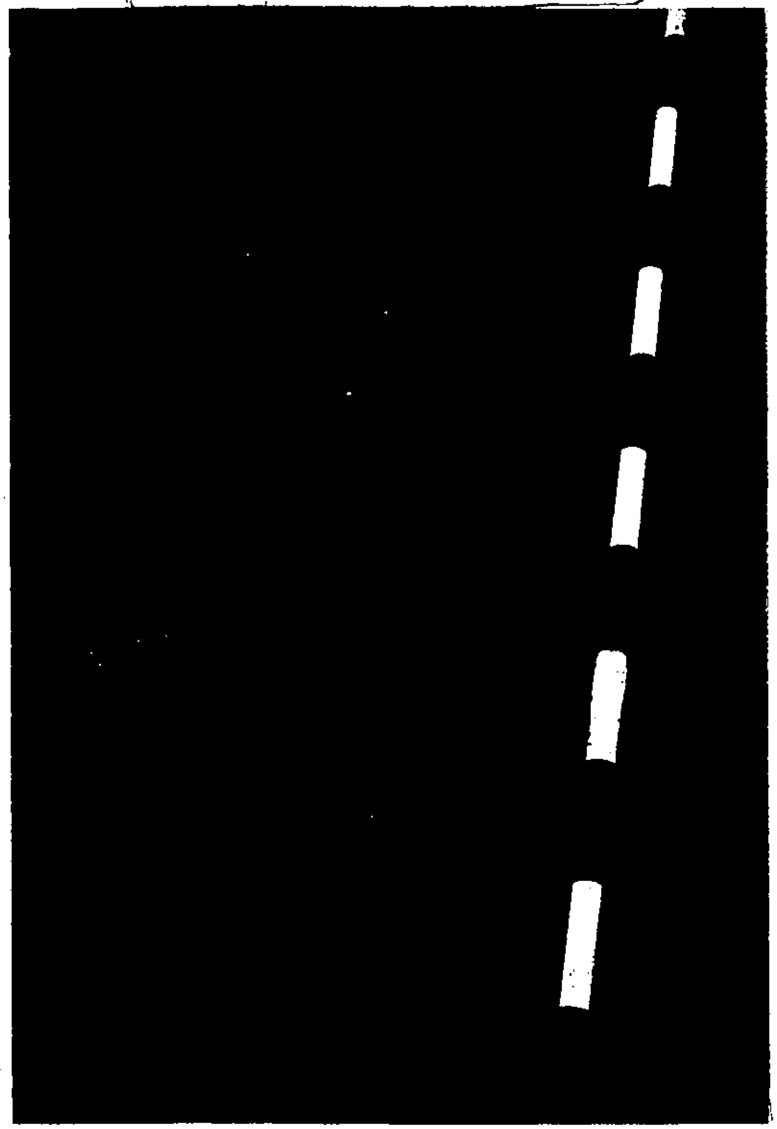

Figure 3.16 Fissure 7, showing lower termination (hollow arrow), and short upper dike-like section (fluidized intrusion) (between solid arrows). Scale in dm.

COLOURED PICTURES
Images en couleur

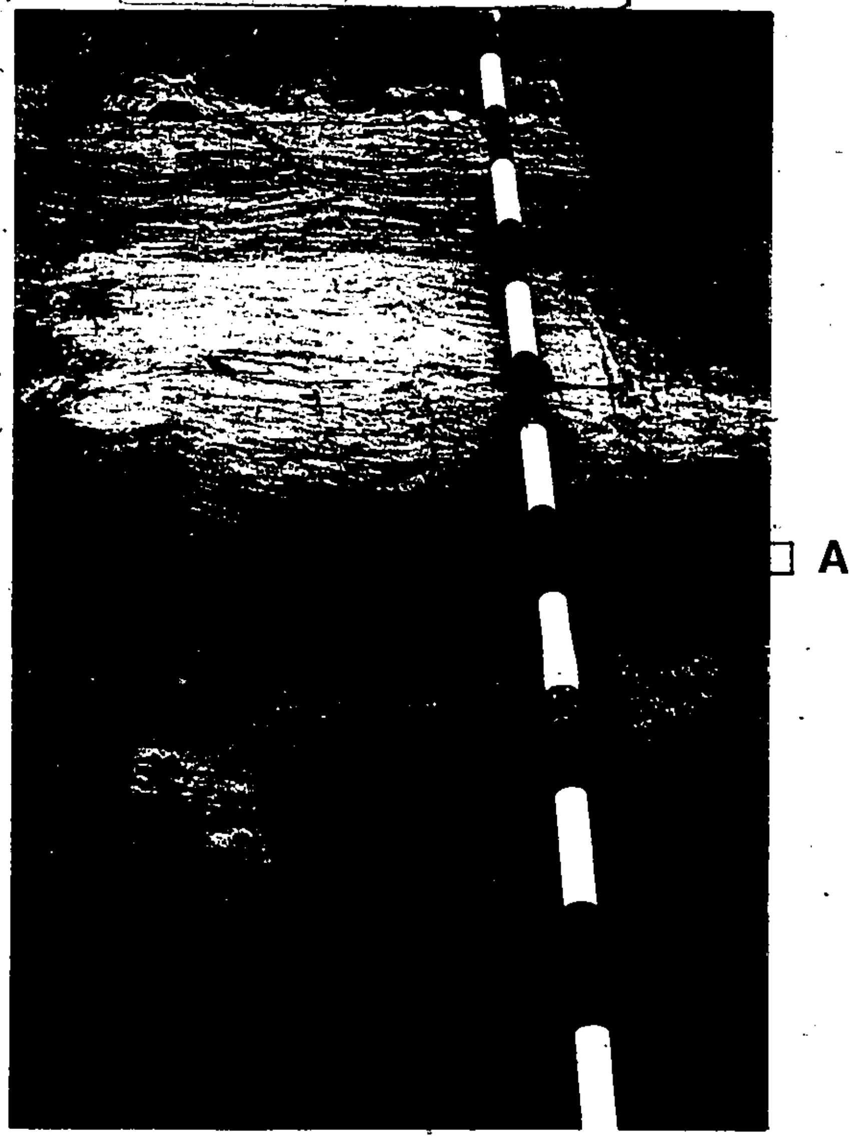

Figure 3.17 Central part of fissure 6. Note 8 cm thick bed at A of well sorted, structureless fine sand, above which there is slight upturning of the sediments adjacent to a >1 cm wide central fissure. Scale in dm.

beds, or, more rarely, are thicker and cut the sediment sharply and cleanly, in a dike-like manner (figs. 3.16 through 3.20). Fissure 6 continues upward in the former manner for 70 cm, changing in dip upwards from vertical to 60°, then becomes obscured within a bed of convoluted rippled sand containing balls of foundered clayey silt. From that point upwards the fissure is discontinuous in section, and where visible, it tends to be thicker (5-10 mm), and dike-like, and consists of structureless fine sand. Fissure 7 has a very short (10 cm) section with upturned strata, above which the fissure is thick (2 cm), massive and dike-like, and ends abruptly 10 cm above the top of the section with the upturned strata (fig. 3.16). The fissure re-appears 40 cm above this, in the form of a straight, sub-vertical, 2 cm thick dike, which continues upward for another 50 cm, past the limit of access. Digging into the face a few cm did not reveal a continuation of the fissure between the upper and lower dike-like sections, and it is assumed that the dikes are in the form of patchy, discontinuous but interconnected sheets. Fissure 8 is a thin (1-2 mm), irregular dike through and above the massive zone and continues in this manner upwards for 70 cm to where it becomes obscured in the weathered face of the section. It cuts the surrounding sediment cleanly.

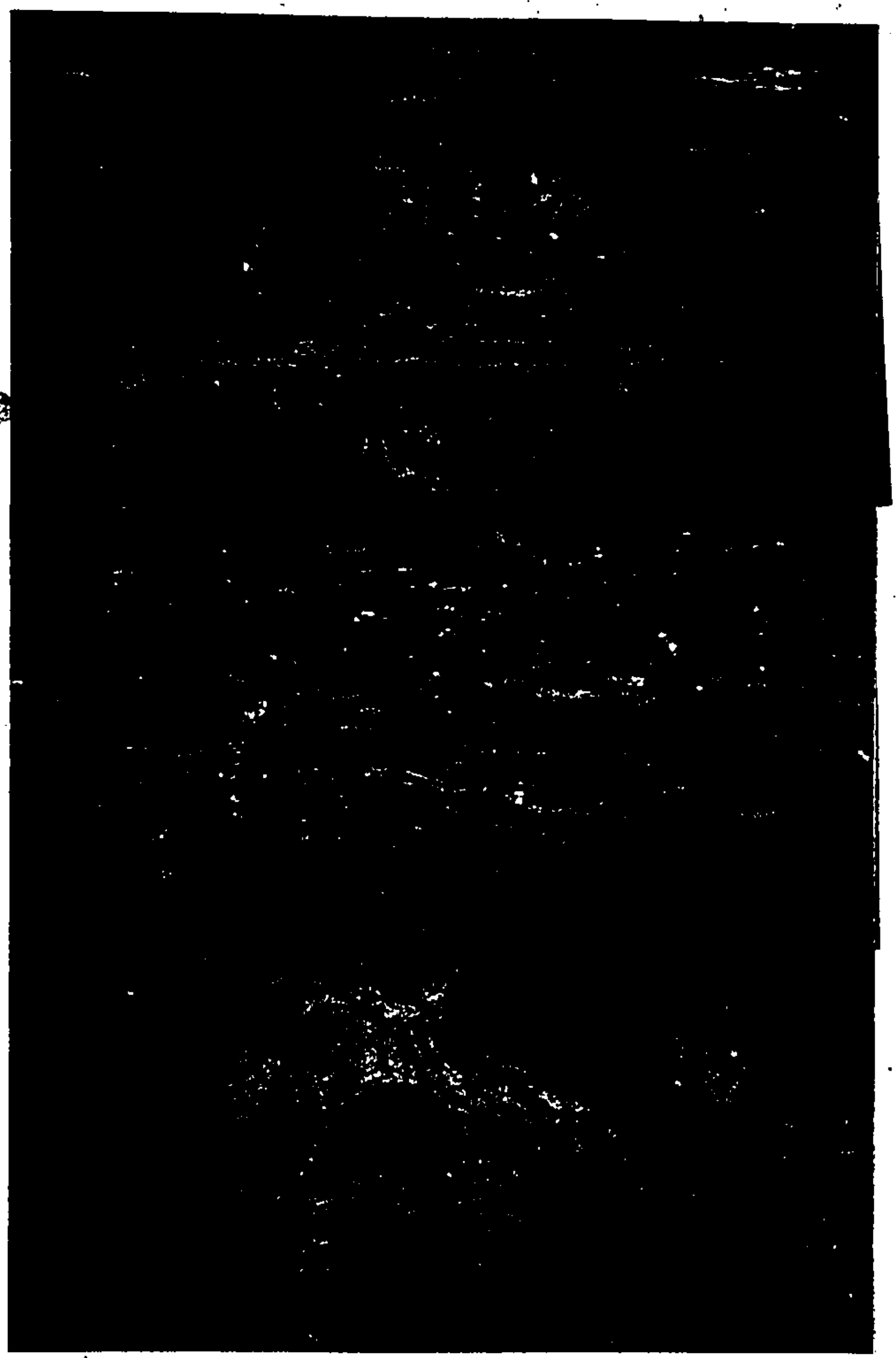

Figure 3.18 Upper part of fissure 6, vertical section. Arrows point to short, discontinuous dike-like segments containing structureless to faintly parallel laminated sand. Distance across top of photo is 1.3 m. Fissures cut earlier formed convolutions.

Figure 3.19 Upper part of fissure 7 (above upper solid arrow in fig. 3.16). Solid arrows indicate discontinuous dike-like segments of fissure; hollow arrows point to massive sand units, representing possible horizontal zones of fluid escape and/or fluidization. Scale in dm.

COLOURED PICTURES
Images en couleur

Figure 3.20 Close-up of upper part of figure 3.19. Arrows as for Fig. 3.19.

FISSURE NUMBER	DEPTH	AVERAGE WIDTH	AVERAGE DIP IN DEGREES	NATURE OF THE TOP OF THE FISSURE	NATURE OF THE BOTTOM OF THE FISSURE
1	>2m	8cm	85	truncated by pit excavation	not exposed
2	>4.5m	12cm	80		
3	>4.2m	10cm	75		
4	>2.5m	5cm	65		
5	>3m	10cm	88		
6	>1m	12cm	80	changes to multiple channels showing slight upturning of laminations adjacent to the channels	
7	>30cm	4cm	70		gradual tapering to undisturbed beds.
8	>1.5m	5cm	85		not exposed
9	>3.2m	12cm	75	truncated by the unconformity at the base of the (Champlain Sea) littoral deposits	not exposed

Table 3.1 Chart of some of the physical characteristics of the fissures. Widths include the adjacent downturned strata.

3.2.5 SIMILARITY OF FISSURES TO FAULTS

The downturning of the beds adjacent to the central fissure resembles drag along a fault (fault drag folds or distributive faulting). Fault-related drag, however, is in the opposite sense on either side of a fault. The deformation associated with the fissures in the Chevrier pit is always in the same direction (downwards) on either side of a fissure. This, together with the fact that there is no net displacement of beds across the fissures, eliminates the possibility that they originated through faulting. The possibility that the fissures are a very recent phenomenon, resulting from relaxation or stress release within the sediments as a result of excavation, can be dismissed, because the fissures do not offset the diagenetic ferruginous bands, they are not parallel to the face of the excavation, fissure 9 ends abruptly at the littoral unconformity, and in any case such features would have the characteristics of faults.

3.2.6 ORIGIN OF FISSURES AS FOSSIL ICE VEINS

Physical resemblance to frost wedges

The fissures are similar to certain types of frost veins and wedges, fossil and active, reported from similar sediments

~~by~~ some workers (French, 1983, and unpublished photographs) (figs. 3.21,3.22); Gangloff et al, 1971; fig. 32 of Johnsson, 1959; fig. 16 of Dionne, 1971; and "sag" veins of Katasonov, 1973, and Romanovskij, 1973; and especially plate 7 of Romanovskij, 1973). The microfaults and downturning of the bedding next to the central fissure is the most similar aspect. In the case of fossil ice veins and wedges, the faulting is an adjustment of the sediments to the loss of support at the centre of the crack or wedge upon melting of the ice core. The slight irregularity of the central fissure as seen in section is another similarity, and Johnsson (1959) reported that it is common to find asymmetric downturning of the beds on either side of the fossil ice wedge casts, as in the case of several of the St. Lazare fissures (fig. 3.13).

Post-glacial climatic conditions

Studies of modern, active ice wedges show that average annual ground temperatures of -6°C or less are necessary for their development in fluvial sands (Black, 1975). A large number of fossil ice wedges and other fossil periglacial features has been reported from southern Quebec (Dionne, 1974; Lagarec, 1973, Gangloff, 1970). These have been attributed to periglacial conditions present near the edge of the retreating ice sheet (Dionne, 1971) or to general climatic cooling associated with the Cochrane ice readvance ~~in Northern~~ Ontario

Figure 3.21 Fossil frost wedge formed in glacial outwash near Lodz, central Poland, during the last (Weichselian) glaciation. Lens cap 6 cm dia. (photo courtesy of H. M. French).

Figure 3.22 Fossil frost wedge in Quaternary sediments at Belhatow, southern Poland, probably formed between 45000 and 25000 y B.P. Fissure is identified as syngenetic, that is, it formed and grew along with deposition of the sediment package. Spade handle 70 cm long. (photo courtesy H. M. French)

at around 8,000 yrs B.P. (Gangloff, 1970), or to other postulated cold periods since the regression of the Champlain Sea (Lagarec, 1973). Several authors, including Terasmae, (1959), and Lasalle (1966), confirmed Potzer's (1953) discovery of pollen evidence for a cold phase in the early Holocene. This phase is referred to as the Cockburn Glacial Phase or Cockburn Stade and has been correlated with European events, including the Poroslav phase in the Soviet Union. Lambert (1972) reported the existence of cryoturbation structures in Champlain Sea sediments at Oka, Quebec, less than 10 km from St. Lazare, at a similar elevation as the St. Lazare fissures. He attributed their development to a climatic perturbation corresponding to the Cockburn readvance in Northern Ontario at 8,500 to 8,000 yrs. B.P. The evidence for the existence of periglacial (tundra) conditions after 11,000 yrs B.P. is, however, equivocal. Some palynological evidence indicates that tundra was not widespread after that time (Dionne, 1974). Andrews (1973), Prest (1970), and Hughes (1965) consider the Cochrane event to have been a surge of the ice sheet from the western side of Hudson Bay, of local importance only, and not due to any climatic perturbations. Davis (1969) reported, however, that tundra clearly persisted as far south as southern New England until 9500 yrs B.P., and Richard (1971) suggested that permafrost may have been present in the Laurentians, 350 km northwest of the study area, until 7200 B.P. Lagarec (1973) reported the existence of fossil periglacial features, including polygonal ice (or soil) wedge forms, in sediments of the Champlain Sea and suggested that there may have been several cold episodes since 6000 yrs B.P. (mean annual temperature -2° to $-4^{\circ}C$). Uplift curves for the Montreal region (Hillaire-Marcel, 1979, and Corbeil, 1984, (see fig. 3.23), indicate that 100 metres of isostatic uplift took place in the first 1700 years after deglaciation, which was sufficient to have exposed the St. Lazare plateau to subaerial conditions by 10,200 yrs B.P. (fig. 3.23). It seems possible, therefore, that the st. Lazare plateau may have been subjected to several hundred years of periglacial conditions at some point after regression of the Champlain Sea.

Current theories on the origin and growth of frost wedges require at least a few hundred years of permafrost conditions for frost wedge networks to develop in fine sands (Dionne, 1974). They may also develop in areas of discontinuous permafrost (Black, 1975). Only a few decades of these conditions may be necessary for narrow frost veins to develop (incipient frost wedges, or "sag veins" of Romanovskij, 1973). Many workers have, moreover, recorded the presence of seasonal frost cracks in non-permafrost areas due to severe winter freezing (Washburn, 1980). The fissures at St. Lazare, if formed by frost processes, would represent only the early stages of frost wedge development (ice veins, according to Washburn) because of their narrowness and the fact that they do not form a polygonal network.

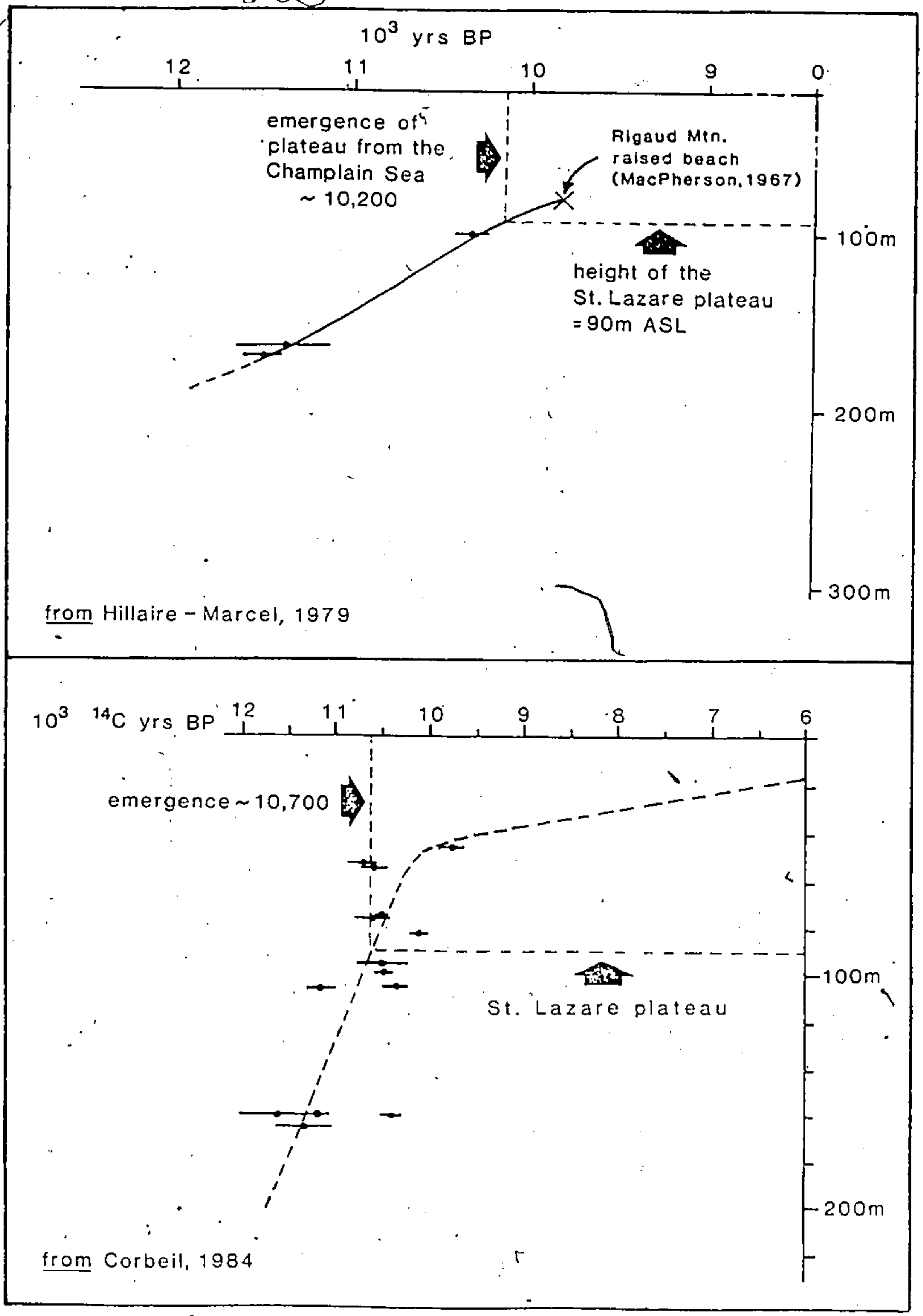

Figure 3.23 Emergence curves for the Champlain Sea, Montreal region. Emergence of the St. Lazare Plateau occurred by at least 10,000 y BP.

Arguments against origin of fissures by frost cracking

1. The fissures are deeper than the average depth of frost wedges (3-4 m, French, 1983). Black (1983) states that wedges more than 4 m deep occur only in ice-rich fine grained sediments [silts and clays]. The St. Lazare fissures are in sand, and are significantly deeper than what would be expected in incipient frost wedge development, despite the fact that the observed depths are less than the true depths (table 3.1). Depths of seasonal frost cracks recorded by Washburn et al (1963) are less than 1 m. Thus, the depth to width ratios of the fissures at St. Lazare are far larger than would be expected from frost cracking.

2. Black (1975, p. 11), in his list of criteria for recognition of ice-wedge casts, states that "single wedges are suspect anywhere". In addition, frost wedge networks tend to develop, especially in the initial stages, with 90° (orthogonal) intersections between wedges (French, 1983). Only two out of the nine fissures at St. Lazare were observed to intersect with each other, and the angle of intersection is 30°. Even if these features represent the earliest stage in the development of a frost wedge network, non-orthogonal intersection of fissures does not fit the accepted morphology of frost wedge networks.

4. Black (1983) observed that ice wedges form in silts and clays much more readily than in clean sands, and, where

frost wedges are found in coarser material today, they are always better developed in nearby fine grained deposits. No frost cracks or wedges have been reported in the Vaudreuil area (H. Richard, pers. communication, 1983), and Dionne (1974) notes that no ice-wedge casts have been reported from areas that were submerged by the Champlain Sea.

5. The downturning that occurs adjacent to the central fissures is not vertically consistent, that is, the amount of sediment laterally affected by downturning varies along the length of the same fissure, in some cases from >20 cm to virtually nothing. This is difficult to explain by frost cracking, as the width of frost veins and wedges, and hence the amount of space left to be infilled by sediment when the ice melts, is relatively consistent with depth, or it diminishes consistently with depth because of downward tapering of the original ice wedge.

6. Fissures 6, 7, and 8 do not extend to the surface, at least not in a form which resembles any known type of fossil frost crack, vein, or wedge, but end at least 2 m below the surface. The only likely explanation for this, if the fissures were frost veins, is that they were formed before the strata above the termination were laid down. If the veins were then buried by later deposits, subsequent degradation and melting of the ice veins might account for the water escape features observed (with upturning of strata next to the central fissure). This would correspond to a form of syngenetic ice

wedge, as described by many Soviet authors. The objection is that there must have been more than a hundred metres of marine water above the outwash fan as it was being deposited (see discussion on timing of maximum extent of the Champlain Sea, chapter 2), precluding the development of frost cracks.

7. The most significant piece of evidence against the frost cracking hypothesis is shown in fig. 3.24, where the the top of a fissure is truncated by the unconformity beneath the overlying wave-reworked sediments. This indicates that the fissures predated the regression of the Champlain Sea, as it is not possible for frost cracking to occur subaqueously, unless the entire water column above the sediment was frozen. This evidence restricts the crack development to the very brief period during regression of the Champlain Sea when the water depth above the fan was shallow enough to permit development of winter sea ice from the water's surface down to the top of the fan, but before the top of the fan was at wave base. In the writer's opinion this is very improbable, as ice above the sediment would insulate it from the large and sudden temperature drops needed to initiate and propagate frost cracks. The formation of active ice wedges below sea ice has not been reported.

COLOURED PICTURES
Images en couleur

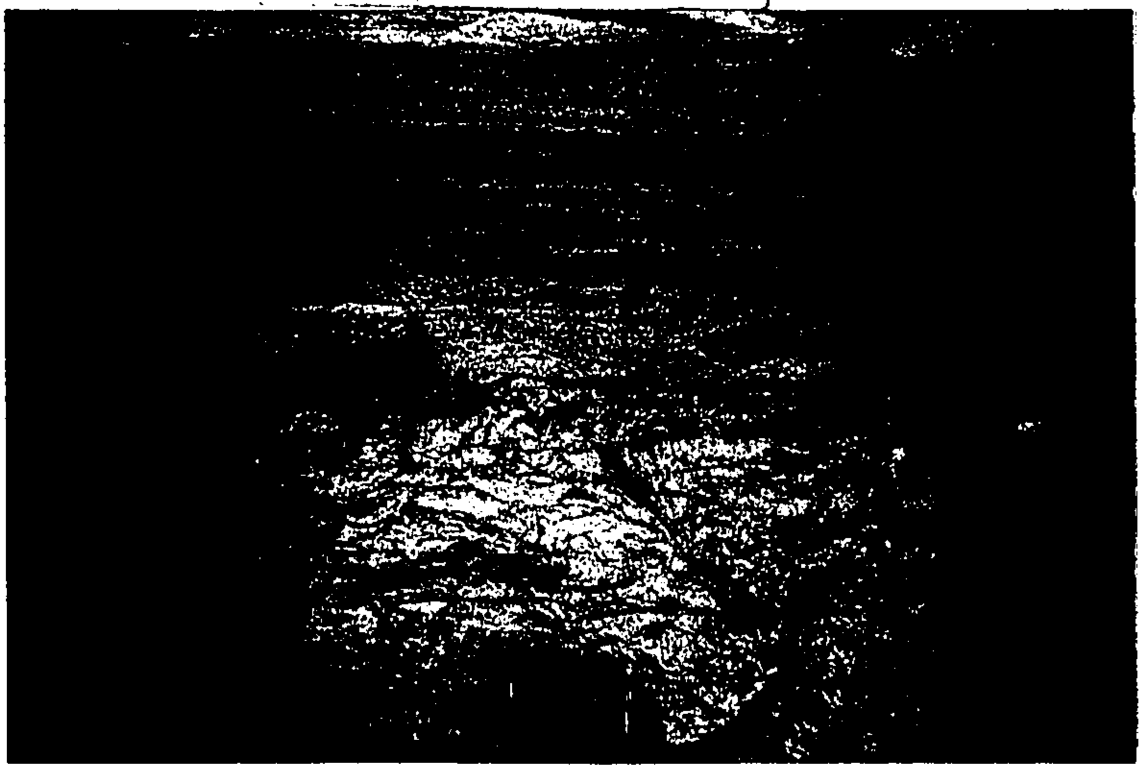

Figure 3.24 Top of fissure 9, where it is truncated by the erosional unconformity which represents the base of the sediments reworked by littoral processes in the Champlain Sea. Note that the fissure does not continue above the unconformity. Shovel handle 12 cm across.

3.2.7 EXPLANATION OF FISSURES AS WATER ESCAPE STRUCTURES

Water escape structures form in unconsolidated sediments as a result of expulsion of excess pore water accompanied by readjustment of all or part of the sediment into a more stable and more tightly packed fabric. The escaping pore fluid tends to be confined and channelled within the sediment, creating localized zones in which the escaping fluid moved at relatively high velocity. This flow may cause the sediments within the channels to become entrained and flow with the escaping pore water in a process called fluidization. Lowe and LoPiccolo (1974) were the first to explain the genesis of water escape fissures (pillar structures), and did so in the context of the formation of dish structures, common in many sedimentary sequences. The most comprehensive review and analysis of various water escape structures to date is that of Lowe (1975),who showed that the process of fluidization of sediments or part of a sediment package is an integral part of the formation of pillar structures. Lowe and LoPiccolo define fluidization as a process in which "the individual sediment grains become partially or entirely supported by the drag of upward moving water". This is distinct from liquefaction, where "loosely packed, metastable grains are shaken loose from each other and briefly settle unsupported through the pore fluid". Kunii and Levenspeil (1969) defined a point at which the upward velocity of the pore fluid becomes high enough to entrain the sediment grains, thus initiating fluidization. At lower velocities, fluid escape takes place by seepage through sediment which remains undisturbed. The grain size of the sediment is the most important factor controlling its susceptibility to fluidization. Fine grained sand is most easily fluidized (Lowe, 1975). Fluidization is most likely to occur in sands deposited at high rates of sedimentation because they have the highest initial pore water content.

Lowe (1975) defined five different types of water escape pillars, (or fluidization channels, as they are known in engineering terminology). All five classes include both cylindrical and planar forms, and Lowe makes no attempt at distinguishing between the two. Cylindrical pillars (or water escape pipes of other authors, see Plint, 1983), differ from planar, or sheetlike, pillars in morphology only, not in genesis or internal structure. Lowe's second, or "B" type of pillar, includes large (up to "many" metres), planar vertical and subvertical forms. Internally, the pillars may be massive or faintly laminated. Although not discussed by Lowe, there must be a gradation between type B pillars and Lowe's "fluidized intrusions", which he has classified in a separate category under the general heading "soft sediment intrusions".

Lowe (1975) described fluidized intrusions as channels along which fluidized sediment moved. They are recognized by the presence of homogenized sediment in tabular bodies.

Fluidized intrusions are one in a group of three types of soft sediment intrusions, the other two types being hydroplastic intrusions and liquefied intrusions. The distinction between the three types is made on the basis of the inferred differences in the interactions between the sediments and the pore fluid. Fluidized intrusions are characterized by turbulent flow. Lowe states that the structures resulting from fluidized intrusions are clastic dikes and sills.

Peterson (1968) described and illustrated sandstone dikes and the nature of their internal structures. He noted that bedding and laminations parallel to the walls are common within the dikes.

Lowe (1975) stated that "the upward flow of sediment and water within fluidization channels is commonly accompanied by a more or less continuous subsidence of surrounding grain-supported sands...and occasionally by slumping of the pillar walls...similar to spouting beds of industrial fluidization systems". Two of Lowe's figures (1975, figs. 6a and 6b) illustrating type B pillars show downturning of the sediments immediately adjacent to the pillar walls, in a manner similar to the St. Lazare fissures. Plint (1983) described downturning in fluidization pipes in Eocene sands, and, most notably, in his figure 7 downturning occurs as a series of microfaults. In another (1983b) paper, Plint illustrated (his fig. 6) and described collapse of adjacent bedding into the fluidized core of a dewatering pipe. Gill and

Kuenen (1958) depicted the internal structure of some sand volcanoes in Carboniferous sandstones in Ireland, and their cross sections show downturning of beds at the margin of the feeder pipes of the sand volcanoes (which are type B pillars or fluidization channels by Lowe's definition). Experiments involving laboratory-produced fluidization channels showed that the fluid flowing within the channels was relatively dilute, in other words had a low sediment-water ratio (Gill and Kuenen, 1958).

It seems most likely that the fissures in the Chevrier pit are a form of water escape structure. The intimate association of the fissures with definite water escape structures (exhibiting upturned strata and dike-like fluidization channels) is strong circumstantial evidence. Lamination parallel to the fissure walls is common to clastic dikes (Peterson, 1968)(fig. 3.15). Neither of these structures is characteristic of fossil frost veins (Black, 1976).

In the St. Lazare features, the downturning of the beds beside the fissures resulted from failure of the fissure walls and slumping into an open central fissure created by removal of sediment by the upward movement of escaping pore water. This flow would have been relatively dilute, and failed to support the adjacent fissure walls. Where the fissures dip at a relatively low angle, the beds on the lower side of the fissure are supported from below and slumping occurs only on the upper side.

An alternate explanation is that a zone of fluidization existed, in which the degree of fluid support varied in a gradient from fully fluidized along the fissure, gradually reaching zero support along the margin of the downturned zone. When upward pressure decreased the sand subsided downward to a degree proportional to the original upward support. This explanation is not preferred, for the following reasons:

1. Lateral gradients of fluid support are not observed to occur in laboratory fluidization experiments (Kunii and Levenspeil, 1969); rather, channelization of the escaping fluid is the most common occurrence, and is the least desired effect with respect to engineering concerns.

2. The fissures intersect beds of very fine material such as fine silt and clay, which would have not fluidized or would have been much more resistant to fluidization than the subjacent sand (Lowe, 1975). These beds would certainly have interfered with a zoning or gradient of fluidization, and would have resulted in an interruption of the smooth downturning along the fissures. The characteristic aspect of downturning does not change across these beds of very fine material. The former explanation seems to fit much better here - the clayey silt bed would have been breached by a relatively narrow zone of escaping pore fluid.

3. The fact that there is downturning at all implies that sediment was removed from somewhere along the fissure to provide space for the slumping to occur, and the latter explanation does not provide for this. It might be argued that melting of buried ice directly below the fissures provided the void into which the sediment collapsed, but adjustment of unconsolidated material to a large void space is distributed upwards and outwards from the void, so that the effect of the void is rapidly diminished upward. That there is approximately the same amount of downturning along the length of the fissures indicates that sediment was removed along the length of the fissures.

4. The places where one side of the fissure has remained completely undisturbed are difficult to explain with the second hypothesis. It seems easier to see that no collapse occurred on the lower side of some fissures that were shallowly dipping because they were supported from beneath (first hypothesis), than because for some reason during the fluidization event the sediments on the lower side of the fissure failed to undergo any fluidization (second hypothesis).

In the upper part of fissures 6, 7, and 8, where there is upturning, or little or no downturning, the material moving through the channels was much denser (higher sand-water ratio) and provided support to the fissure walls, and, in some places, exerted enough shear against the fissure walls to cause upturning of the beds. When flow ceased in these sections, the sand-water slurry in the fissures "froze" in place, creating a plug of massive or faintly structured sand. Change from downturning to upturning may have been caused by a diminution of fluid velocities consequent upon branching of the main channel. Branching tended to occur where the channel encountered a bed of high enough permeability to allow flow of pore fluid within it, relieving the pressure in the main fluidization channel (zone A, fig. 3.17). Beds of well sorted sediment deposited mainly from suspension are most likely to have provided these relief channels, and may or may not have themselves been fluidized as a result. These beds would have had the highest initial porosities and high permeability and may have had a massive primary structure (see figs. 3.16 through 3.20). Upward from the point at which this lateral branching or relief of the fissures took place, most of the water escape channels are irregular and discontinuous, and would have had internal fluid velocities less than in the lower sections. It appears that in fissure 6 (fig. 3.17), during waning flow after the fluidization event, flow of escaping fluids in this section of the fissure may have continued upward across zone A.

The St. Lazare fissures cut convoluted beds, so are clearly post-depositional. The fissures are themselves cut by diagenetic ferruginous bands and therefore predate them. The fissures are believed to have been formed before regression of the Champlain Sea, because the dewatering processes described above take place subaqueously. The high pore water pressures may have been provided by remnants of glacier ice buried at some depth within the fan sediments (beneath the fissures). Elsewhere in the Chevrier pit there is evidence of melting of buried ice (see chapter 2). This would have charged the sediments with high pore water pressures, and upward relief of this pressure might have taken place first by seepage, then by concentration of seepage flow into planar channels where velocities of flow surpassed those necessary for fluidization.

In view of the relative rarity of large planar dewatering structures reported in the literature, the question arises as to why the relief of excess porewater pressure took place in the St. Lazare case by way of planar rather than the more common cylindrical or pipe forms. Although there is little or no total displacement of the beds across the St. Lazare fissures, stresses favoring the incipient development of minor faults within the sediment, over a cavity produced by the melting of buried ice, may have controlled their formation. The release of stress would tend to take place along planes, even if the cavity was relatively equidimensional. In addition, there exists the possibility that there were meltwater channels within the buried ice mass (either newly formed or relict) that collapsed and provided elongate cavities that controlled the nature of the stresses within the sediment.

The downturning was not caused by simple collapse into a cavity as the downturning tends to be regular and continuous along the length of the fissure. Adjustment of a mass of sediment to fill a cavity diminishes rapidly away from the source of disturbance. In addition, fissure 7 was observed to terminate downwards in undisturbed sediment.

3.3. CHAPTER 3 SUMMARY AND CONCLUDING STATEMENTS

Post-depositional structures in the Chevrier pit that resemble certain types of fossil frost wedges are interpreted as water escape fissures. They were formed before regression of the Champlain Sea, possibly in response to elevated pore pressures at depth within the subaqueous fan deposits, caused by melting of remnant glacier ice. The fissures are characterized by an adjacent zone in which the host sediments are downturned. Although climatic conditions favorable to the development of frost wedges may have been present in the early Holocene, there is strong evidence against formation by frost cracking processes. The two main points are: (1) the fissures predate the subaerial exposure of the fan deposits by regression of the Champlain Sea, and (2) three of the cracks end at depth within the sediment and water escape channels extend upwards from these terminations.

The morphology of the fissures is a result of fluidization of the sediment within planar channels. Excess pore water, possibly due to the melting of buried ice, initiated flow of relatively dilute sediment-water mixtures, and led to erosion of the host sediments along the fissure. Slumping of the fissure walls followed, as the dilute sand-water slurry moving up the fissure was not dense enough to provide support. Some of the fissures may have branched or bled off laterally along permeable beds of massive sand, and continued upwards as denser fluidized intrusions, which remained as massive or faintly structured sand dikes upon cessation of flow within the channels. Minor faulting over cavities created by melting ice may have controlled the (planar) form of the fissures. The lack of reports of this type of water escape structure in the literature, even from other deposits of glacifluvial sands in the Ottawa Valley, indicates that the following combination of depositional conditions is unique to deposits of this type. Characteristic features of the St. Lazare outwash fan deposits are:

1. Permeable, easily fluidized sediments are underlain by relatively impermeable clay-rich diamictons.

2. The areal extent of the deposits is relatively large, which increased the chances of remnant ice being buried, and of any one particular place in the sediment package

being hydrologically connected to melting remnant ice.

3. Laterally extensive interbeds of fine-grained material deposited from interflows or overflows, especially common in the marine environment, are observed in the deposits at St. Lazare (See discussion, chapter 4) and, acting as temporary permeability barriers, may have served to localize or direct buried meltwater release.

4. The existence of cavities created by melting remnant ice induce faults of limited displacement which control the development of the water escape fissures.

CHAPTER 4: INTERPRETATION AND DISCUSSION

4.1 THE ICE - PROXIMAL GLACIMARINE ENVIRONMENT

4.1.1 SUBWASH

Rust and Romanelli (1975) introduced "subaqueous outwash" to describe deposition of glacigenic sediments at the margin of a glacier, below wave base in a marine or lacustrine environment. Recently workers have recognized that this is not an uncommon situation, and indeed that many mapped ice-marginal features may have some component of subaqueous deposition (Fox and Powell, 1985; Domack, 1984; McCabe, 1984; Thomas, 1984; Fenton et al, 1983; Dredge, 1983; Cheel, 1980; Proudfoot et al, 1980; Rust, 1977; Banerjee and McDonald, 1973; Gustavson et al, 1973; Wisniewski, 1973; and Saunderson, 1973).

Goldthwait (1985) has included subaqueous outwash in the most recent revision of the "Analytical Classification of Glacigene Landforms", a project initiated by the Second Inqua Commission in 1973. He coined the shortened term "subwash", which is preferred by this author. Goldthwait classified subwash under the broad category of "indirect glacially-induced landforms", under a sub-category of "proglacial landforms", and thirdly under a second sub-category of "glaciolacustrine/glaciomarine deposits".

TABLE 4.1

EXCERPT FROM GOLDTHWAIT'S (1985) CLASSIFICATION OF GLACIGENIC LANDFORMS: [present author's comments in square brackets]

I. direct glacial landforms
   A. subglacial landforms
      1. streamlined topography
      2. drumlin field
      3. ground moraine
      4. minor (pressure) moraine
   B. ice marginal landforms
      1. minor (dumped) moraine
      2. lateral moraine complex
      3. end moraine system
II. indirect glacially-induced landforms
   A. ice marginal glacifluvial landforms
      1. hillside channel (meltwater erosional form)
      2. esker system or ose
      3. kame field
         a. moulin kame
         b. kame plateau
         c. kame terrace
         d. kame delta (marginal ose): pitted but gently sloping top, apex channel hanging atop ice-contact slope; gravel topsets, long foresets, lobate into temporary lake or sea-level.
   B. proglacial landforms
      1. Scabland topography
      2. outwash systems (sandur) [subaerial fluvial deposits]
         a. outwash fan: symmetric gentle cone, distributary dividing channels; coarsest gravel at head, finest sand at outer edge; bedding parallel to surface.
         b. valley train
         c. pitted plain
         d. outwash delta: wherever plain (a,b, or c above) reaches lake or sea; lobate underwater edge; sand with fine gravel topset; topset/foreset structure.
      3. glacial lake or marine plain: glacilacustrine/ glacimarine deposition [subaqueous deposits]
         a. outwash delta (as above II, B, 2,d) glacifluvial with subaqueous flows.
         b. SUBAQUEOUS OUTWASH (SUBWASH): overlaid irregular lobate mounds, poorly sorted sand to pebbles, lenticular current beds arched (slightly backset and foreset); believed deltas from underwater ice-cliff tunnel[s].
         c. strandline
         d. varved laminae (rhythmites)
         e. marine clay

4.1.2 SUBWASH FANS

Goldthwait has distinguished between subwash fans (category II,B,3,b), and deltas (categories II,A,3,d,kame delta; II,B,2,d, outwash delta, [subaerial component, or topset beds]; and II,B,3,a, outwash delta, [subaqueous component]). Cheel (1980, p. 23) emphasized this important distinction between true deltas, which by definition form with a subaerially exposed upper surface (Barrel, 1912), and subaqueous fans, which lack the control on the upper surface that an air-water interface imposes. This is a distinction that is not always made when discussing subwash fans, even when they are recognized as such (Thomas, 1984; Dredge, 1983; Gustavson et al, 1973; Banerjee and McDonald, 1973; Aario, 1972; Axelson, 1967; DeGeer, 1940). (Unfortunately, Goldthwait has used the term "delta" in his description of subwash deposits). Harrison (1972, p. 7), proposed the term "attenuated deltas" for subwash fans in the North Bay area, Ontario. Completely subaqueously deposited fans occur in environments other than the ice-proximal, of course, for example at the bottom of shelf slope channels on continental margins, and, on a much smaller scale, in tidal channels. Fenton et al (1983) identified fans composed of glacifluvial sediment, but formed by turbid underflows at the mouths of glacier spillways where they emptied into Glacial Lake Agassiz ("underflow fans").

The most significant implication of this with respect to facies interpretation is the lack of topset beds formed through ordinary subaerial fluvial processes on the top of a subwash fan (Gustavson et al, 1975). According to Hjulstrom (1958) deltas have characteristically greater foreset slopes than do subaqueous fans. Axelsson (1967, p. 9) made the observation, however, that some river-mouth deltas have quite gentle foreslopes and lacked true foreset bedding. Submarine fans in continental slope regions, which are dominated by resedimentation processes, typically have a subdued concave to partly convex upward longitudinal profile (similar to alluvial fans). Problems of scale, however, make comparisons with the much smaller subwash deposits tenuous. McCabe et al (1984, p. 727), and Thomas (1984, p. 19) illustrated in their depositional models of subwash a gentle, slightly convex upward wedge of sediment, decreasing in thickness outward from the ice front. Slumping and resedimentation play an important role in the formation of these fans. Fenton et al (1983, p. 56) and Cheel and Rust (1982, p. 291, 292) indicated similar fan morphology where slumping is not believed to have dominated the depositional processes. Dredge (1983, p. 120), however, identified subwash fans from Glacial Lake Agassiz, deposited in contact with the Keewatin ice front, in the form of "distinctive flat-topped pads with steeply dipping foreslopes". Fan or delta morphology does not appear to be a reliable criterion for distinguishing between subaerial or subaqueous deposition. There are two processes which may contribute to the creation of a flat top on a subaqueous fan: The first is that the top of the fan may be maintained at a certain height as the glacier margin slowly retreats during deposition, although the surface would be quite irregular due to the highly variable conditions as the ice recedes. The second is that subsequent reworking by waves as the proglacial water body drains or recedes will tend to truncate and flatten the top of the feature. Fans formed in proglacial lakes, which, if ice-dammed, may drain catastrophically, will have their original (presumably irregular) morphology preserved. Marine incursions such as the Champlain Sea are generally controlled by isostatic rebound and drain more slowly. The author believes that the deposits at St. Lazare represent a relatively flat-topped subwash fan with a relatively steep and morphologically distinct front fan margin, characterized by foresets in the distal areas with dips in the order of 10° - 15°. The flat top is primarily due to littoral reworking.

4.2 PROCESSES OF SUBWASH DEPOSITION

The following is a discussion of the various mechanisms by which sediment derived from subaqueous outwash is deposited. The specific environments of the St. Lazare fan are dealt with in section 4.3.

4.2.1 TURBIDITY CURRENTS AND TURBIDITY UNDERFLOWS

Kuenen (1951) defined a turbidity current as one which has a higher density than the body of water in which it flows due to the sediment suspended within it. He reserved the term "density current" for one which has increased density due to lower temperature or the presence of a solute phase (brine, for example). He noted that a turbidity current usually flows along the bottom ("underflow" of Bell, 1942), but will flow at any level within the water body where the density of the turbidity current matches the surrounding water. Gould (1951) expanded the definition to include overflows, where the inflowing turbid suspension is less dense than the surrounding water and flows over the top of the water mass. Overflows would be commonly expected in glacimarine environments, considering the difference in density between the fresh glacier meltwater and seawater.

In the glacilacustrine environment, underflows are common. Gustavson (1975, p. 258) demonstrated that a difference as little as 0.01% in density was required for underflows to form. Combined with the extreme temporal variability of the strength of meltwater efflux, this leads to the development of the common characteristically well-laminated glacilacustrine sediment (rhythmites and varves).

Similar rhythmites have not been observed until recently in glacimarine deposits (Domack, 1984). It was assumed that this was because underflows did not form, and because flocculation of clay size material in the saline environment suppressed sorting. Domack (1984) observed that flocculation and bioturbation tend to inhibit and obscure rhythmites in fine grained glacimarine material in distal basins, but that in the proximal areas turbid underflows are a major influence on sedimentation.

4.2.2 OVERFLOWS AND INTERFLOWS

Overflows and interflows may form directly at the subglacial or englacial tunnel mouth if the density of the debouching fluid is less than the surrounding water, or underflows may rise from the bottom to form interflows or overflows when decreasing sediment concentration reduces their density to less than the surrounding water (Powell, 1983). The velocities of these flows can be high enough (5 to 40 cm/sec) to carry up to fine sand sized material some distance away from the glacier front (Gilbert, 1982). Deposits from interflows and overflows are suspension deposits and in the open marine environment will form draped, structureless to graded laminae of clay to silt, or exceptionally, fine sand, at any position in the fan setting.

4.2.3 VARIABILITY OF MELTWATER DISCHARGE

The source of glacifluvial streams is meltwater from the glacier ice and runoff from precipitation that falls on the surface of a continental glacier and becomes incorporated into the sub- and englacial channel system. Weather, therefore, is the major control on the rate of flow in meltwater channels, and hence the amount of water debouching at subaqueous ice-marginal openings. Gustavson <u>et al</u> (1975) identified three nested cycles of discharge:

First order:	annual: winter freeze-up drastically reduces or stops discharge
Second order:	weather patterns (days to weeks)
Third order:	diurnal (present in summer only): results in fluctuation of flow strengh in Alaskan glaciers by a factor of ten (Mackeiwicz <u>et al</u>, 1983)

A fourth variable, superimposed on the above cycles, is the sudden release of meltwater filling pockets or cavities within the glacier, and the catastrophic discharge of ponded superglacial or subglacial lakes (Sugden and John, 1976).

Gustavson et al (1975) observed that meltwater discharge from the Malaspina Glacier in Alaska is drastically reduced but not always halted during the winter. Considering the very rapid rates of retreat postulated for the Wisconsinan ice sheet, (from 100 m/yr to a maximum of 500 m/y, Flint, 1963, p. 210) it seems reasonable to assume that there may have been continuous efflux of meltwater throughout the year, albeit greatly reduced during the winter.

4.2.4 VARIATION IN MELTWATER SEDIMENT CONCENTRATIONS

The concentration of sediment within glacifluvial systems is also variable. Hooke et al (1985) reported that the highest concentrations in subglacial streams in a Norwegian glacier occur during the first spring discharge, and thereafter the streams are more dilute. Ostrem (1975) observed that 60% of the total summer sediment flux was transported from a glacier on eastern Baffin Island during one 24 hour period. Short-term fluctuations in sediment concentrations were observed as well, on the order of hours to days, apparently unrelated to trends in total water discharge. The total sediment load usually reaches its maximum before the peak of meltwater flow (Ostrem, 1975); but the the peak of sediment concentration in meltwater commonly occurs up to several hours after peak flow (Fahnestock, 1963; Ostrem et al, 1967, in Mackiewicz et al., 1984, p. 120).

4.2.5 INITIATION OF TURBIDITY UNDERFLOWS IN THE GLACIMARINE ENVIRONMENT

A suspended sediment concentration of at least 34 g/l is required to exceed the density of marine water (Powell, 1983). Powell (1983) noted that subaerial glacial meltwater streams in Alaska have measured suspended sediment loads of up to 72 g/l. Inflowing subglacial streams of that concentration can be expected to form an underflow directly (hyperpycnal flow). This is in part due to the high viscosity of the cold water increasing its capacity to carry fine and very fine sand, and in part to the very high velocities that subglacial streams can attain - up to 50 m/sec (Mackeiwicz _et al_, 1984). Mackiewicz _et al_ also pointed out that the debris loads of (rapidly retreating) continental glaciers may be significantly greater than those of valley glaciers.

Powell (1983) proposed that the bedload of englacial streams may play an important role in the formation of underflows. The traction and saltation fraction of a high-yield debouching stream may separate from the main body of the stream and form an underflow, similar to to the process suggested for the Congo River at the head of its submarine canyon. Some subaerial glacial streams carry from 30% to 90% of their sediment load as bedload (Mackiewicz _et al_, 1984). In addition, sand settling out from overflows, if present in large enough amounts, may produce the same results. Figure 4.1 summarizes the foregoing conditions. Mackeiwicz et al (1984, p. 121) postulated that two additional methods may contribute to underflow generation. Hydraulic conditions in pipe-full glacial channel flow may allow for more sediment in suspension and a more even distribution of that sediment; and turbulence due to a hydraulic jump at the mouth of the tunnel may erode and entrain sediment from the fan at that point.

A final method of generating a turbid underflow is through slumping of material already deposited on the fan, forming a classic turbidity current. There is a fundamental difference, however, between underflows generated in this way and flows initiating directly from meltwater. Slump-generated turbidity currents constitute a single sedimentary event, with a distinct beginning and end to deposition. The turbid underflow generated from meltwater, although subject to fluctuations in flow and sediment concentration, will tend to be sustained over a period of time, up to a few days in the case of a second order storm discharge, or weeks at the peak of the first order (annual) cycle. In the latter case, overprinting of third order fluctuations will lead to a turbidity underflow with variations in flow strength, a situation which must rarely or never occur in slump-generated (surge) turbidity currents. For these reasons, meltwater-generated underflows should be termed continuous

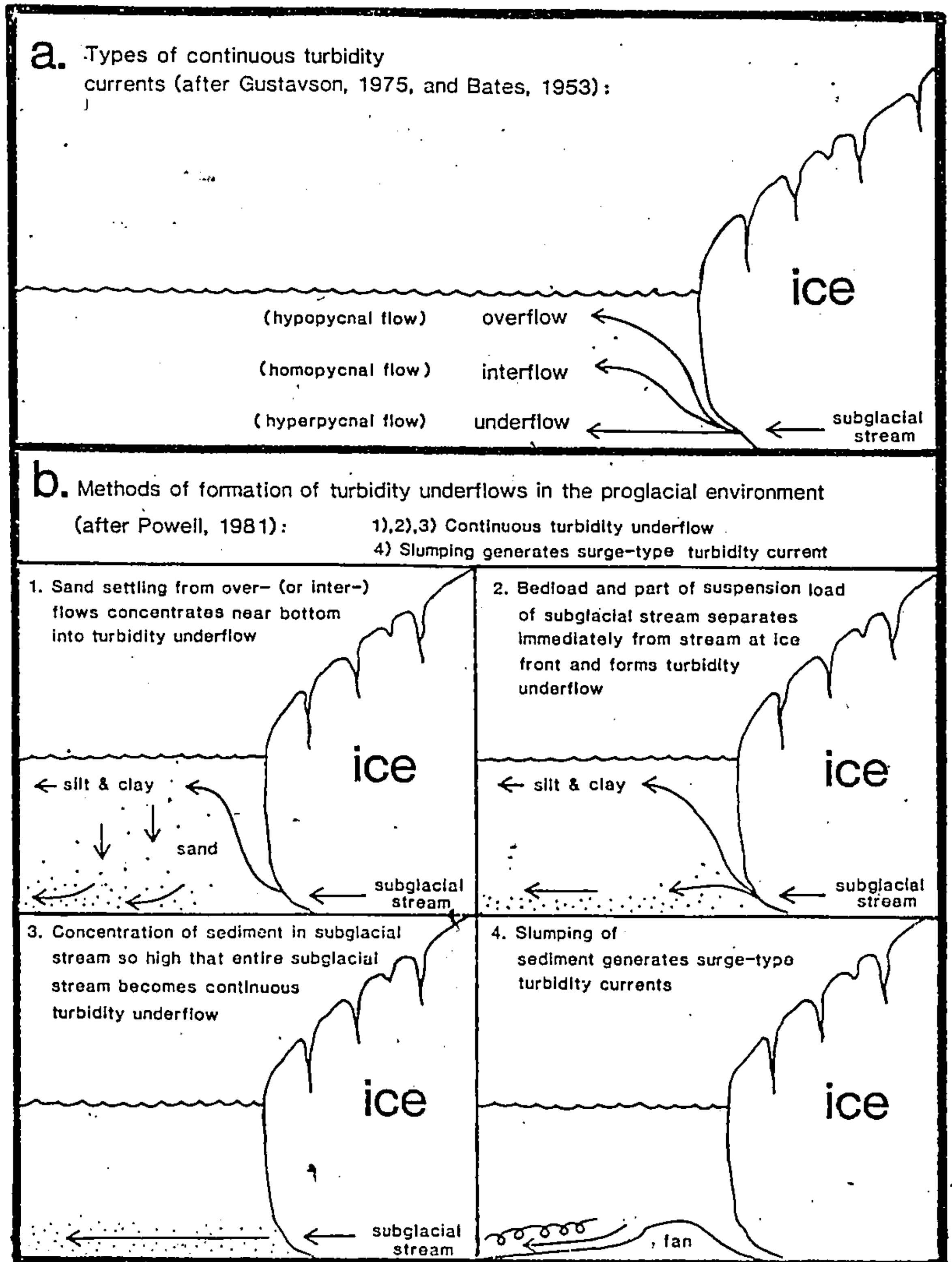

Fig. 4.1 Turbidity currents in the glacimarine environment.

turbidity underflows, and these are a subset of continuous turbidity currents, which include turbid interflows and overflows. This is the equivalent of the two-dimensional turbidity currents (continuous underflows) of Luthi (1980).

4.2.6 LATERAL VARIABILTY IN ICE-PROXIMAL DEPOSITIONAL ENVIROMNENTS

Domack (1984) and Rust and Romanelli (1975) attributed channelling, cross-lamination and trough crossbedding to the action of proximal underflow currents. Because the high energy of meltwater streams is localized at the tunnel mouth, it would be expected that low energy environments are also part of the ice-proximal environment, away from the influence of debouching streams. If the turbidity underflows are channelized on the fan surface, the high energy environment is extremely restricted at the ice margin and across the fan to medial or even distal areas where the underflows leave the channels (Gustavson et al, 1975). Proudfoot et al (1982) described clay being deposited near the ice margin adjacent to channelized debouching streams in subwash fans they refer to as "kame-deltas". This would result in rapid facies change within the fan deposits.

4.3 THE ST. LAZARE SUBWASH FAN

4.3.1 GEOMORPHOLOGICAL CONSIDERATIONS

The steep northern and northwestern sides of the plateau indicate that the deposits were confined there by ice. The faulting and contortions of the strata in pit 3, which is located along the northern side, may be a result of partial collapse of that side after the ice support was removed.

The sediments of the plateau are perched on a bedrock high and are draped across it to the south. The surficial deposits are very thin along the northwestern edge, and the topography along that side is partially controlled by bedrock. The smaller (Hudson) feature to the northwest also has a steep northwestern ice-contact side.

4.3.2 DISTAL FAN (PIT 1 - SABLIERE BARBE)

Underlying diamicton

This unit is well exposed only in face 1.2, but it appears to be a lodgement till deposited by active ice. The shearing and contortions of the wispy bedding within the unit (fig. 2.17) support this interpretation. Probably this unit discontinuously overlies bedrock in the area, as it does elsewhere in the Ottawa Valley (Gadd, 1977; Richard, 1980).

The sandy diamicton mapped by Richard (1982) at several places on the plateau (fig. 1.1a) is probably this unit, as these exposures occur either adjacent to bedrock outcrops or where the total thickness of the surficial deposits is very thin. Borehole data show that at the apex of the fan (NE corner of the plateau), neither clay nor diamicton is present between the sand and the bedrock.

Fossiliferous marine clay

The fossiliferous clay in section 2.1 (and exposed in the middle of the Barbe pit) is the product of normal marine sedimentation, with some influence from outwash currents (sand interbeds) and probably from ice rafted debris (scattered pebbles and boulders). The Champlain Sea was at least 112 m deep at this point; the marine limit on Rigaud Mountain is 192 m (Richard, 1978), and the approximate elevation of the fossiliferous clay is 80 m. The abundant faunal assemblage which was flourishing here (bivalves, gastropods, siliceous sponges) was buried by the influx of large amounts of fine sand.

Lacustrine phase at St. Lazare?

The recent discoveries of lacustrine sediments beneath glacimarine material in the Ottawa Valley (see section 1.2.3

above) prompts close examination of the base of the marine sequence at St. Lazare. Romaine (1951) identified raised beaches as high as 216 m on Rigaud Mountain. No record of marine fauna exists for any strandline above 180 m (Richard, 1978). The clay above the diamicton at face 1.2 was not examined for lacustrine microfauna, but it does not seem likely that any lacustrine sediment is present, as the marine macrofossils occur directly above the diamicton. If the highest beaches on Rigaud Mountain are lacustrine, no corresponding lacustrine record exists in the lutites at St. Lazare.

Radiocarbon dates

The shells of Hiatella arctica from the profan sediments at the base of the fan sequence gave an average date of 9865 ± 120 radiocarbon years BP and the Macoma balthica shells 11,025 ± 160 yrs BP. No explanation is offered for the discrepancy between species. The Macoma date fits reasonably well with the 11,200 yrs obtained by Richard (1978) for the deglaciation of Rigaud Mountain.

Subwash fan sediments at face 1.2

The section at face 1.2 is unique in that it represents the entire fan package, however attenuated and abbreviated at this point by the intermittent or wandering influence of underflow currents, and truncated by Champlain Sea wave activity.

The sand coarsens upward at this location, indicating that the subwash fan was prograding into this area from the site of the ice tunnel opening, some 6 km to the NNE. The paleocurrents measured throughout the sand at section 2.1 show flow from that direction.

The only indication of faunal activity above the clay unit is the presence of Monocraterion and Planolites burrows, although units containing substantial amounts of silt are heavily bioturbated. The extensive bioturbation indicates that breaks in sand deposition must have occurred. The overlying units are laterally continuous for 50 m, possibly up to 150 m or more. This can clearly be seen along the partially slumped face which forms the eastern boundary of the pit, about 75 m east of face 1.2 (fig. 4.2). These beds are dipping at 15 towards the SSW. It can be seen from fig. 1.3 that pit 1 is located at the relatively steep (3^o–8^o) southern margin of the fan. This is the expression of the foresets at the front of the fan, modified by littoral processes.

The sediments are mostly horizontally laminated, although the bedding is partially to completely obscured by bioturbation in places. The lower metre and a half of sand contains significant amounts of silt and probably represents

COLOURED PICTURES
Images en couleur

Figure 4.2. Oblique view of large fan foresets in the distal region, pit 1. Foresets dip at about 10° SSW. Section about 7 m high.

lower flow regime deposition. Above this there are rippled and crossbedded units, in predominately medium sand. The traction current structures are proof that underflows were active here. The lateral continuity of the bedding indicates that there was broad sheet flow across the foresets at the distal regions of the fan. Some of the rippled horizons contain silt drapes (flasers). These represent suspension deposition from interflows or overflows, probably from underflows which had lifted from the bottom at some point upcurrent and were depositing silt as interflows at this point. The coarsening upward trend is due to an increase in energy of the underflow currents. This indicates that channelized underflows were bringing coarser sediment farther out from the glacier margin before opening up into sheetwash. At all other sections in the plateau, abundant channelization is evident. Two thirds of a metre of facies 3 (alternating beds) are present near the top of the section, the significance of which is discussed below.

Origin of facies 3 sediment (alternating beds)

The beds of facies 3 sediments have considerable lateral extent, up to a hundred metres or more. They are unchannelized or occupy very broad, shallow channels (fig. 2.09). The coarse beds, and some of the finer beds, are composed of well sorted sand with traction current structures such as ripple cross lamination, tabular (sand wave) crossbedding, occasional trough crossbedding, and upper flow regime plane lamination. High energy is also indicated by the straight erosional contact truncating the burrowed horizon at fig. 2.44. This shows that turbid underflows occcupied broad channels or moved across fan foresets as sheetwash.

The alternation of bedding style and sediment size resulted from the fluctuation of the meltwater currents. The finer beds are moderately to poorly sorted and were formed in part by the settling of silt sized material from interflows and overflows. The extensive burrowing and bioturbation of these finer beds indicate that there were periods of non deposition, or at least slow enough deposition that colonization by burrowing fauna could take place. In some places, where the coarse beds were deposited under upper flow regime conditions, the intervening beds are partially or completely eroded (fig. 2.44). Evidence of the former existence of an overflow/interflow layers within the sequence is inferred by the occasional Monocraterion burrow within the upper flow regime sands. It is assumed that the worms that formed the burrows colonized the area during a significant lull in deposition, and would not have survived in the high energy environment of the horizontally laminated sand. In all cases the burrows are truncated at one horizon within the upper flow regime sands (fig. 2.44).

The extent of bioturbation in the poorly sorted fine beds points to first order or annual cycles in meltwater flow.

Daily fluctuations certainly would not provide enough time for bioturbation. Second order fluctuations caused by weather systems are not believed to be responsible for the overall aspect of the alternating bed facies, because the coarser beds containing traction current structures, which are very laterally extensive, would have taken longer to accumulate than the several days of peak flow that may have accompanied a major storm. It is more likely that the coarse beds were deposited during annual peak flow (a number of weeks) when underflows could be maintained beyond the channels on the main part of the fan out across the distal foresets. Unusual discharge events at other times could complicate this pattern, and many of the thinner beds of coarser material can be attributed to this. The alternating bed facies, therefore, can be considered to be proximal varves. Fig. 4.3 shows alternating beds from face 1.1b photographed in May 1985 which, atypically, have the clay laminae of the winter layer preserved. These resemble the "sandy proximal varves" of DeGeer (1940), from a Pleistocene submarine outwash fan in Sweden. Annual meltwater fluctuations were proposed by Domack (1984) as the most likely control on the rhythmic proximal glacimarine bedding of The Late Pleistocene Whidbey Formation in Washington.

The finer, poorly sorted horizontally laminated beds of facies 3 contain significant amounts of silt and are largely a product of suspension deposition from interflows or overflows.

COLOURED PICTURES
Images en couleur

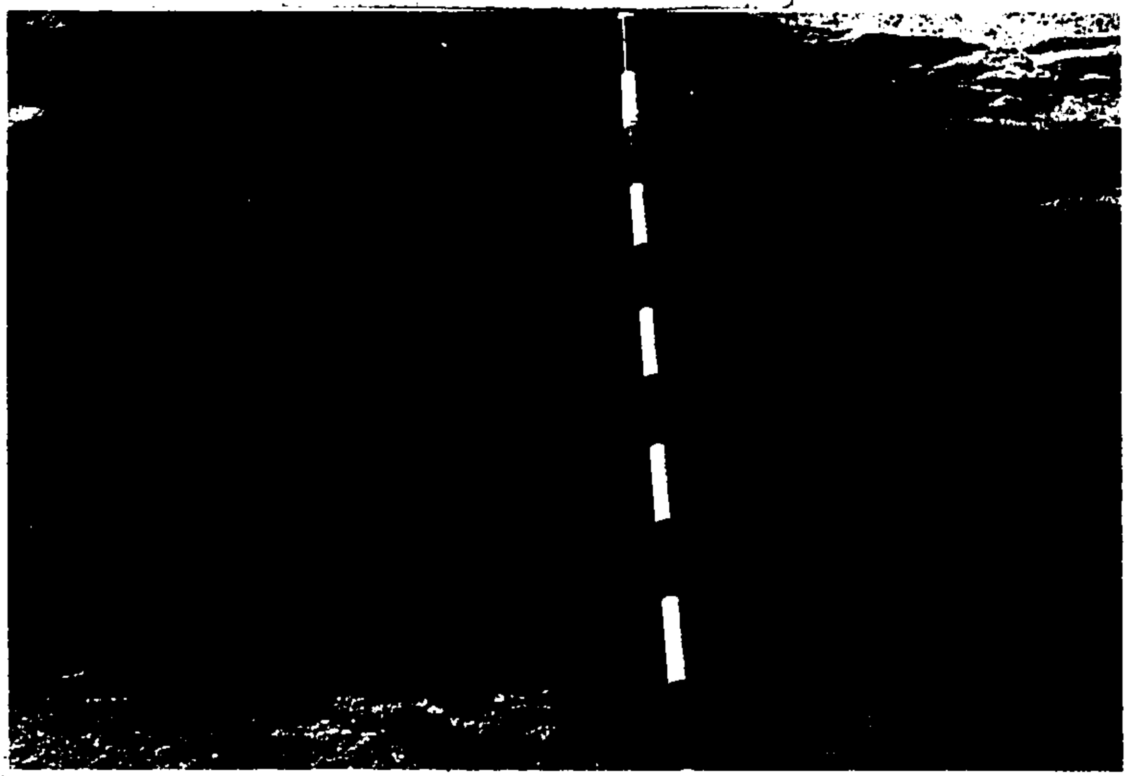

Figure 4.3 Facies 3 beds (interpreted as proximal varves), face 1.1a. Traction current beds alternate with mainly suspension deposited beds. Scale in dm.

Because of their relative remoteness from the ice margin, they probably also contain contribution from interflows derived from underflows that lifted from the bottom as sediment loss reduced their density.

This property of underflow deposition would lead to sharp contacts between coarse underflow deposits and their overlying interflow equivalents, as observed in facies 3 beds. The sharp lower contacts of the coarse beds are due to the sudden startup of underflows during the season of peak flow (Domack, 1984,p. 598). Domack suggested that sharp upper and lower contacts of an underflow deposit imply a relatively short episode of sedimentation, and that rather, as in the case of the rhythmites of the Whidby Formation, a gradual lessening of the strength and frequency of underflow deposits over the season led to a fining upward transitional contact between peak flow tractional underflow sediment and the overlying fine grained overflow deposits.

Grading is occasionally present, however, within the alternating bed facies in pit 1. Fig 4.4 is a section through facies 3 beds showing draped lamination overlain by type A climbing ripples which grade upward into type B climbing ripples. There is general fining upward within each bed. No bioturbation is present here (perhaps due to continuous rapid deposition), but these beds are of the same order of thickness and occur in the same place in the fan as the bioturbated strata, and are attributed to annual meltwater cycles.

COLOURED PICTURES
Images en couleur

Figure 4.4 Clay drape grading upward to silty and sandy climbing ripples, indicating gradual increase in current and underflow activity, probably at the beginning of seasonal meltwater efflux. Knife handle 2 cm wide.

Two reasons are proposed for the sharp rather than gradational upper contact of the coarse underflow deposits, and the general lack of grading within either the coarse or the fine members of facies 3: 1. Bioturbation may have homogenized originally graded fine grained members (unlikely). 2. As discussed above, a continuous turbidity underflow will lift off the bottom as soon as its density is lower than the ambient fluid, with consequent cessation of traction activity downstream of that point.

Time required for deposition of the fan

Gustavson et al (1975, p. 276) estimated the time required for deposition of glacilacustrine deltas at from tens of years to several hundred years at most. Using the average thickness of the proximal varve couplets at St. Lazare (30 cm), and the maximum thickness of section in pit 1 (14 m, including an estimate of the depth to the top of the diamicton), an estimate of 47 years is derived. This fits very well with the figure of Proudfoot et al (1982) for the time required for deposition of a subwash fan in Alberta derived from the varve- dated duration of the glacial lake into which it was deposited (40 years for 11 m). The size, average flow rates and sediment loads of glacial tunnels must be quite variable, and depend on such factors as the configuration of the glacial tunnel network, melting rates and sediment supply.

Thus the rate of deposition of subwash fans must be expected to vary widely within the end member figures of Gustavson et al (1975), and perhaps more. These depositional rates (in the order of 30 cm/yr) are quite reasonable when compared with rates of over 400 cm/yr for silt and clay rhythmites in Glacier Bay, Alaska (Powell, 1981).

Other distal fan facies

Facies 3 sediments make up over 50% of the exposures at pit 1. Facies 1 is the next most abundant, and is discussed below. Facies 3 sediment (current rippled sand) comprises up to 25% of the exposures at face 1.1. Facies 2 sand differs from the traction current part of facies 3 sediment in the abundant presence of climbing ripples, and in the thickness of the bedding. Facies 2 beds are considerably thicker, on the order of a metre or more.

Thick sequences of climbing ripples can be deposited experimentally in a matter of hours (Gustavson et al, 1975). A single very high discharge event, lasting only a few days, may have deposited an entire metre thick unit of facies 2 climbing ripples. Climbing ripple cross lamination is a very common mode of deposition in deltas, where relatively high velocity streams carrying high sediment loads are suddenly slowed as they enter the depositional basin and large amounts of sediment are forced out of suspension. The same situation would have existed at the distal end of fan-top channels at St. Lazare under high flow conditions when very large amounts of sediment were being delivered to the fan front. The estimate of the time of deposition of the entire fan should be reduced in inverse proportion to the amount of climbing rippled sand in the section.

Ice rafted debris

The component of ice rafted debris in the St. Lazare sediments is low. Outsize clasts have been observed in the sand, and most boulders show evidence of having been dropped into the sediment (fig. 4.5). Only one of these dropstones showed obvious evidence of glacier scour (fig. 4.6). The glacier would have been in extensional flow in the study area, having descended from the highlands a short distance north or northeast from St. Lazare, and experienced flow expansion down-ice from the sub-ice constriction imposed by Oka and Rigaud Mountains. There would have been little or no subglacial material brought up into the glacier snout, and calving bergs would have been relatively clean. Outwash-derived currents may also have quickly removed bergs from the fan area, especially if the currents were debouching in a small calved bay in the ice margin. Outsize boulders are particularly abundant at the littoral unconformity, and are all of Grenville origin. Some may have been derived by

COLOURED PICTURES
Images en couleur

Figure 4.5 Ice-rafted boulder, face 2.6, showing deformation of subjacent beds. Boulder 30 cm across.

COLOURED PICTURES
Images en couleur

Figure 4.6 Striated ice-rafted boulder, face 2.5. Scale in dm.

drifting of shore ice from the abundant boulder beaches on Rigaud Mountain after ice retreated from the area, and deposited at the base of the littoral sediments as a lag. Boulders abundantly scattered over the top of the plateau may have a similar origin. Lack of supraglacial debris is indicated by the absence of any flowtill diamicton interbedded with the sand.

Facies f: faintly horizontally stratified channel fill

The channels and their sediments bear a strong resemblance to mass flow deposits in Pleistocene glacilacustrine sediments in the Netherlands (Postma et al, 1982, especially their fig. 6d; and fig. 385 of Ruegg, 1983), and near Ottawa (Cheel and Rust 1980, their type B channel-fill), both of which were attributed to the erosive action of slump-generated mass flows. In the case of the channel fill near Ottawa the steep channel walls and the inverse to normal grading at the base ~~are the~~ most similar features. The similarity to the channels of the Netherlands are (1) the steep channel sides, (2) the concentration of pebbles along bedding planes near one side of the channel, (2) faint horizontal stratification, (3) identical convolutions near the top of channels (fig. 383 of Ruegg, 1983), and (4) the dark laminae near the base of some channels (fig. 4.7), which pinch out within the channel, and which Ruegg (1983, p. 68) attributes to slumping of the un-

COLOURED PICTURES
Images en couleur

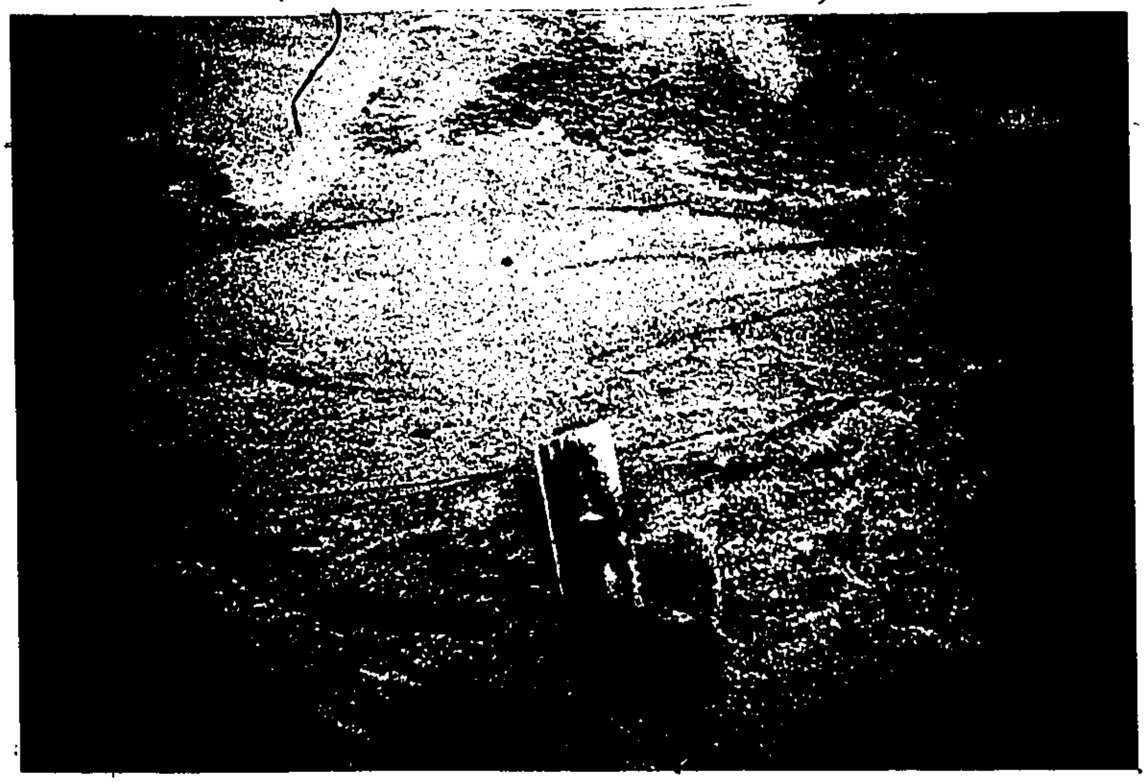

Figure 4.7 Laminae rich in heavy minerals at the base of a facies 1 channel, pinching out within the channel, similar to that of Roepp (1983, fig. 6d) (top and to the left of scraper). Face 1.1b. Scraper is 10 cm wide.

stable channel wall during sedimentation of the channel fill. The major differences between the channel fills are (1)the St. Lazare near-massive channel-fill is of very well sorted sand (apart from the very minor pebble component), and (2) does not exhibit an overall decrease in grain size from bottom to top, and (3) the channels of Postma et al do not show the strong asymmetry of the St. Lazare type.

On the other hand, the following characteristics of facies 1 sediment tend to indicate that the channels were carved by dilute currents rather than by mass flows: (1) The channel fill consists of small fining upward beds of well sorted sand. (2) Facies 1 channels are asymmetric. (3) Pebbles and rip-up clasts commonly lie along bedding surfaces, concentrated toward the steep, or "cut bank" side of the channels. (4) Pelecypod valves, when they occur, tend to lie in a horizontal, convex-upward position.

The strongest piece of evidence against a dilute current origin (fluidal flow, Lowe, 1979) for the St. Lazare channels is the very steep channel walls. In the absence of stabilizing vegetation, saturated sand has very little cohesive strength and therefore could not have maintained steep channel walls. This argues for the presence within the channels, during their formation, of sediment of sufficient concentration such that it would have provided support for the channel walls. Dispersive pressure present in density modified grain flows (Lowe, 1976a) may have been capable of providing support.

Postma et al proposed that the "diffuse banding" (vague horizontal stratification) of their type B channel fill may have originated by the progressive "freezing" of a basal layer of highly concentrated sediment. This process would lead to the development of inverse grading in each layer due to dispersive pressures (Hiscott and Middleton, 1979, p. 323). Because almost all the beds in the St. Lazare type are normally graded, this process could not have been responsible. The occasional reverse graded bed may be attributed to this process, however.

The succesive upward fining within the individual beds of facies 1 channel fill at St. Lazare implies pulses of flow, with deposition of finer material as the flow waned. It is proposed that the mode of deposition of the faintly stratified facies 1 sand is by a relatively concentrated dispersion of sand, possibly corresponding to the density-modified grain flow of Lowe (1976a). Sediment was sufficiently concentrated that dispersive pressure partially contributed to grain support (and helped to maintain the high-angle channel walls), yet dilute enough that some aspects of fluidal flow were obtained (ability to erode, normal grading, asymmetric channel profiles, deposition of pelecypod valves in convex-upward position). Slump-generated mass flow may not have been the source of sediment (if they were, channel fill with features more characteristic of mass flow depositon should be expected to be found more proximally). The channel fill may be a result of continuous turbidity underflows that were confined and concentrated within their channels to the extent that dispersive pressures became significant. The fact that there is no overall upward fining of the sand within the channels also supports the hypothesis of deposition from continuous (but fluctuating) turbity currents rather than episodic (slump-generated) flows.

The reverse-to-normal grading in the lowermost few cm at the base of most channels is probably a result of the transition from erosion to deposition, when the concentration of sand at the base of the channel was high enough for dispersive pressures to have become predominant. This inversely graded layer also occurs above reactivation surfaces within the channels, indicating a freshening of the strength of the currents and re-initiating of erosion. The irregular, stepped aspect aspect of some of the channel walls is attributed to enlarging of the channel during reactivation.

Large convolutions which are present near the top of many of the channels, and are truncated by the overlying beds, formed after deposition of the channel fill as a result of dewatering of the (rapidly deposited) sediment. The convolutions may have been influenced by currents above the bed, but preferred orientations of the convolutions were not measured (or noted) in the field.

The presence of rip-up clasts of clayey silt within the channels shows that there were interflow/overflow deposits present upstream of pit 1, further proof of the existence of winter suspension deposits which tend to have been eroded by the action of underflows.

4.3.3 PROXIMAL FAN DEPOSITS AT PIT 2 (CHEVRIER PIT)

Pit 2 is situated in a relatively proximal position on the fan. All facies are present here except for facies 3 (alternating beds), which is believed to be restricted to distal fan areas. The predominant facies type in pit 2 is facies 4, or crossbedded sand, confined within relatively steep walled channels of varying sizes. Most of it is trough crossbedding and planar-tangential crossbedding formed by migrating straight- and sinuous-crested subaqueous dunes, indicating that in this subproximal position the energy of the outwash currents was high. Some planar-tabular (sand wave) crossbedding, ripple cross lamination and trough cross laminated fine sand exists within the channels; this is an indication of lower flow strengths of the meltwater underflow currents. No indication of interflow or overflow deposition is present in the southern two thirds of face 2.5; the peak flow strength in this area was always high enough to erode all traces of suspension deposition. The paleocurrents within the crossbedded units indicate flow from the WNW. Because of the strength of flow implied by the crossbedding and the proximity of the ice margin, an ice tunnel opening to the northwest, about one quarter of the way down the northwest side of the fan, is inferred.

The lower part of the adjacent exposure of face 2.2 consists of fine sand, consisting of type B climbing ripples and non-climbing ripples. Fig. 2.23 shows upper flow regime discontinuous plane lamination grading upward into non-climbing ripples, indicating a waning of the velocity of the underflow current at that place. Several units of tabular crossbeds represent the migration of individual sand waves. Most of the rippled sand shows flow from the west, but climbing ripples in the lowest part of the north end of face 2.2 point towards the west and may be regressive ripples formed in the manner recorded by Aario (1972). A large part of the sediment within pit 2 may be fine rippled sand, as similar material is present in face 2.1 and in scattered small exposures elsewhere in the pit. These sediments indicating easterly paleoflow may be the deposits of currents originating from a meltwater tunnel on the west side of the fan which was active after tunnels at the inferred fan apex deposited the beds observed in pit 1. Deposits in this sub-proximal position in the fan may not show any rhythmic aspect because of the high energy of the flows; fine grained off-season suspension deposits were likely not preserved through peak flow.

At the north end of face 2.5 there is evidence of shallow, broad channels filled with much finer sediment (very fine sand, silt, and clayey silt). The upper few metres of face 2.2 are composed of similar sediment in one broad (>60m) channel. In face 2.5 there is abundant evidence of overflow/interflow deposition in the form of draped lamination and poorly sorted horizontally laminated fine silty sand. Several thin beds of massive well sorted fine to medium sand are also attributed to fallout from overflows or interflows (fig. 2.22). Fine sand is expected to be deposited from overflows proximally (Gilbert, 1982). Fig. 4.4 shows a coarsening up sequence starting with draped clay and overlain by climbing ripples in silt and sand, with a regular upward decrease of angle of climb of the ripples. This indicates a change from suspension sedimentation to a gradually increasing underflow current and a decrease in the ratio of material falling from suspension to that carried in traction. Although no burrowing is present, the presence of a clay layer strongly suggests winter deposition, and the coarsening up sequence a gradual seasonal increase in meltwater activity.

The variety of facies in pit 2, and the divergence of its paleoflow trends from those measured elsewhere across the fan, suggest that more than one major ice tunnel contributed sediment to the fan. Any one ice tunnel may have varied in importance over time according to the configuration of the network of subglacial tunnels.

"Flaser" bedding

Flaser-like bedding within facies 2 sand (fig. 2.24) results from draping of clayey silt over ripples during interflow or overflow events when underflow deposition is temporarily interrupted. This may be an expression of third order (diurnal) flow fluctuations (probably, in the case of fig. 2.24), or it may represent lulls between storms or weather pattern influence.

Convolute lamination

There are several convoluted beds in face 2.2 (<u>sensu</u> Reineck and Singh 1975). These beds are laterally continuous within a broad, shallow channel and average 25 cm in thickness. The convolutions die out gradually over a space of about 5 cm below, and are truncated abruptly above. There is no preferred lateral orientation to the convolutions. They are interpreted as a product of reverse density gradation where a layer of sand overlies a layer of silt or silty clay which has a lower density than the sand. The straight upper contact may not be an erosional contact, but simply the upper surface of the sediment at the time that the convolution occurred (similar to fig. 131 of Reinick and Singh, 1975). Elswhere in pit 2 similar convolutions were found that must have occurred after the overlying beds were deposited, as a sharp upper contact is missing, and instead the convolutions affect the overlying beds (fig. 4.8). It is clear that at least two different generations of convolutions are present. Convolute bedding is indicative of high depositional rates and high pore water content, conditions that certainly would be expected to occur in fine grained subwash fan sediments. Convoluted bedding is distinct from contorted bedding in genesis and in form. Contorted bedding lacks the sometimes quite regular anticline/syncline form of convoluted beds. Contorted bedding in the study area results primarily from distortion by shearing as masses of sediment adjusted or subsided to fill voids created by melting remnant glacier ice.

Proximal bank-attached channel bar (face 2.6)

Face 2.6 is approximately 1 km NE of the main part of the Chevrier pit. The littoral unconformity is at 4m depth in the section. The sediments above the unconformity are identical to those in face 2.5. Below the unconformity is a large channel, 100 m wide, and two thirds filled with large planar tabular crossbeds. It was formed by the down-channel migration of a cross-channel, bank-attached bar (alternate bar sensu McCabe, 1975, in Collinson, 1983, p.57) (fig. 2.37). The crossbeds are composed of moderately sorted fine to coarse sand. Regressive ripples migrated obliquely up the foresets near the bank-attached side. In the thalweg at the open end of the bar,

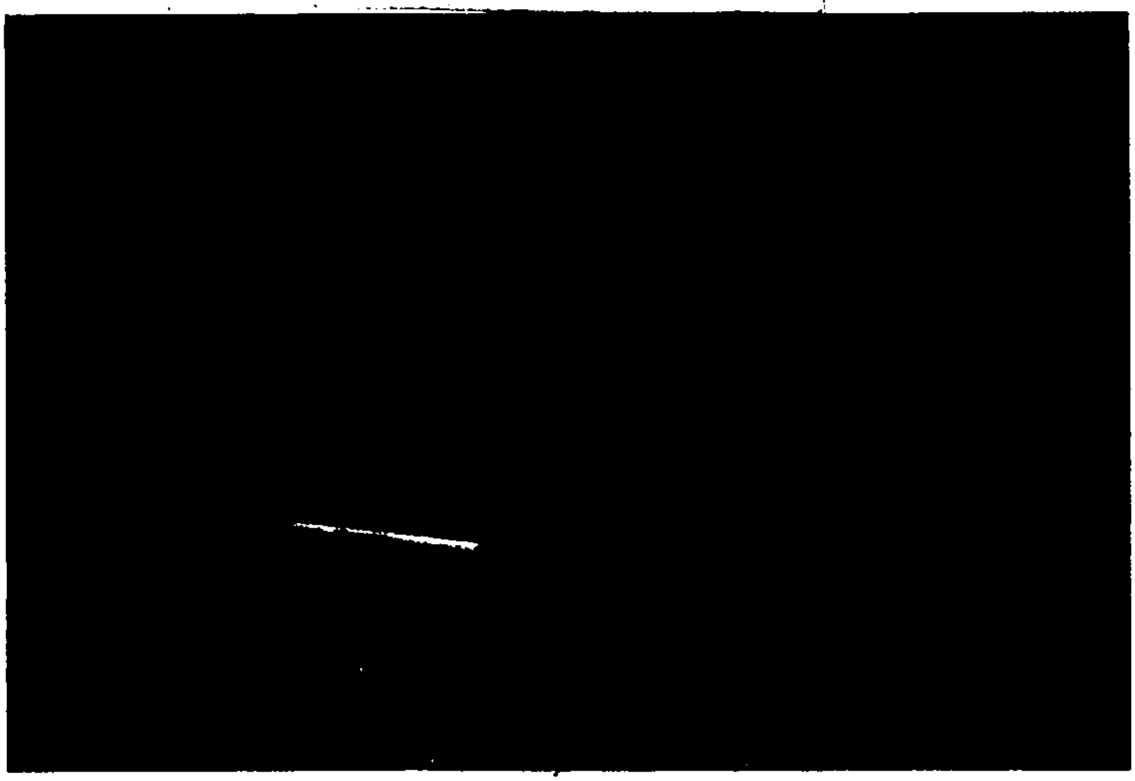

Figure 4.8 Convoluted bedding with disturbed overlying sediment, pit 2, indicating that convolution occured after deposition of superjacent beds (vertical section). Pen 15 cm long.

migrating sinuous-crested dunes formed trough crossbeds. The paleoflow indicated by these trough cross beds matches the direction of dip of the bar foresets, and is similar to those measured elsewhere in pit 2 (130°). The channel is cut in rippled fine sand. This is further evidence of an active ice tunnel on the west side of the fan.

4.3.4 PROXIMAL FAN FACIES AT PIT 3 (DAOUST PIT)

Face 3.1

Pit 3 is in the most proximal position with respect to an ice tunnel at the northern apex of the fan. This is compatible with the fact that the coarsest material found in any of the pits is located here. Part of face 3.1 is made up of coarse pebbly sand, interbedded with medium sand and overlying fine rippled sand.

The finest grained sediment anywhere in the fan is also present here. Disconformably overlying the coarse pebbly sand is a lens-shaped unit of blocky, laminated and variegated silty clay. Gadd (1977) identified similar gray/red variegated silty clay from the upper part of the Champlain Sea deposits in boreholes in the Ottawa valley. The laminations within the clay are disturbed, faulted and contorted throughout. The contact with the underlying sand is relatively straight and regular although slightly loaded in places. The underlying sand is highly disturbed, with injections of one unit into another, microfaulting (mostly reverse) and contorted bedding.

It is probable that channels were carved then abandoned on the fan surface, through channel avulsion or by the sudden cessation of meltwater flow from the ice tunnel. In the absence of meltwater influence, or in a near-channel backwater, clay may have filled the channel. In light of the disturbances of the underlying sand, however, it is suggested that the clay lens was deposited in a kettle formed by the melting of buried glacier ice. The injections and other contortions of the sand units formed as the ice melted and subsidence began. Two smaller units of similar silty clay are interbedded with the sand units beneath the clay lens; this shows that slumping of pebbly sand occurred intermittently as clay sedimentation proceeded, as described by Hayward and French (1980) from deposits in the Ottawa area. Probably some residual subsidence during the deposition of the entire clay unit contributed to the contortion and faulting within the clay, which seems too severe to be due simply to differential compaction. The reverse faults throughout the section conform to the criteria for melt-out of buried ice proposed by McDonald and Shilts (1975).

The clay lens is truncated above by the littoral unconformity. The amount of sediment that was reworked by the shoaling Champlain Sea is not known, but the presence of a prominent, flat littoral unconformity at depth throughout the fan indicates that the original profile of the top of the fan was flattened by wave activity.

Face 3.2

Face 3.2 is predominantly planar crossbedded medium and fine sand, with inferred paleoflow from the north. The abundance of relatively low energy deposits close to an ice tunnel which is believed to have deposited similar material 7 km to the south implies variable strength of the subglacial streams debouching from the ice tunnels.

There is a considerable amount of disturbance of the beds here, similar to face 3.1 and attributed to the same process, namely meltout of buried ice. Small reverse faults abound throughout. Two foundered balls of fine sand in a medium sand unit (one is shown in fig. 2.41) are attributed to partial liquefaction of the lower bed. Injection of a unit of fine silty sand into two less disturbed units is also a result of ice melt-out. Some of the upper units are relatively flat-lying and less disturbed, and may have been deposited by mass flow into a kettle from adjacent highs (Hayward and French, 1980). Collapse of part of the northeastern edge of the fan after retreat of the ice margin from the fan may have contributed to the faulting in pit 3.

Faunal presence in the subwash fan

There is evidence for a considerable amount of faunal life within the fan sediments. There was certainly a diverse assemblage thriving not far from the ice front (<10 km), in the pro-fan silty clay, as indicated by the biocoenosis at face 1.2. The occurrence of disarticulated pelecypod valves within the facies 1 channels in face 1.1 indicate the presence of colonies of pelecypods more proximal than pit 1. The preservation potential of shells within the very permeable sand at St. Lazare is poor. Some burrows in pit 2 are believed to be of pelecypod origin. Abundant colonization of the distal fan areas (probably by annelids - Guy Narbonne, pers. comm. 1984) is borne out by the burrows and bioturbation in pit 1.

Littoral unconformity

The uppermost part of the sequence was truncated by reworking of the top of the fan by wave processes as the Champlain Sea regressed. This must be the usual situation with subwash deposits, and only in restricted basins would diminished fetch allow for a minimum of wave attack and reworking. In the case of ice-dammed lakes, relatively catastrophic drainage may help preserve the uppermost sediments by reducing the amount of time the feature would be at waterlevel. In the case of the St. Lazare fan, the uppermost beds were reworked quite significantly. Abundant geomorphic evidence of shore processes, such as terraces and extensive boulder beaches, is present in the Vaudreuil region. In pit 2, the littoral unconformity extends to a depth of 3 m below the top of the present pit level. The sections in pit 2 clearly show the lag of boulders above the unconformity, coarse horizontal or low angle storm beach bedding and discontinuous subhorizontal beachface bedding above this (Davis 1983, p.413) (figs 2.34 and 2.35). The sand above the unconformity everywhere is stained orange from iron oxide, in strong contrast to the buff-coloured sand immediately beneath the unconformity, reflecting the oxidizing conditions in the littoral environment. No evidence of fluvial deposition, such as channels, was seen above the unconformity, nor is there any evidence that these sediments were subaerially exposed during deposition.

Aeolian lag

At face 1.2, the unconformity is at 1.2 m depth in the section. It can be seen in fig. 4.2, where it strongly resembles deltaic topset bedding, and has been mistaken for such in the past (Richard, 1976). The bedding in this unit has been obscured at this location by a number of processes, namely cryogenic disturbances during cold postglacial climatic events (see discussion, section 3.2.6); disturbance by modern vegetation; and tilling by farm machinery (alfalfa is presently being grown in the adjacent field). The uppermost part of the unit consists of coarse pebbly sand. As mentioned in section 1.3.3, evidence of aeolian processes are widespread on the plateau. This upper pebbly sand is probably a deflation lag created by aeolian winnowing of fines. This is not an uncommon occurrence in glacial deposits (Flint, 1963, p. 118). Frost churning of the sediment prevented a lag concentrate from armouring the surface and halting this process, such that the effects extended to a depth of almost 1 m.

4.3.5 DEPOSITIONAL MODEL

A calved bay at St. Lazare

The two ice contact sides of the fan (a long one to the northwest and a short one to the north) combined with the inferred position of a major ice tunnel at the northeastern corner of the fan, suggest that there was a triangular indentation in the ice front, coinciding with the bedrock high on which the fan is located. The bedrock relief up-ice of the fan is considerable; the bedrock channel on the northwestern side of the fan combined with the bedrock high beneath the fan form a steep cliff of over 100 m. It is oriented obliquely to the flow of ice indicated by striae to the northeast, but

Rigaud Mountain may have deflected the thinning leading edge of the ice towards the southeast.

The combination of the restriction on glacier flow posed by the two mountains and the steep relief of the bedrock surface between them may have initiated the calving of a triangular bay. This calved bay may have been as deep as 7 km, and maintained long enough for deposition of the fan (fig. 4.9). The potential gradient of water pressure within the glacier would have been affected by this indentation in the ice front such that the drainage was deflected, with time, towards the bay. Meltwater activity would have increased during at least the initial stages of the deposition of the fan. Multiple meltwater channel openings would have developed within the bay. Given an average rate of retreat of the ice of 100m to 200m per year (Flint, 1963), it could have taken 35 to 70 years for the main ice front to have retreated past the apex of the fan. This figure agrees well with the estimate of the time required to deposit the fan based on the average thickness of the proximal varves recognized in the distal areas of the fan (47 years).

No evidence of deformation by overriding ice exists anywhere in the fan, so readvance of the ice front cannot be postulated at this location. The overall slight coarsening upward trend to the sediments within the fan is attributed to increase of meltwater activity with time as a meltwater tunnel network developed within the ice to feed the fan apex, progradation of the fan itself, and the channelling of sediment laden underflows across the fan.

On a broader scale, the St. Lazare fan is the major component of a complex of outwash deposits in the ice-lee of Oka Mountain. Rigaud Mountain has a similar but smaller lee accumulation (fig. 4.10). This may be a common occurrence in the lee of large obstacles that induced crevassing and calving down-ice from them.

A combination of circumstances, therefore, combined to produce the St. Lazare fan: 1. A rapidly retreating ice sheet produced large amounts of meltwater, and had an extensive and well developed network of meltwater tunnels within the ice; 2. The local bedrock consists of an easily erodable accumulation of resistant clastic particles; 3. Flow expansion between, and down-ice from, Rigaud and Oka Mountains induced crevassing and weakening of the ice margin; 4. Steep bedrock relief (the bedrock high at St. Lazare) induced calving of a re-entrant and provided a restriction to flow which briefly stabilized the ice margin.

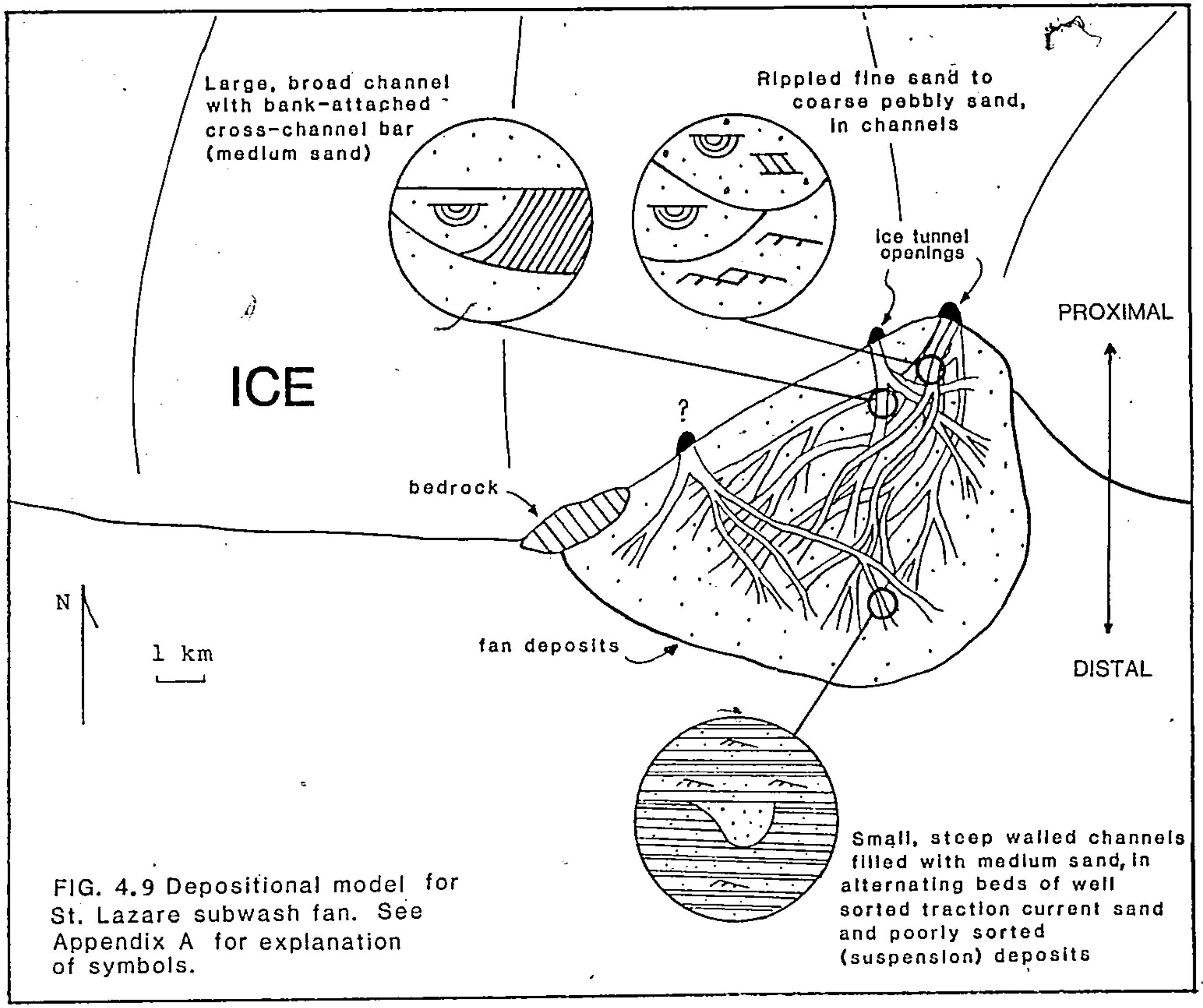

FIG. 4.9 Depositional model for St. Lazare subwash fan. See Appendix A for explanation of symbols.

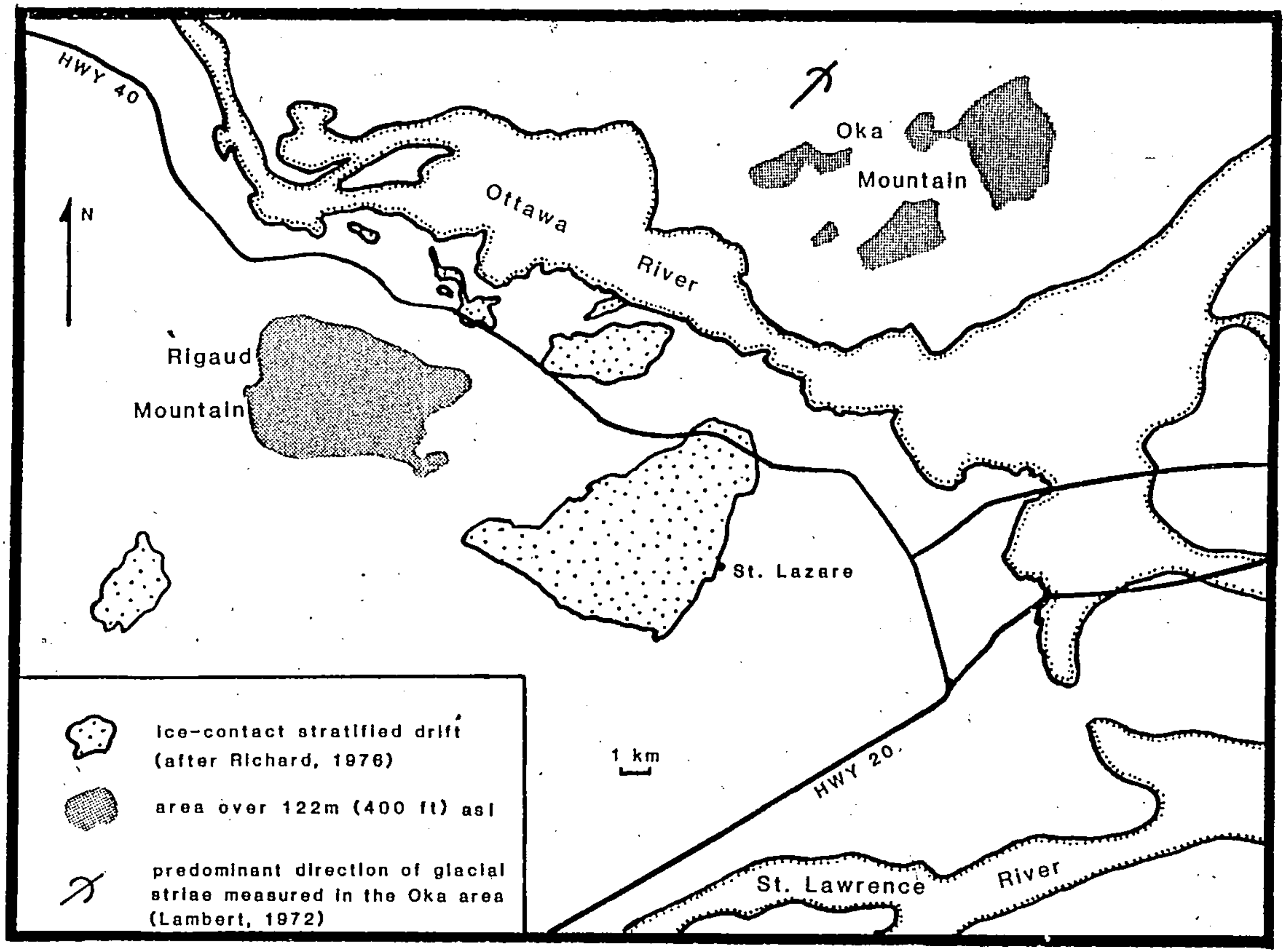

Fig 4.10 Relationship of the St. Lazare fan and related deposits to Oka and Rigaud Mountains.

REFERENCES

Aario, R. 1972. Associations of bed forms and paleocurrent patterns in an esker delta, Haapajarvi, Finland. Ann. Acad. Sci. Fennicae. Ser. A. vol. 3. 55p.

Anderson, T. W., Mott, R.J. and Delorme, L. D. 1985. Evidence for a pre-Champlain Sea glacial lake phase in the Ottawa Valley, Ontario, and its implications. In Current Research, Geol. Surv. Can. Paper 85-1A, 239-245.

Andrews, J. T. 1968. Postglacial rebound in Arctic Canada: similarity and prediction of uplift curves. Can. Journ. of Earth Sciences. 5, 39-47.

Andrews, J. T. 1973. The Wisconsin Laurentide ice sheet: dispersal centers, problems of rates of retreat, and climatic implications. Arc. and Alp. Res. 5, 185-199.

Axelsson, V. 1967. The Laiture Delta; A study of deltaic morphology and processes. Geog. Annal. Ser. A, vol.49, 1-127.

Banerjee, I. and McDonald, B. C. 1975. Nature of Esker Sedimentation. In Glaciofluvial and Glaciolacustrine Sedimentation, ed. A. V. Jopling and B. C. McDonald. S.E.P.M. Spec. Publ. 23, 132-154.

Barrell, J. 1912. Criteria for the recognition of ancient delta deposits. Geol. Soc. Am. Bull. 41, 359-382.

Bates, C. C. 1953. Rational theory of delta formation. Bull. Amer. Assoc. Petr. Geol. 37, 2119-2162.

Bell, H. S. 1942. Density currents as agents for transporting sediment. J. Geol. 50, 512-547.

Bertouille, H. 1976. Contribution à l'étude des ferruginisations et encroutements calcaires: role des thermomigrations. Rev. Geog. Montr. 30, 327-338.

Black, R. F. 1976. Periglacial features indicative of permafrost: ice and soil wedges. Quat. Res. 6, 3-26.

Black, R. F. 1983. Pseudo ice-wedge casts of Connecticut, Northeastern United States. Quat. Res. 20/1, 74-89.

Bryson, R. and Wendland, W. M. 1967. Tentative climatic patterns for some late glacial and post-glacial episodes in central North America. In Life, Land, and Water, ed. W. J. Meyer-Oakes. U. of Manitoba Press, 271-298.

Bryson, R., Wendland, W. M., Ives, J. D. and Andrews, J. T. 1969. Radiocarbon isochrones on the disintegration of the Laurentide ice sheet. Arc. Alp. Res. 1/1, 1-14.

Chapman, L. J. and Putnam, D. F. 1973. The Physiography of Southern Ontario. 2nd ed. U. of T. Press, 386 p.

Cheel, R. J. 1980. Late Quaternary glacio-marine deposits of the Stittsville area, near Ottawa, Canada. M.Sc. thesis, U. of Ottawa, 154 p.

________ and Rust, B. R. 1982. Coarse grained facies of glacio-marine deposits near Ottawa, Canada. In Research in Glacial, Glacio-Fluvial, and Glacio-Lacustrine Systems, ed. R. Davidson-Arnott, W. Nickling and B. D. Fahey. Geo Books Norwich, 279-295.

Clark, P. and Karrow, P. F. 1984. Late Pleistocene water bodies in the St. Lawrence Lowland, New York, and regional correlations. G. S. A. Bull. 95, 805-813.

Collinson, J. D. 1983. Alluvial Sediments. P. 15-60 in Sedimentary Environments and Facies, ed. H. G. Reading. Elsevier, New York. 569 p.

Corbeil, P. 1984. Géologie du Quaternaire de la région de Rigaud/Rivière-Beaudette (Quebec): Quelques applications a l'environment. M.Sc. thesis, U. de Québec à Montréal, 103 p.

Crimes, T. P., Legg, I., Marcos, A. and Arboleya, M. 1977. ?Late Precambrian-low Lower Cambrian trace fossils from Spain. In Trace Fossils 2, ed. T.P. Crimes and J. C. Harper, Geol. Jour. Spec. Issue 9, 91-138.

Cronin, T. M. 1977. Champlain Sea Foraminifera and Ostracoda: a systematic and paleoecological synthesis. Géog. Phys. Quat. 31/1-2, 107-122.

Davis, M. B. 1969, Palynology and environmental history during the Quaternary Period. Am. Scient. 57/3, 317-332.

DeGeer, G. 1940. Geochronologia Suecica Principles. Kungl. Svenska Vetenska. Handl. Series 3, 18, 367 p.

Dionne, J. C. 1971. Fentes de cryoturbation tardiglaciaires dans'la region de Québec. Rev. Géog. Montr. 25/3, 245-264.

Dionne, J.-C. 1974. Paleoclimatic significance of late Pleistocene ice-wedge casts in southern Quebec, Canada. Paleogeog., Paleoclim., Paleoecol. 17, 65-77.

Domack, E. W. 1984. Rhythmically bedded glaciomarine sediments on Whidbey Island, Washington. Jour. Sed. Petr. 54/2, 589-602.

Dredge, L. A. 1983. Character and development of Northern Lake Agassiz and its relation to Keewatin and Hudsonian ice regimes. In Glacial Lake Agassiz, ed. J. T. Teller and L. Clayton. Geol. Assoc. Can. Spec. Pap. 26, 117-131.

Dreimanis, A. 1977. Correlation of Wisconsin glacial events between the Eastern Great Lakes and the St. Lawrence Lowlands. Geog. Phys. Quat. 31/1-2, 37-51.

Elson, J. A. and Elson, J. B. 1959. Phases of the Champlain Sea indicated by littoral mollusks. Abstr., Geol. Soc. Am. Bull 70/12, 1596.

Elson, J. A. 1969. Late Quaternary marine submergence of Quebec. Rev. Géog. Montr. 23/3, 247-258.

Fairchild, H. L. 1907. Gilbert Gulf (marine waters in Ontario basin). G. S. A. Bull. 17, 712-714.

Fenton, M. M., Moran, S. R., Teller, J. T. and Clayton, L. 1983. Quaternary stratigraphy and history in the southern part of the Lake Agassiz Basin. in J. T. Teller and L. Clayton, eds, Glacial Lake Agassiz. Geol. Assoc. Can. Spec. Pap. 26, 49-74.

Flint, R. F. 1963. Glacial and Pleistocene Geology. Wiley and Sons. New York. 553 p.

Fox, K. J. and Powell, R. D. 1985. Deltaic and submarine outwash fan lithofacies of the glacimarine deposystem, British Columbia, Canada. Geol. Soc.

Am. Abstracts with Programs vol. 17/5, p. 14.

French, H. M. 1976. The Periglacial Environment. Longman, Inc., New York, 309 p.

Gadd, N. R. 1963. Surficial geology of the Ottawa map-area, Ontario and Quebec, 31G/5; Geol. Surv. Can. Paper 62-16, 4 p.

Gadd, N. R. 1977. Offlap sedimentary sequence in Champlain Sea, Ontario and Quebec. Geol. Surv. Can. Paper 77-1a, 77-78.

Gangloff, P. 1970. Structures de gelisols reliques dans la region de Montréal. Rev. Géog. Montr. 24/3, 241-253.

Gangloff, P., Clermont, J.-P. and Paquette, G. 1971. Le Problème du Tardiglaciaire au Québec Méridional. Géog. Phys. et Quat. 25, 305-308.

Gilbert, R. 1982. Contemporary sedimentary environments on Baffin Island, N.W.T., Canada: Glaciomarine processes in fiords of eastern Cumberland Peninsula. Arc. and Alp. Res. 14/1, 1-12.

Gill, W. D. and Kuenen, P. H. 1958. Sand volcanoes on slumps in the Carboniferous of County Clare, Ireland. Quart. Journ. Geol. Soc. Lond. 113/4, 441-461.

Goldthwait, R. P. 1985. Analytical Morphological Classification of Glacigenic Landforms. Geol. Soc. Am. Abstracts with Programs vol. 17/5, p. 12.

Gould, H. R. 1951. Some quantitative aspects of Lake Mead turbidity currents. In Turbidity Currents and the Transportation of Coarse Sediments to Deep Water, ed. J. L. Hough. S.E.P.M. Spec. Publ. 2, 34-52.

Gustavson, T. C. 1973. Sedimentation and physical limnology in proglacial Malaspina Lake, southeastern Alaska. In Glaciofluvial and Glaciolacustrine Sedimentation, ed. A. V. Jopling and B. C. McDonald. S.E.P.M. Spec. Publ. 23, 249-263.

Gustavson, T. C., Ashley, G. M. and Boothroyd, J. C. 1975. Depositional sequences in glaciolacustrine deltas. In Glaciofuvial and Glaciolacustrine Sedimentation, ed. A. V. Jopling and B. C. McDonald. S.E.P.M. Spec. Publ. 23, 264-280.

Harrison, J. E. 1972. Quaternary Geology of the North-Bay Mattawa region, Geol. Surv. Pap. 71-26, 26p.

Hayward, M. 1979. Aspects of the Champlain Sea Event in the South Ottawa region. M.A. Thesis, U. of Ottawa, 122 p.

Hayward, M. and French, H. M. 1980. Pleistocene marine kettle-fill deposits near Ottawa, Canada. Can. Journ. of Earth Sciences. 17, 1236-1245.

Hillaire-Marcel, C. 1979. Les mers post-glaciaires du Québec: quelques aspects. Thése de Doctorat d'état, U. Pierre et Marie Curie, Paris. Two vols., 540 p.

________ and Occhietti, S. 1980. Chronology paleogeography and paleoclimatic significance of the late and post-glacial events in eastern Canada. Zeitschrift fur Geomorph. N.F. 24, 373-392.

Hiscott, R. N. and Middleton, G. V., 1979. Depositional mechanics of thick-bedded sandstones at the base of a submarine slope, Tourelle Formation (Lower Ordivician), Quebec, Canada. In Geology of Continental Slopes, ed. Doyle, L. J. and Pilkey, O. H. Jr. S.E.P.M. Spec. Publ. 27, 307-327.

Hitchcock, C.H. and Hitchcock, E., 1861. Geology of Vermont. Claremont, New Hampshire. Two vols., 558 p.

Hooke, R. LeB., Wold, B. and Hagen, J. O. 1985. Subglacial hydrology and sediment transport at Bondhusbreen, southwest Norway. Geol. Soc. Am. Bull. 96/3, 388-397.

Hough, J. L. 1958. Geology of the Great Lakes. University of Illinois Press. Urbana, Illinois. 313 p.

Hughes, O. L. 1965. Surficial geology of part of the Cochrane district, Ontario, Canada. Geol. Soc. Am. Spec. Pap. no. 84, 34 p.

Jopling, A. V. and Walker, R. G. 1968. Morphology and origin of ripple-drift cross-lamination, with examples from the Pleistocene of Massachusetts. Jour. Sed. Petr. 38, 971-984.

Karrow, P. F. 1961. The Champlain Sea and its Sediments. In Soils in Canada, ed. R. F. Legget. Roy. Soc. Can. Sp. Publ. 3, p.97-108.

Katasonov, E. M. 1973. Present-day ground- and ice veins in the region of the Middle Lena. Biul. Peryglac. 23, 81-89.

Katasonov, E. M. and Ivanov, M. S., 1973. Cryology of Central Yakutia. Guidebook, Second International Conference on Permafrost, Yakutsk, 38 p.

Kuenen, Ph. H. 1951. Properties of turbidity currents of high density. In Turbidity Currents and the Transportation of Coarse Sediments to Deep Water, ed. J. L. Hough. S.E.P.M. Spec. Pub. 2, p. 14-33.

Kumarapeli, P.S., and Saull, V.A. 1966. The St. Lawrence Valley System: A North American Equivalent of the East African Rift Valley System. Can. Journ. of Earth Sciences. 3, 639-657.

Kunii, D. and Levenspeil, O. 1969. Fluidization Engineering. John Wiley, New York, 534 p.

Lagarec, D. 1973. Postglacial permafrost features in Eastern Canada. In Sec. Int. Permafrost Conference, N. Am. Contribution, Natl. Ac. Sc., Washington, 126-131.

Lajoie, P. and Stobbe, P. 1950. Soil Survey of Soulanges and Vaudreuil Counties. Canada Dept. of Agriculture. King's Printer, Ottawa. 72 p.

Lambert, P. 1972. Geomorphologie des environs d'Oka. Thesis D.E.S. U. de Montreal, 270 p.

Lasalle, P. 1966. Late Quaternary and glacial history in the St. Lawrence Lowlands, Canada. Leidse Geol. Mededel. 38, 91-128.

Lowe, D. R. and LoPiccolo, R. D., 1974. The characteristics and origins of dish and pillar structures. Jour. Sed. Petr. 44/2, 484-501.

Lowe, D. R. 1975. Water escape structures in coarse grained sediments. Sedimentol. 22, 157-204.

__________ 1976. Grain flow and grain flow deposits. Jour. Sed. Petr. 46, 188-199.

Luthi, S. 1980. Some new aspects of two-dimensional turbidity currents. Sediment. 28, 97-105.

Mackiewicz, N. E., Powell, R. D., Carlson, P. R. and Molnia, B. F. 1984. Interlaminated ice-proximal glacimarine sediments in Muir Inlet, Alaska. Marine Geol. 57, 113-147.

McCabe, A. M., Dardis, G. F. and Hanvey, P. M. 1984. Sedimentology of a Late Pleistocene submarine-moraine complex, County Down, Northern Ireland. Jour. Sed. Petr. 54/3, 716-730.

Ostrem, G. 1975. Sediment transport in glacial meltwater streams. In Glaciofluvial and Glaciolacustrine Sedimentation, ed. A. V. Jopling and B. C. McDonald. S.E.P.M. Spec. Publ. 23, 101-122.

Peterson, G. L. 1968. Flow structures in sandstone dikes. Sed. Geol. 2, 177-190.

Péwé, T.L. 1966. Paleoclimatic significance of fossil ice wedges. Biul. Perygl. 15, 65-73.

________ 1973. Ice wedge casts and past permafrost distribution in North America. Geoforum 15, 15-34.

Plint, A. 1983a. Liquefaction, fluidization and erosional structures associated with bituminous sands of the Bracklesham Formation (Middle Eocene) of Dorset, England. Sediment. 30, 525-535.

________ 1983b. Sandy fluvial point-bar sediments from the Middle Eocene of Dorset, England. In Modern and Ancient Fluvial Systems, ed. J. D. Collinson and J. Lewin. Spec. Pub. Int. Assoc. Sediment. 6, 355-358.

Postma, G., Roep, T. B. and Ruegg, G. H. J. 1983. Sandy-gravelly mass-flow deposits in an ice-marginal lake (Saalian, Leuvenumsche Beek Valley, Veluwe, The Netherlands), with emphasis on plug-flow deposits. Sed. Geol. 34, 59-82.

Potzger, J. E. 1953. Nineteen bogs from southern Quebec. Can. Jour. Bot. 31, 383-401.

Powell, R. D. 1983. Glacial-marine sedimentation processes and lithofacies of temperate tidewater glaciers, Glacier Bay, Alaska. In Glacial-Marine Sedimentation, ed. B.F. Molnia. Plenum, N.Y. 185-232.

________ 1981. A model for sedimentation by tidewater glaciers. Ann. Glac. 2, 129-134.

Prest. V. K. 1970. Quaternary Geology of Canada. In Geology and economic minerals of Canada, ed. R. J. W. Douglas, part B, ch. XII. Geol. Surv. Can. Economic Geology Rpt. no. 1, 676-764.

Proudfoot, D. N., May, R. W., Rutter, N. W. and Shaw, J. 1982. Field Excursion Guide Book, Excursion 20B, Eleventh International Congress on Sedimentology. International Association of Sedimentologists. 159 p.

Reinick, H. -E. and Wunderlich, F. 1968. Classification and origin of flaser and lenticular bedding. Sedimentol. 11, 99-104.

Richard, P. 1971. Two pollen diagrams from the Quebec City area, Canada. Pollen Spores 13, 523-559.

Richard, S.H. 1972. Surficial Geology of Vaudreuil, Ontario and Quebec Map 1488a.

Richard, S. H. 1976. Surficial geology mapping, Valleyfield-Rigaud area, Quebec (31 G/1, 8, 9). Geol. Surv.

Can. Paper 76-1A, 205-208.

_________ 1978. Age of Champlain sea and "Lampsilis Lake" episode in the Ottawa-St. Lawrence Lowlands. Geol. Surv. Can. Paper 78-1C, 23-28.

_________ 1980. Surficial geology: Papineauville-Wakefield region, Quebec. Geol. Surv. Can. Paper 80-1C, 121-128.

_________ 1982. Surficial Geology, Vaudreuil, Quebec. Geol. Surv. Can. Map 1488A.

_________ 1982. Surficial Geology, Huntingdon, Quebec. Geol. Surv. Can. Map 1489A.

_________ 1982. Surficial Geology, Winchester, Ontario. Geol. Surv. Can. Map 1491A.

_________ 1982. Surficial Geology, Kemptville, Ontario. Geol. Surv. Can. Map 1492A.

_________ 1982. Surficial Geology, Morrisburg, Ontario. Geol. Surv. Can. Map 1493A.

__________ 1982. Surficial Geology, Ottawa, Ontario. Geol. Surv. Can. Map 1506A.

__________ 1982. Surficial Geology, Russell, Ontario. Geol. Surv. Can. Map 1507A.

Robin, G. de Q. 1962. The ice of the Antarctic. Scient. Am. 207/3, 132-146.

Romaine, V. 1953. The physical geography of the Two Mountains area. M.A. thesis, McGill University, 135p.

Romanelli, R. 1975. The Champlain Sea episode in the Gatineau River Valley and Ottawa Area. Can. Field Nat. 89, 346-360.

Romanovskij, N. N. 1973. Regularities in formation of frost fissures and development of frost fissure polygons. Biul. Peryglac. 23, 237-277.

Ruegg, G. H. J. 1983. Glaciofluvial and glaciolacustrine deposits in the Netherlands. In Glacial Deposits in Northwestern Europe, ed. J. Ehlers. Balkema, 379-392.

Rust, B. R. and Romanelli, R. 1975. Late Quaternary subaqueous outwash deposits near Ottawa, Canada. In Glaciofluvial and Glaciolacustrine Sedimentation, ed. A. V. Jopling and B. C. McDonald. S.E.P.M. Spec. Publ. 23, 177-192.

Rust, B. R. 1977. Mass flow deposits in a Quaternary succession near Ottawa, Canada: diagnostic criteria for subaqueous outwash. Can. J. Earth Sci. 14, 175-184.

Saunderson, H. C. 1975. Sedimentology of the Brampton Esker and its associated deposits: an empirical test of theory. In Glaciofluvial and Glaciolacustrine Sedimentation, ed. A. V. Jopling and B. C. McDonald. S.E.P.M. Spec. Publ. 23, 155-176.

Schroeder, R.A., and Bada, J.L., 1978. Aspartic acid racemization in late Wisconsin Lake Ontario sediments. Quat. Res. 9, 193-204.

Sugden, D. E. and John, B. S. 1976. Glaciers and Landscape. Butler and Tanner Ltd. England. 376 p.

Terasmae, J. 1959. Notes on the Champlain Sea episode in the St. Lawrence Lowlands, Quebec. Science 130/3371, 334-336.

Terasmae, J. 1965. Surficial geology of the Cornwall and St. Lawrence Seaway project areas, Ontario. Geol. Surv. Can., Bull. 121, 54 p.

Thomas, G. S. P. 1984. Sedimentation of a sub-aqueous esker-delta at Strabathie, Aberdeenshire. Scot. Jour. Geol. 20/1, 9-20.

Tremblay, J.J.L. and Hobson, G.D. 1962. Vaudreuil Map Area, Quebec. Geol. Surv. Can. Paper 61-20: Part 1, Ground-water Resources of the East Half, 1-13; Part 2, The Seismic Method Applied to a Bedrock Channel Problem, 15-18.

Tucker, M.E. 1982. The Field Description of Sedimentary Rocks. Wiley and Sons, Toronto. 112 p.

Washburn, A. L., Smith, D. D. and Goddard, R. H. 1963. Frost cracking in a middle-latitude climate. Biul. Peryglac. 12, 169-189.

Washburn, A. L. 1980. Geocryology, a Survey of Periglacial Processes and environments. Wiley and Sons, New

York. 406 p.

Wilson, A. 1941. Geology of Valleyfield, Ontario and Quebec. Can. Department of Mines and Resources Map 660a.

________ 1941. Geology of L'Orignal, Ontario and Quebec. Can. Department of Mines and Resources Map 662a.

Wisniewski, E. W. 1973. Genesis of the Lammi Esker (Southern Finland). Societas Geogr. Fennia, Fennia 122, 31 p.

APPENDIX A

LEGEND FOR STRATIGRAPHIC SECTIONS

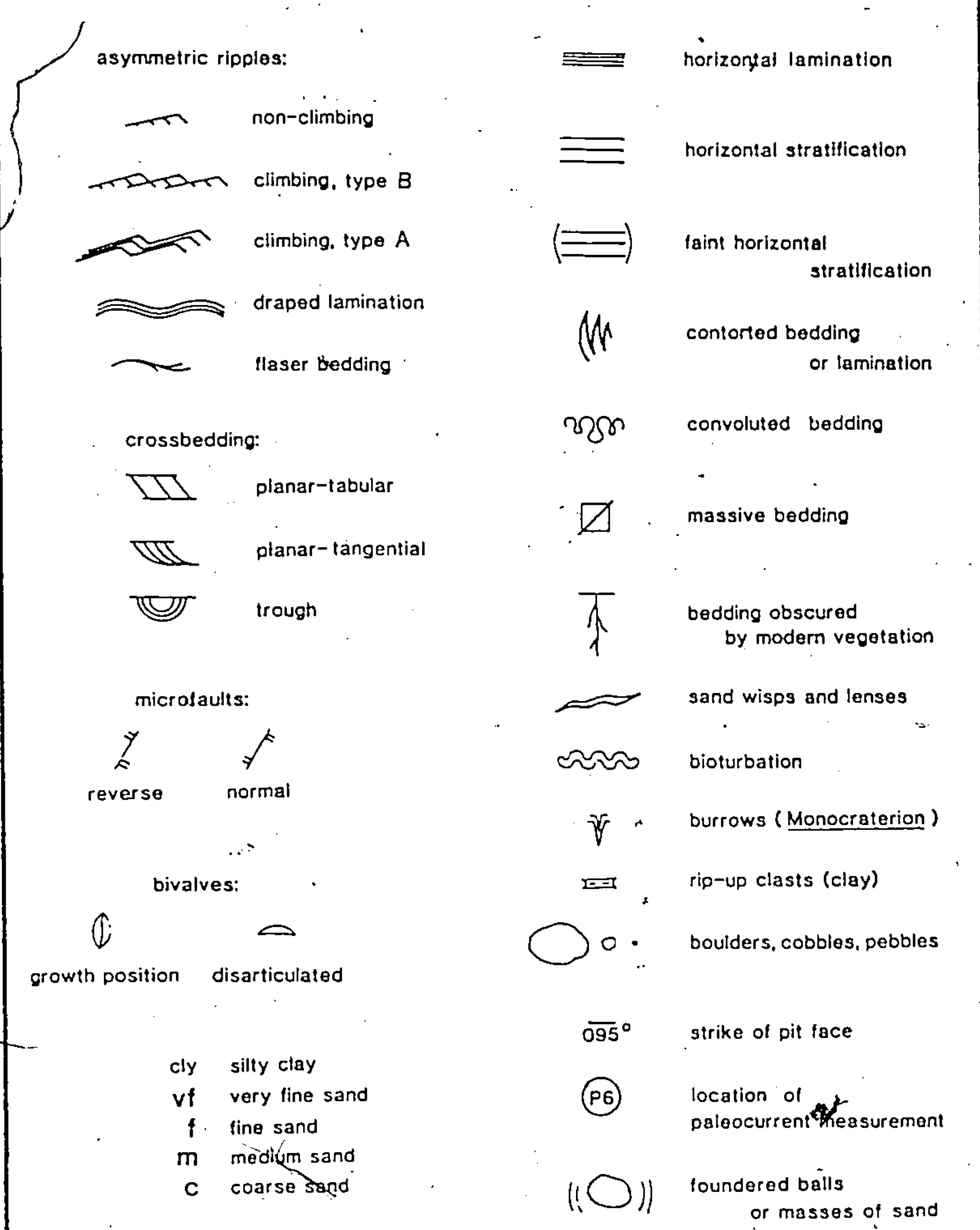

APPENDIX B

PALEOCURRENT DATA

LOCATION 1: RIPPLES

100 088 110 119 108 068 107 114 084 101 083 102 131 107 080

106 095 116 101 072 121 105 099 107 099 107 099 100 101 083

120 100 103 092 044 104 100 127 113 107

VECTOR MEAN AZIMUTH=101°; MAGNITUDE=97%

LOCATION 2: TROUGH CROSSBEDS

065 119 110 113 118 130 128 116 145 139 142 117 100 110 081

125 115 112 105 104 155 143 123 115 093 155 150 160 133 156

VECTOR MEAN AZIMUTH=121°; MAGNITUDE=93%

LOCATION 3: RIPPLES

160 147 156 134 167 151 153 139 149 099 161 100 160 159 120

125 177 147 099 120 176 137 125 099 152 164 139 145 157 144

162 123 113 135 103 121 180 131 126 138

VECTOR MEAN AZIMUTH=138°; MAGNITUDE=93%

LOCATION 4: RIPPLES

027 011 002 029 055 021 013 027 035 020 010 033 046 017 027

043 025 027 342 035 034 355 031 039 034 012 030 023 339 006

041 032 042 010 005 040 028 344 039 010

VECTOR MEAN AZIMUTH=023°; MAGNITUDE=96%

LOCATION 5: RIPPLES

113 090 115 091 087 087 092 080 117 119 145 100 123 099 083
077 113 085 115 070 079 087 095 093 107 083 117 055 121 103
121 045 127 071 065 093 087 093 107 089

VECTOR MEAN AZIMUTH=095°; MAGNITUDE=93%

LOCATION 6: RIPPLES

055 061 053 065 069 035 073 056 061 041 049 064 045 065 040
081 056 029 078 044 065 075 054 062 061 084 046 051 071 074
056 043 051 099 055 068 064 062 057 066

VECTOR MEAN AZIMUTH=060°; MAGNITUDE=97%

LOCATION 7: RIPPLES

179 159 166 178 173 195 171 187 176 164 213 183 198 161 194
162 179 157 157 204 170 173 161 235 194 209 273 168 173 173
166 200 205

VECTOR MEAN AZIMUTH=179°; MAGNITUDE=92%

LOCATION 8: TROUGH CROSSBEDS

206 238 202 205 226 200 182 219 196 212 182 205

VECTOR MEAN AZIMUTH=207°; MAGNITUDE=97%

LOCATION 9: RIPPLES

251 249 227 292 307 306 297 271 260 228 314 312 317 338 338

251 237 309 242 247 227 235 247 225 197 207 229 200 248 249

VECTOR MEAN AZIMUTH=260°; MAGNITUDE=79%

LOCATION 10: TROUGH CROSSBEDS

224 218 200 215 181 213 194 212 185 227 216 131

VECTOR MEAN AZIMUTH=208°; MAGNITUDE=87%

LOCATION 11: RIPPLES

261 235 225 249 250 226 223 233 233 243 235 237 242 243 241

221 226 264 263 257 236 254 248 260 247 261 238 257 258 228

VECTOR MEAN AZIMUTH=244°; MAGNITUDE=97%

LOCATION 12: TROUGH CROSSBEDS

210 153 181 192 189 198 191 219 189 188 157 191 146 158 171

170 157 136 168 136 146 154 141 187 178 155 166 170 151 198

VECTOR MEAN AZIMUTH=171°; MAGNITUDE=93%

LOCATION 13: RIPPLES

229 231 205 289 231 184 210 221 219 210 227 237 181 238 217

243 231 237 191 181 170 224 206 230 260 223 232 221 238 232

VECTOR MEAN AZIMUTH=219°; MAGNITUDE=95%

LOCATION 14: TROUGH CROSSBEDS

157 140 153 161 165 181 184 169 151 165 163 141 163 149 165

150 148 173 171 135 136 176 168 175 157 165 158

VECTOR MEAN AZIMUTH=161°; MAGNITUDE=96%

LOCATION 15: RIPPLES

009 007 008 038 358 018 018 044 004 024 359 017 354 031 039

011 041 011 033 021 035 351 017 356 026 007

VECTOR MEAN AZIMUTH=015°; MAGNITUDE=96%

LOCATION 16: RIPPLES

257 242 259 253 241 227 253 231 248 244 235 241 237 251 225

241 243 273 249 249 269 253 250 245 221 234 261 249 242 227

VECTOR MEAN AZIMUTH=247°; MAGNITUDE=98%

LOCATION 17: TROUGH CROSSBEDS

099 079 091 055 091

VECTOR MEAN AZIMUTH=078°; MAGNITUDE=96%

LOCATION 18: TROUGH CROSSBEDS

092 088 065 131 166 192 090 111 104 140 121 142 082 086 119

182 161 097 125 157 075 123

VECTOR MEAN AZIMUTH=108°; MAGNITUDE=73%

LOCATION 19: TROUGH CROSSBEDS

155 137 143 131 109 145 158 101 068 122 182 120 105 171 143

162 122 132

VECTOR MEAN AZIMUTH=134°; MAGNITUDE=92%